THE ROLE OF CONNECTIVE TISSUE GROWTH FACTOR (CTGF) IN OVAL CELL AIDED LIVER REGENERATION IN THE 2-AAF/PHx MODEL

By

LIYA PI

A DISSERTATION PRESENTED TO THE GRADUATE SCHOOL
OF THE UNIVERSITY OF FLORIDA IN PARTIAL FULFILLMENT
OF THE REQUIREMENTS FOR THE DEGREE OF
DOCTOR OF PHILOSOPHY

UNIVERSITY OF FLORIDA

2005

This document is dedicated to my dear mother and father.

ACKNOWLEDGMENTS

I would like to express my deepest gratitude to my mentor, Dr. Bryon Petersen, for his encouragement, support, and understanding throughout the course of my work for this dissertation. I would also like to sincerely thank the members of my doctoral thesis committee: Dr. Chen Liu, Dr. Laurence Morel, Dr. Edward W. Scott, and Dr. Naohiro Terada. Their advice was crucial to my success in this research. I would also like to extend my thanks to Drs. Seeh-hong Oh, Rafel Witek, Jie Deng, Takahisa Fijikawa, Martha Campbell-Thompson and Thomas Shupe. I would like to thank Donghang Zhen, Youngmi Jung, Heather Hatch and Jennifer LaPlante for all of the experimental advice, friendship, and support they have shown me throughout my time at the University of Florida. Finally, I would like to give a special thank to my husband, Wen-Yuan Song; my parents, Kaijin Pi and Fulian Zhang; my two children, Joanna Song and Eric Song; as well as my sisters Lijun Pi, Lili Pi for all of the support they have offered to me over the years.

TABLE OF CONTENTS

page

LIST OF TABLES

LIST OF FIGURES

Abstract of Dissertation Presented to the Graduate School
of the University of Florida in Partial Fulfillment of the
Requirements for the Degree of Doctor of Philosophy

THE ROLE OF CONNECTIVE TISSUE GROWTH FACTOR (CTGF) IN OVAL CELL AIDED LIVER REGENERATION IN THE 2-AAF/PHx MODEL

By

Liya Pi

May 2005

Chair: Bryon Petersen
Major Department: Pathology, Immunology and Laboratory Medicine

Recruitment and proliferation of Thy-1^+ oval cells are a hallmark of liver regeneration following 2-acetylaminofluorene (2-AAF)/partial hepatectomy (PHx) in rats. Oval cell activation, as part of a process of the progenitor dependent liver regeneration, is an orchestrated response induced by specific external stimuli and involves sequential changes in gene expression, growth factor production and morphological changes. To understand the molecular mechanism underlying oval cell response, we identified genes that are differentially expressed in Thy-1^+ oval cells utilizing suppression subtractive hybridization methods. It turned out that connective tissue growth factor (CTGF), which is a heparan-binding, secretory protein and can promote the growth, migration, apoptosis, angiogenesis and differentiation in a cell type specific manner, is one of the candidates. The upregulation of CTGF was confirmed at both the RNA and protein levels in Northern and Western analyses. The induction pattern in CTGF coincides with that of oval cell activation. In addition, CTGF expression in

Thy-1^+ oval cells were verified by approaches including quantitative real time PCR, immunofluorescent staining and *in situ* hybridization. Furthermore, Northern analysis showed that CTGF upregulation was associated with those of TGF-β1, procollagen type I and fibronectin gene expression. To inhibit CTGF synthesis, Iloprost, which is a stable prostacyclin derivative and has been shown to block TGF-β induced CTGF synthesis, was administrated to rats treated with 2-AAF/PHx. Iloprost administration blocked CTGF induction in treated animals but did not affect TGF-β1 expression. The inhibition of CTGF induction by Iloprost was associated with a significant decrease in oval cell proliferation and a lower level of α-fetoprotein (AFP) expression as compared to control animals. These results demonstrate that CTGF induction is important for robust oval cell response following 2-AAF/PHx treatment in rats. A yeast two-hybrid cDNA library specific for oval cell-aided liver regeneration was constructed and screened. Several interesting interactors including fibronectin, extracellular matrix protein 1 and histine rich glycoprotein were identified. Further characterization of these candidates in the future would help us to understand how CTGF regulates oval cell response during liver regeneration.

CHAPTER 1
LITERATURE REVIEW

The Liver

The liver is a central organ in the body and functions as a biotransformation machine to oxidate or hydroxylate digested substances using enzyme systems and excretes the degraded harmless conjugates as bile through vessels of bile ducts into the duodenum. It also is a place to synthesize a variety of plasma proteins and hormones that are released directly into the bloodstream. As a factory to metabolize lipid and glucogen, it plays a critical role in regulating glucose level in the blood.

Although the liver performs irreplaceable vital functions, it is usually exposed to dangerous xenobiotics ingested with foods. Potential massive death of hepatocytes caused by highly reactive electrophiles after biotransformation of these xenobiotics creates an evolutionary pressure for the liver to regenerate. This chapter covers the structure, cell types of the liver and mechanisms of liver regeneration.

Liver Anatomy and Physiology

In the liver, the smallest structural unit of parenchyma is hepatic lobules, which constitute cellular arrays of one-cell-wide, 0.3-0.5 mm-longed hepatic plates (Jones and Schmucker, 1977; McCuskey and Reilly, 1993). Each hepatic plate contains about 20 hepatocytes, which are stacked one by one to form straight or bifurcated columns of the arrays. The centers of lobules are the branches of the efferent vessels, the hepatic central veins while the edges of lobules are the branches of the afferent vessels including the portal vein and the hepatic artery, together with bile ducts, all three are designated as

portal triad. Bloods of the portal vein come from the intestine and contain lots of nutrients while bloods of the hepatic artery are rich in oxygen. Hepatic plates in a lobule are disposed radially with respect to terminal branches of portal triads. Bile canaliculi form between individual hepatocytes and connect with terminal biliary ducts of the portal triads. Capillary-sized sinusoids located between hepatic plates are full of blood and fluids moving in a direction from portal triad to central vein. The radially disposed plates of hepatocytes are exposed on either side to the blood flowing in sinusoids. The space of Disse is located between the sinusoid and the adjacent hepatocytes. In this lobular pattern, the bloods and fluids flow from the periphery (the terminal branches of the portal triad) toward the center of the lobule (the hepatic vein). The arrays of hepatic plates, the intrahepatic branches of afferent and efferent of vessels, the extensive biliary trees and numerous vascular sinusoids form continuous tridimensional networks of hepatic structures.

The functional unit of the liver is defined differently as the acinus (Rappaport, 1963). The acinus consists of a mass of parenchymal tissue surrounding the fine terminal branches of the portal triad and extends perpendicularly from one portal triad to the next. Hepatocytes in each acinus radiate around the terminal branches of portal triad centrally and are bordered peripherally by central veins. In this definition, the blood flows within sinusoids from the center (portal triad) to the peripheral region (central vein) while bile moves in the opposite direction through bile canaliculi to bile duct in the center region. An acinus is divided into three zones. Zone 1 is referred to hepatocytes surrounding the portal triad and zone 3 is those around the central vein. Zone 2 is the hepatocytes between zone 1 and 3. The liver receives three quarters of its blood supply from the

portal vein, which carries nutrient-rich blood from the intestines. This blood carries digested food substances to the liver for processing. The liver receives the remaining quarter of its blood supply from the hepatic artery, which carries oxygen-rich blood from the heart. A mixture of bloods from the hepatic artery and from the portal vein pass sinusoids and convey into the hepatic veins draining into the inferior vena cava, which then empties into the heart. The micro vascular sinusoids and the branches of afferents and efferents of vessels maintain 25% blood of cardiac output in the liver and make the liver an important organ as blood reservoir.

Types of Hepatic Cells

The liver contains a specific and characteristic set of cells expressing specific phenotypic markers listed in Table1-1. The main cell type of the liver that carried out most of the hepatic function is parenchymal cells, which are epithelial cells including hepatocytes and biliary ductular cells arranged in hepatic plates. Non-parenchymal cells are lined in sinusoids and composed of sinusoidal endothelial cells, kupffer cells, hepatic stellate cells, and pit cells. The individual cell-cell types contact with each other in an intimate relationship and with extracellular structure. These cells form a unique architectural arrangement facilitating the functions of the liver. The roles of each type of cells in normal liver are reviewed below.

Parenchymal cells

Parenchymal cells in the liver are arranged in hepatic plates, which are interconnected to form a continuous tridimensional lattice. The majority of epithelial cells are large hepatocytes (30-40 um) while a minor fraction of them are bile duct and ductular epithelial cells. Hepatocytes constitute the largest cell number (60-65%) of the endogenous liver cell population and the largest proportion of liver mass (90-95%)

(Michalopoulos, 1990; BUCHER, 1963). Individual hepatocytes are polygonal and face at least blood sinusoids at the side of their basal membrane. These hepatocytes carry out most of the metabolic functions of the liver. In different lobular zones, hepatocytes are hetergenous with different metabolic and/or biosynthetic activities. The upstream, periportal hepatocytes are exposed to different compositions of bloods (e.g., more regulatory signals in the afferent blood) compared to those of the downstream, Centro lobular hepatocytes.

The apical membranes between adjacent hepatocytes form bile canalicules. Bile is secreted by hepatocytes and drained starting from bile canalicules, followed by the finer and larger branches of the intrahepatic and extrahepatic portions of the biliary tree. Bile duct epithelia (chaolangiocytes) are lined in bile ducts along the course of the biliary passageways. They form vessels of both the finest intrahepatic branches and the larger extrahepatic ducts. The region connecting terminal hepatocytes and bile duct epithelial cells is called the canal of Hering, which is believed to be the origin of a heptic stem cell, "oval cell". Bile duct epithelia account for 3-5% of the nucleated liver population and express some distinct markers such as cytokeratins 7 and 19, epithelial membrane antigen, carcineoembryonic antigen, carbonic anhydrase and γ-glutamyltranspeptidase (McCuskey and Reilly, 1993). Compared to hepatocytes, bile ductular cells exhibit a lack of cytochrom P-450-dependent monooxygenase activities but possess a number of distinct phase II conjugating enzymes. This different metabolic activity provides bile ductular cells a survival advantage over hepatocytes during the biotransformation of some hepatotoxins or hepatocarcinogens. Under some circumstances when hepatocyte proliferation is arrested, it is believed that oval cells originating from the canal of Hering

are recruited to replenish the liver. Oval cell involvement in liver regeneration will be discussed in later sections of this chapter.

Nonparenchymal cells (NPCs)

Nonparenchymal cells account for 5-10% of the mass and 35-40% of the cell number in the liver. Although they do not directly carry out metabolic functions, they plays important roles to facilitate exchange of substances between bloods and the liver and to defend the liver from exogenous attacks.

Sinusoidal endothelial cells (SECs) account for approximately 15-20% of the total number of liver cells and cover the inside of the sinusoidal wall, which provides a large surface area for nutrient absorption (Arii and Imamura, 2000). One main structural characteristic of the SEC is the formation of numerous fenestrae with a diameter of approximate 100nm. Fenestrae filter fluids, solutes and particles that are exchanged between the sinusoidal lumen and the space of Disse, allowing only particles smaller than the fenestrae to reach the parenchymal cells or to leave the space of Disse. Thus, SECs function as a selective sieve for substances passing from the blood to parenchymal cells through fenestrae, which allows a direct communication between the sinusoidal lumen and the space of Disse and efficiently transports metabolites in plasma to the hepatocytes. SECs also function as a scavenger system to clear the blood from many different macromolecular waste products, which originate from turnover processes in different tissues. They possess endocytotic capacity to take up substances such as heparin, colloidal albumin, antimony sulfur colloid, and albumin. The third characteristic of SECs is that there is no continuous basement membrane in the space of Disse, which is a region between SECs and parenchymal cells. The absence of a regular basal lamina, the

presence of fenestrae and endocytotic capacity make SECs be a unique cell population distinct from any other type of endothelial cell in the body.

Pit cells were first described in 1976 by Wisse and possess typical granules termed as pit (grapes in Dutch) of natural killer cells. They often adhere to SECs and face blood directly. Through their pseudopodia, pit cells can penetrate the fenestrae of the SECs and directly contact the microvilli of hepatocytes. They are considered to originate from blood NK cells, which immigrate into the hepatic sinusoids through adhesion molecules (Vanderkerken et al., 1993). Pit cells function as liver-specific natural killer cells and present antigen. Dendritic cells capture and process antigens, migrate to lymphoid organs and secrete cytokines to initiate immune responses. Pit cells express a typical natural killer cell marker, NKR-P1, which can trigger cytotoxic action. They represent a first line of cellular defense in the liver.

Kupffer cells were account for approximately 31% of sinusoidal cells (Bouwens et al., 1986). They are attached to the sinusoidal wall and possibly migrate along the lumen. Kupffer cells are tissue macrophages and components of the diffuse monoculear phagocyte system. They function as a waste receptacle for all kinds of old, unnecessary, damaged, altered, or foreign material. Upon activation (zymosan or endotoxin uptake), they secrete a number of products with potent biologic effects, including proteases and cytokines with influence on parenchymal and other sinusoidal lining cells. In juried livers, activated Kupffer cells secrete cytokines and growth factors that induce the growth of hepatocytes, stellate cells and the migration of inflammatory cells. Moreover, they are more phagocytic than are their normal states and have impaired capacity to remove endotoxins.

Stellate cells account for 15% of the total number of resident cells and approximately one-third of the nonparenchymal cell population in normal liver (Jezequel et al., 1984). They are spindle-shaped with oval or elongated nuclei and located in the space between the basolateral surface of hepatocytes and the ablumenual side of sinusoidal endothelial cells. One major characteristic of stellate cells in normal liver is cytoplasmic droplets which contain vitamin A (80% of retinoids of the whole body), primarily in the form of retinyl esters.

Stellate cells can recruit inflammatory cells through expression of adhesion molecules, secretion of chemokines and cytokines and hence play regulatory roles in liver inflammation. During tissue remodeling, quesicent stellate cells become activated and transdifferentiate into myofibroblast-like cells. They lose retinoids and become very proliferative, fibrogenic and contractile (Friedman et al., 1993). The specialized stellate cells express a high DNA binding activity of several transcription factors including c-Myb, NFkB, KLF6 and Sp1. Activated stellate cells are also an important source of cytokines and synthesize a large amount of extracellular matrix components including collagen, proteoglycan and adhesive glycoproteins. The production of ECM component is mediated through integrin-dependent signaling events including focal adhesion kinase, tyrosine kinase and ERK activation. Transforming growth factor (TGF)-β is a major promoter of myfibroblast differentiation, which is characterized by the expression of α-SMA and adhesive receptors and the increasing synthesis of extracellular matrix molecules including ED-A fibronectin. Normally, activated stellate cells ensure a fine-tuning of the wound-healing response according to the duration, the type and the amount

of damage through extra cellular matrix production. However, overexpression of extracellular matrix components by these cells causes hepatic fibrosis.

Stellate cells express some phenotypic markers such as desmin and a smooth muscle actin (specific for activated stellate cells). Interestingly, they also express neuroendocrine markers including glial fibrillary acidic protein, neural cell adhesion molecule, the class VI intermediate filament protein nestin and synaptophysin (Niki et al., 1996; Niki et al., 1999). Such characteristic raise the question of a possible neural crest origin of stellate cells.

Extracellular matrix (ECM) in the liver

The ECM was thought to be simple proteinaceous material rich in collagen and termed "ground substance". Now a notion that ECM is a highly dynamic complex that varies in composition according to its tissue localization and physiological circumstances has been developed. Its essential nature has been demonstrated in the lethality of transgenic mice lacking functional fibronectin gene at the early embryo stage (Georges-Labouesse et al., 1996).

ECM comprises less than 3% of the relative area on a normal liver section. Although it is restricted in Glisson's capsule, portal tracts, Disse's space and the central veins of the liver, it is part of the frontier between the blood flow and the parenchyma.

ECM consists of the array of various macromolecules forming a scaffold of the liver. These macromolecules include fibronectin, collagen, laminin, vitronectin and proteoglycans. Proteoglycans include heparan, dermatan, chondroitin sulphate, perlecan, hyaluronic acid, biglycan, and decorin. A classic basement membrane is formed to surround the bile duct structures in the portal triads. The basal lamina consisting of type IV collagen and laminin is associated with the bile ducts and ductules and the adjacent

hepatocytes. Across the liver acinus, the ECM gradually changes to components such as fibrillar collagens, fibrinectin, undulin, trace amounts of collagen V and laminin, tenascin and proteoglycans in the Disse's space (Martinez-Hernandez and Amenta, 1995; Martinez-Hernandez and Amenta, 1993). One major characteristic of the ECM in the Disse's space is that the basement membrane-like matrix along the sinusoid wall is not electron-dense, unlike a typical basement membrane. The low density of this matrix is critical for allowing easy diffusion between blood and liver cells and for maintaining the differentiated function of all resident liver cells.

Besides the mechanical coherence, liver ECM also influences the phenotype and function of hepatic cells. As a binder of cytokines and growth factors, ECM can concentrate, present and sequester these molecules specifically (Schuppan et al., 1998). The release of cytokines and growth factors from ECM provides the initial signal for tissue repair, prior to the activation of cells during liver injury. In addition, ECM components can communicate with cells through integrins, the cell surface transmembrane proteins. Integrins consist of α and β heterodimeric subunits. The cytoplasmic side of α and β subunits consists of a short segment that is physically connected to the cytoskeleton. Through this linkage, external ligands (e.g.,ECM components) may affect directly the internal structure of the cell and may facilitate cells to colonize in the sites where they are to function. Also, when an integrin is engaged by the appropriate ligand, its cytoplasmic domain undergoes activation, initiating events that impact on the regulatory machinery of the cell (Ruoslahti and Engvall, 1997). ECM components such as fibronectin have been shown to bind to the long extracellular segment of integrin and modulate cell function.

The components of the ECM are maintained constantly by an active process of synthesis and degradation. The concentration of each component may be transiently or permanently changed according to the types of liver injuries during physiological processes such as hepatic development and pathological processes such as hepatic fibrosis. In the regenerative response ECM components are produced to make new sinusoids and restore the original liver architecture. In fibrosis, type I collagen are predominant to be synthesized and are the main component of scar tissue. The remodeling process is fundamental in the change of the liver architecture in normal or abnormal state.

Liver Regeneration

Liver regeneration is a compensatory hyperplasia after cell loss or injury to restore the original mass and architecture as shown by Higgins and Anderson by the two-thirds partial hepatectomy model in rodents (1931). Morphologically and functionally, the residual hepatocytes still maintain an active urea cycle, albumin synthesis and drug metabolism as well as exhibit normal polarity of membrane domains during this process (DuBois et al., 1994). However, the removed lobes of the liver do not grow back, unlike the regeneration of limbs in amphibian models. Instead, a hyperplastic response involving massive cell replication and tissue remodeling occurs in the remnant liver.

Based on the parenchyma cell type involved in this process, liver regeneration after hepatic injury can take place through two different mechanisms: hepatocyte driven liver regeneration or progenitor cell dependent liver regeneration. Both regeneration are the systematic replacements of lost tissue through an orchestrated series of events including ECM rearrangement; setting into motion the cell cycle for mitosis; cellular division of all cell types at different times; shutting down the cell cycle and reorganization of the newly

formed tissue. These processes are strictly regulated and end as the liver regains its original mass.

Hepatocyte-Driven Liver Regeneration

Normally, hepatocytes are quiescent in G_0 stage and exhibit minimal replicative activities. However, injuries resulting from either up to 75% of liver mass removal (such as partial hepatectomy, PHx), chemical toxicity caused by carbon tetrachloride (CCl_4) or biological insults can trigger the synchronous entry of the remaining hepatocytes and other existing mature hepatic cells into cell cycles in rats. The kinetics of cell proliferation and the growth factors produced by proliferating hepatocytes suggest that hepatocytes provide the mitogenic stimuli leading to proliferation of the other cells. Thymidine labeling studies show that hepatocytes in zone 1, where the lobules surround the portal triads, first enter cell cycles followed by hepatocytes in zone 2 in pericentral areas. There are two peaks of hepatocyte proliferation. The first peak occurs at 24 hours after PHx while the second one is at 48-72 hours with much smaller magnitude after PHx. Biliary ductular cells are the second cell type to replicate with a peak at 48 hours and followed immediately by stellate and Kupffer cells. SECs are last to replicate with a slow shoulder of replication at day 3-8 post PHx (Michalopoulos and DeFrances, 1997). Unlike hepatocytes, DNA synthesis in NPCs is not initially localized to the portal triads but is diffuse throughout the liver remnant (Bucher, 1963).

Liver histology at day 3 to 4 after PHx is characterized by clumps of small hepatocytes surrounding capillaries. The clumps of small hepatocytes are first in periportal areas and subsequently in the centrolobular region (Martinez-Hernandez and Amenta, 1995). Typical hepatic histology is gradually restored through the following steps: stellate cells penetrate the hepatocyte clumps and start producing several types of

laminin. Endothelial cells invade these clusters to restore one-cell-thick cords that have tow surfaces lined by sinusoids. Eventually, the small hepatocyte clumps become rearranged into the typical hepatocyte plates seen in the mature liver. The capillaries of the small hepatocyte clumps (surrounded by typical capillary basement membrane) change into true hepatic sinusoids (surrounded by very scant matrix and lined by fenestrated endothelial cells and kupffer cells). The hepatic matrix composition also changes from one of high laminin content to that typical of mature liver with very scent matrix containing primarily fibronectin, collagen types IV and I, and several other protiens and glycosaminoglycans in smaller amounts. By day 7, hepatic histology consists of lobules larger in size than before regeneration. Hepatocytes become arranged in plates consisting of two cell layers (as opposed to the one cell layer of the normal liver). The spatial distribution of proliferating hepatocytes in the regenerating liver has a predictable pattern during these processes.

Progenitor Cell Dependent Liver Regeneration

When a damage to a liver is too much or proliferation of hepatocytes is inhibited as a result of either the metabolism of foreign compounds to hepatotoxic intermediates or heptotropic virus infection, progenitor cells such as oval cells are recruited to proliferate and replenish the function of damaged hepatocytes in rats (Shinozuka et al., 1978). Morphologically, oval cells are small in size (approximately 10μm), with a large nucleus to cytoplasm ratio, with an oval shaped nucleus (Farber, 1956). After activation, a large number of oval cells appear near bile ductules and then migrate into the hepatic parenchyma (Alison et al., 1996b; Paku et al., 2001). Activated oval cells firstly differentiate into basophilic small hepatocytes and eventually become mature adult

heaptocytes (FARBER, 1956; Golding et al., 1995). Besides hepatocyte lineage, oval cells are also able to differentiate into intestinal type epithelium in rats in vivo (Golding et al., 1995), bile ductular epithelial cells and pancreatic-like cells in culture (Shiojiri et al., 1991; Yang et al., 2002).

The origin of oval cells is still controversial. Traditional belief is that they come from the canals of Hering, which is a transitional zone between the periportal hepatocytes and the biliary cells lining the smallest terminal bile ducts (Farber. 1956). In supporting this, selective damage of bile ductular epithelia in periportal zone reduces oval cell proliferation (Petersen et al., 1997). Furthermore, oval cells have been found to express markers of bile duct epithelium (CK19) and hepatocytes (albumin). They also express α fetal protein (AFP) and are positive for monoclonal antibodies, such as OV6, OC.2 and BD1. Recently, it has been found that oval cells also express some hematopoietic stem cell markers such as CD-34, c-kit and Thy1 as well as Flt-3 (Yin et al., 1999; Fujio et al., 1994; Petersen et al., 1998; Omori et al., 1997). These findings raise an intriguing possibility that part of the oval cell population may come from bone marrow.

In 1989, Evarts et al. showed that the oval cell compartment is activated extensively in rat livers treated with 2-acetylamino-fluorene (AAF) and 2/3- partial hepatectomy (PHx). Since then, this 2-AAF/PHx model of oval cell activation has been widely used to analyze the oval cell compartment during the last ten years. There are two basic surgeries to induce oval cell activation in the 2-AAF/PHx protocol. At first, 2-AAF pellet is inserted intraperitoneally by a small surgery into the rats. This intraperitoneal administration of 2-AAF prior to and during hepatic injury inhibits hepatocyte proliferation and induces oval cell replication because this compound specifically blocks

the cyclin D1 pathway in the hepatocytes. 2-AAF induced oval cells characterized by expression of AFP, albumin and hepatic transcription factors emerge within 96 hours after exposure to the chemical (Paku et al., 2001). In the second surgery, two-thirds of livers in animals are removed at 5-7 days post 2-AAF exposure. This severe hepatic injury provides a necessary growth stimulus for the massive proliferation, expansion and finally differentiation of the AAF-induced oval cells in the liver parenchyma. At 3 days after the partial hepatectomy, the oval cells have been found to infiltrate the liver lobules and form elongated ductular structure. Approximately at day 7-11 post PHx, undifferentiated oval cells proliferate to the maximal amount. After day 10-11, oval cells start to differentiate into foci of hepatocytes and intestinal-type structures (Evarts et al., 1996; Alison et al., 1996a).

Recently, analysis of morphological changes using immuno-electromicroscopy and immunostaining reveals that activated oval cells form elongated ductular structures, which are surrounded by basement membranes and terminated at hepatocytes located at the limiting plate and accompanied by activated and proliferating stellate cells. The surrounded base membranes may provide a substrate and scaffold for proliferation and migration of oval cells. More interestingly, a number of proliferating stellate cells are always intimately associated with these ductules and sometimes form direct cell-cell contact with the ductular epithelial cells (Paku et al., 2001). This connection between oval cells and stellate cells may represent mutual interaction through reciprocal growth factors and growth factor receptors.

The Molecular Aspects of Liver Regeneration

The understanding of the molecular mechanism of liver regeneration has been mainly investigated on the 70% partial hepatectomy model in rodent. Cell cycle genes,

metabolic genes, genes coding for ECM proteins, growth factors, cytokines and transcriptional factors are involved in different phase to mediate liver regeneration. Genes can be divided into three categories before cells enter mitosis and DNA replication in liver regeneration following PHx (Figure 1-1): I. the expression of immediate early genes. II. delayed early genes and III. cell cycle genes. A tight regulation of cells to enter cell cycles after injury and to exit cell cycles after appropriate tissue remodeling occurs during liver regeneration.

More than 100 immediate early genes are induced rapidly after PHx and their expression lasts for approximately 4 hrs ((Figure 1-1). Their activation doesn't require protein synthesis. Growth factors trigger intracellular signals during liver regeneration and result in activation of some latent and prexisting transcription factors such as post-hepatectomy factor/nuclear factor-κB (PHF/NF-κB) and signal transducer and activator of transcription Stat3. These transcription factors further activate the effector genes, which ultimately mediate the primary growth response (Taub, 1996). The largest category of immediate early genes is transcriptional factors including c-fos, c-jun, junB, c-myc, c-ets, IκBα, insulin-like growth factor binding protein-1 (Haber et al., 1993). Some immediate-early genes also encode other factors such as liver regenerating factor -1 (LRF-1), nuclear receptor, phosphatases, metabolic enzymes and liver specific transcription factors such as CAAT enhancer binding protein and hepatocyte nuclear factors (HNF). These factors can interact with growth-induced factors to facilitate the maintenance of metabolic homeostasis of the liver during liver regeneration.

Delayed early genes are induced after the immediate early gene response and before the maximal expression of cell cycle genes ((Figure 1-1). The transcription of

these genes requires protein synthesis. These groups include the liver-specific genes C/EBPα and Bcl-XL genes. Cell cycle genes are the third groups and induced after delayed early genes (Figure 1-1). These genes include p53, p21, cyclins and cyclin-dependent kinases (cdks) (Albrecht et al., 1993; Loyer et al., 1994). The induction of cyclin D1 is the most reliable marker for cell cycle progression in hepatocytes. Cyclin D1/cdk4 complexes can phosphorylate Rb and E2F factors to overcome a late G1 restriction point in the cell cycle. Once hepatocytes pass the restriction points and express cyclin D1, the cells is irreversibly committed to replicate (Albrecht and Hansen, 1999).

At the molecular level, several factors have been identified to be critical for the normal hepatic regeneration. The earliest event, occurring within one minute after the surgical removal, is a large increase of the blood-borne hepatocyte growth factor (HGF) (Lindroos et al., 1991). This rapid increase is a result of remodeling of extracellular matrix (ECM) and release of HGF from ECM in the liver. Active HGF then binds to its receptor c-met and activates a signal transduction pathway leading to entry of hepatocytes into the cell cycle. Other factors such as Interleukin 6 (IL-6), tumor necrosis factor –α (TNF α), epidermal growth factor (EGF), acidic fibroblast growth factor (aFGF), and transforming growth factor α (TGF α) are also involved in the hepatocyte-driven liver injury response. IL-6 and TNFα knockout mice both show significantly delayed regeneration after PHx (Yamada et al., 1997; Cressman et al., 1996; Yamada and Fausto, 1998). EGF is a primary mitogen for hepatocytes in tissue cultre (Lindroos et al.1991). TGFα mRNA and protein levels increase markedly within hours after PHx (Mead and Fausto, 1989). TGFα overexpression can drive hepatocyte replication in vitro. Norephinephrine, insulin and glucagon are co-mitogens. They alone have little effect on

DNA synthesis but are capable of modulating the effect of other growth factors on hepatocyte DNA replication.

In progenitor-dependent injury response, although it is not clear whether the same positive and negative regulatory signals contribute to liver regeneration, injury-induced changes in cytokines and growth factors definitively modulate the fate of proliferating oval cells. A number of growth modulators, including stem cell factor (SCF), transforming growth factor a (TGF-α), epidermal growth factor (EGF), hepatocyte growth factor (HGF), urokinase-type plasminogen activator (uPA), leukemia inhibitory factor (LIF) and their receptors are involved in oval cell proliferation. The cellular localization of the different components indicates that an intricate network of paracrine and autocrine mechanisms of growth modulation is involved.

The other distinct response associated with activation of oval cells is a large expansion of stellate cells and an increased production of growth factors and ECM molecules in the periportal regions of injured livers. It is believed that stellate cells secretes these growth factors such as HGF, TGFα, TGF-β1 and ECM components such as fibronectin and regulates expansion and differentiation of the oval cell population. In addition, autocrine productions of TGF-α, acidic fibroblast growth factor (aFGF) and IGF-II (insulin-like growth factor II) in oval cells are suggested to mediate the progenitor-dependent liver regeneration. These factors, as well as others as of yet undetermined factors, could be the signals needed to cause oval cells to differentiate down the hepatic lineage. Identification and characterization of the roles of these factors in oval cell proliferation and differentiation would give sight on elucidating the mechanism of the progenitor-dependent liver regeneration. This may, in turn, lead to a

clinical relevance with an application in the treatment of patients through stem cells therapies.

Less knowledge is known about the mechanisms to terminate liver regeneration. Several negative regulatory signals have been proposed including TGF β1, P53, p21 and C/EBPα. Mice lacking p53, p21 and C/EBPα show continuous hepatocyte turnover and hyperproliferaion of hepatocytes (Yin et al., 1998). TGF β1 is a known inhibitor of proliferation in hepatocyte cultures (Carr et al., 1986; Ueda et al., 2003). When TGF-beta or activin signaling in intact rat liver was eliminated by adenovirus-mediated transfer of the gene encoding truncated type II TGF-beta receptor (AdextTR) or truncated type II activin receptor (AdextAR), blockade of either TGF-beta or activin signaling leads to the initiation of DNA synthesis in intact liver (Ichikawa et al., 2001). Therefore, they proposed that TGF-β and activin inhibit hepatocyte growth even in intact liver and may play a critical role in the maintenance of constant liver mass. However, intact signaling by TGF-β appeared to be not required for termination of liver regeneration in Tgfbr2 conditional knockout mice (Oe et al., 2004). This is explained by that increased signaling by activin A may compensate to regulate liver regeneration when signaling through the TGF-beta pathway is abolished, and may be a principal factor in the termination of liver regeneration.

ECM Remodeling during Liver Regeneration

Most regenerative responses in the liver are associated with changes in the ECM. Remodeling of the ECM precedes and accompanies cell proliferation during liver regeneration. Transcripts of the tissue inhibitor of metalloproteinase TIMP-1 increase greatly at the time of the peak of DNA replication and are localized mostly in portal and

perisinusoidal mesenchymal cells. Increases in urokinase-type plasminogen activator and plasmin as well as fibrinogen degradation occur rapidly and persist for several hours after PH (Mars et al., 1995). The activation of plasminogen, an abundant serine protease zymogen to plasmin is mediated through a complex system of proteins that include urokinase-type plasminogen activator (uPA); tissue-type plasminogen activator (tPA); a receptor for uPA, the urokinase-type plasminogen receptor (uPAR); and a number of physiologic inhibitors of plasminogen activation. The activation of proteolytic cascades facilitates cell migration through ECM. A number of growth factors including HGF and transforming growth factor beta (TGF-β) are secreted as latent proteins and bound to the ECM components, where they are activated by proteases (Mars et al., 1993).

With the restoration of hepatic structure, the expression of ECM components is also changed. Upregulation of procollagen α1 and α2 transcripts occurs after the cessation of DNA replication and is associated with increased serum amino-terminal procollagen type III peptide. The changes in the expression of ECM components suggest that matrix synthesis coincide with the restoration of quiescence of hepatocytes.

Taken together, dynamic ECM remodeling with a broad program of changes modulates cell behaviors leading to activation, proliferation, migration and differentiation of hepatic cells at different stages of liver regeneration.

Transforming Growth Factor Beta (TGF-β)

The Biological Activities of TGF-β

TGF-β is a multifunctional peptide that regulates proliferation, differentiation, migration and other funcitons in many cell types during development, differentiation and tissue remodeling (Massague, 1990). Mammals contains three isoforms including TGF-

β1, -β2 and -β3. All three are present in liver but, interestingly, are not expressed uniformly in individual cell types (Bissell et al., 1995), posing the possibility of distinct individual roles. TGF-β1, -β2 and -β3 all function through the same receptor signaling systems.

TGF-β has one of the widest ranges of activities in tissue remodeling and wound healing. Subcutaneous injections of TGF-β into newborn mice led to the formation of granulation tissue formation followed by fibrosis (Roberts et al., 1986). TGF-β is chemotactic and mitogenic to cells of mesenchymal origin including monocyte, macraphage and fibroblast. It stimulates these cells to produce molecules that constitute and interact with the extracellular matrix such as procollagen type I, serum procollagen type III, collagens type I, VI, and X, β-actin, fibronectin, vitronectin and proteoglycans. Some these genes such as collagen type I, fibronectin and type 1 plasminogen activator inhibitor (PAI-1) have been proven to be regulated by TGF-β at the transcriptional level by Smad signal transduction pathway (Yue et al., 2004; Falcone et al., 1995; Inagaki et al., 1994).

On the other hand, TGF-β inhibits the proliferation of epithelial, endothelial and hematopoietic cells. It is believed that the arrest pathway mediated by TGF-β is through the activities of the Smad complexes, which turn off *c-myc* transcription and turn on the transcription of the inhibitors of cyclin-dependent kinases p15 and p21. These activities result in the arrest of the cell cycle prior to the G1 restriction points and ultimately cause the activation of the central retinoblastoma pathway of cell cycle control (Laiho et al., 1990).

Activation of TGF-β Signaling

TGF-β is secreted as a latent factor and its activity is blocked by its carboxyl-terminal propeptide latency-associated peptide (LAP). The secreted latent factor of TGF-β is also associated with a latent TGF-β-binding protein (LTBP). The LTBP/TGF-b complex is primarily in the extracellular matrix. The amino-terminal region of LTBP-1 is covalently cross-linked to ECM proteins by transglutaminase. Then, proteolytic processing is required for the activation of TGF-β. Candidate proteases involved in this processing include plasmin, thrombin or cell-specific and membrane-associated proteases. The plasmin proteases MMP-2 and -9 involve in matrix degradation and TGF-β activation (Schultz-Cherry and Murphy-Ullrich, 1993; Yu and Stamenkovic, 2000). In addition to proteolytic activation of latent TGF-β, a number of pericellular factors act to sequester or limit the activity of this cytokine. These factors consist of the ECM components, which bind to integrins. Integrins are another TGF-β activitors and participate in TGF-β receptor activation (Bissell et al., 2001). All of TGF-β activators are intimately associated with fibrogenic process. Integrinβ6$^{-/-}$ knockout mice are highly resistant to lung fibrosis induced by the profibrotic drug bleomycin (Munger et al., 1999). Thrombospondin-1 null mice share some similar phenotypes with TGF-β1 null animals (Crawford et al., 1998).

Active TGF-β is a homodimeric 25kDa protein and exerts its multiple biologic actions by the interaction with two transmembrane serine/threonine kinase receptors, type I and type II. Type II receptor is constitutively active and TGF-β β binding results in the recruitment and phosphorylation of type I receptor. The intrinsic serine/threonine kinase activity of type I receptor phosphorylates Smad 2 and 3, which combine and form a

heteromeric complex with unphosphorylated Co-Smad 4. The resulting Smad complex then moves into the nucleus, where it regulates target gene transcription either by directly binding DNA sequences or by complexing with other transcription factors or coactivators (Cheng and Grande, 2002). The other group of Smad proteins such as Smad6 or Smad7 prevents Smad2 and 3 phophorylation and subsequent nuclear translocation of heterocomplexes with Smad4. Betaglycan, a transmembrane proteoglycan, which is known as type III receptor of TGF-β, allows high-affinity binding of TGF-β to TGF-β receptor type II but does not itself transduce signal.

TGF-β/Smad signaling is regulated by MAP kinase signaling cascades. Addition of TGF-β results in a transient activation of the ras/MEK/ERK cascade in epithelial cells, mesangial cells and fibroblasts (Hartsough et al., 1996; Mulder and Morris, 1992). The linker region of Smad3 can be phosphorylated by ERK. Ras/MEK/ERK MAP kinase cascade phosphorylates and modifies Smad activity (Mulder, 2000). This cascade is required for TGF-β-induced gene expression (Yue and Mulder, 2000).

Cross talk exists between TGF-β and cyclic AMP signal transduction pathways at the level of transcriptional complex formation (Wenner and Yan, 2003). Treatment of cells with a stimulator of adenylate cyclase or TGF-β increased the amount of phosphorylated CAMP response element binding protein (CREB) and the coactivator, CREB binding protein (CBP) that were bound in a complex to the Smad binding element.

TGF-β Signal Transduction Pathway in Liver Fibrosis

TGF-β is a pro-fibrogenic cytokine during liver injury. In normal liver, TGF-β1 and TGF-β2 mRNAs are predominantly expressed by Kupffer cells while TGF-β3 is expressed by stellate cells. During fibrosis, the expression of TGF-β 1 is significantly

upregulated in stellate cells and SECs whereas TGF-β2 and 3 are downregulated (De Bleser et al., 1997). Up-regulation of TGF-β1 results in the formation of autocrine and paracrine loops, which sustain high cytokine levels in injuried liver. TGF-β1 induces accumulation of H_2O_2 in stellate cells and is a major cytokine to activate stellate cells and upregulates the expression of α1 (I) collagen mRNA (De Bleser et al., 1999; Garcia-Trevijano et al., 1999). Downstream mediators such as CTGF and ED-A form of fibronectin are required for the enhancement of cellular responses and prolongation of fibrotic response mediated by TGF-β.

In addition, liver fibrosis has been demonstrated to be associated with enhanced expression of TGF-β receptors (Gao and Brigstock, 2003; Roulot et al., 1999). Overexpression of dominant negative TGF-β receptor type II improved liver fibrosis (Qi et al., 1999). Smad2, Smad3, and Smad4 were reported to contribute in liver fibrosis *in vitro* and *in vivo* (Lee et al., 2001; Schnabl et al., 2001; Inagaki et al., 2001; Tahashi et al., 2002).

TGF-β Signal Transduction Pathway in Liver Regeneration

The temporal expression of TGF-β in liver regeneration is different from that in liver fibrosis. Its mRNA increases in the SECs and stellate cells as early as 4 hours, with the peak occuring at 72 hrs in PHx treatment. In CCl4-induced acute liver damage, TGF-β1 mRNA rises significantly after 24 hours post-injury, peaks at 48 hours after the major wave of hepatocyte cell division and mitosis. In oval cell mediated liver regeneration, TGF-β1 mRNA also increases in oval cells and stellate cells (Jakowlew et al., 1991; Fausto et al., 1991).

In the context of hepatocyte driven liver regeneration, TGF-β is believed to be antiproliferative rather than pro-fibrogenic. Infusion of TGF-β into partially hepatectomized rats could transiently depress DNA synthesis after PHx (Russell et al., 1988). TGF-β inhibits the proliferation of hepatocytes in culture in the presence of HGF, TGF α, EGF (Nakamura et al., 1985). TGF-β 1 can depress the basal DNA synthesis of hepatocytes in culture (Oberhammer et al., 1991). However, during liver regeneration, hepatocytes acquire temporary resistance to TGF-β, allowing them to proliferate despite rising levels of this cytokine. In epithelial cells, overexpression of constitutively active members of the ras/MEK/ERK cascade blocks nuclear accumulation of Smads. This may explain why transformed epithelial cells that show constitutive activation of Ras are not responsive to TGF-β (Kretzschmar et al., 1999).

Return of TGF-β sensitivity at later stages is believed to limit hepatocyte prliferation and terminate liver regeneration. Thus, TGF- β is a candidate to limit and/or stop liver regeneration following PHx. Recently, Oe et al (2004) investigated TGF-β type II receptor gene (Tgfbr2) conditional knockout mice and found that TGF- β regulated G1 to S phase transition of hepatocytes, but intact signaling by TGF- β was not required for termination of liver regeneration. Increased signaling by activin A may compensate to regulate liver regeneration and is a principal factor in the termination of liver regeneration.

TGF-β Signal Transduction Pathway and ECM Proteins

TGF-β is one of the most potent cytokines to stimulate ECM synthesis and regulates ECM production in normal tissue repair and remodeling process (Shek and

Benyon, 2004). TGF-β overproduction causes a pathological deposition of ECM components, which eventually form scarring of tissues.

TGF-β affects extracellular matrix homeostasis by two major mechanisms: one is to increase the production of extracellular matrix proteins and protease inhibitors. The other is to downregulate the expression of various metalloproteinases. The balance between matrix metalloproteinases (MMPs) and tissue inhibitors of these enzymes (TIMPs) is essential in remodeling the extracellular matrix. TGF-β influences the plasminogen activator/plasmin system by reducing plasmin activator activity and by increasing the synthesis of plasminogen activator inhibitor-1 (PAI-1) (Laiho et al., 1987; Lund et al., 1987). TGF-β induces TIMP-1 and represses MMP-1 (Hall et al., 2003; Greenwel and Rojkind, 1997). TGF-β is a potent inducer of metal metalloproteinase-13 gene expression through Smad 3 (Leivonen et al., 2002). TGF- β enhances the synthesis of ED-A fibronectin (ED-A Fn), which is required for TGF-ß1-triggered enhancement of -SMA and collagen type I expression (Serini et al., 1998). TGF- β induction of collagen occurs directly in an immediate-early fashion, requiring action of the general TGF- β signaling meidators, the Smads, the p38 MAPK pathway and other promoter elements such as Sp1 (Varela-Rey et al., 2002; Greenwel et al., 1997). In addition, TGF-β has been shown to increase expression of collagen types III, VI, VII and X, fibronectin, and proteoglycans (Massague, 1990). The net effect of these actions is an accumulation of ECM. Furthermore, TGF-β modulates the expression of integrins, the cell-surface receptors for ECM components facilitating cell adhesion and matrix deposition (Enenstein et al., 1992; Heino and Massague, 1989). TGF-β mainly acts on stellate cells to regulate increased ECM deposition in liver, particularly liver fibrosis.

Connective Tissue Growth Factor (CTGF)

The CCN Gene Family

The newly emerging CCN family was named after CTGF, cysteine-rich 61 (CYR61), and nephroblastoma overexpressed (NOV) proteins (Bork, 1993). This family also contains other three members including Elm1/WISP-1, Heparin-induced CCN-like protein/rCop-1/CTGF-3/WISP-2 and WISP-3. Orthologs of the CCN proteins have been found among vertebrates from *Xenopus* to human. CCN proteins are secreted, extracellular matrix associated. All members of this family exhibit a high degree of amino acid sequence homology (50-90%), possess a secretory signal peptide at their N terminus and contain some of the four distinct modules as shown in Figure 1-2. Domain I is homologous to the N-terminal cysteine-rich regions of the six "classic" insulin like growth factor (IGF)-binding proteins, IGFBP-1 to -6 (Bork, 1993), and contains a motif (GCGCCXXC) that is involved in binding IGF with low affinity (Kim et al., 1997). However, the physiological role of this binding to IGF still remains to be defined. Domain II comprises a Von Willebrand type C domain (VWC) that occurs in Von Willebrand factor as well as various mucins, thrombospondins, and collagens (Bork, 1993). It is proposed to be involved in oligomerization, which is common in many proteins carrying it. Domain III is a thrombospondin type 1 (TSP1) that contains the local motif WSXCSXXCG and appears to be a cell attachment motif that binds sulfated glycoconjugates (Holt et al., 1990; Rich et al., 1990; Guo et al., 1992). Domain IV is a C-terminal (CT) module that also occurs in the C termini of a variety of unrelated extracellular mosaic proteins including TGF β and PDGF and is responsible for dimerization and receptor-binding (Bork, 1993). Notably, WISP-2 doesn't contain

domain IV. Bioactive forms of CTGF lacking domain I and 2 or 1-3 and of NOV lacking domain I have been reported (Ball et al., 1998; Brigstock et al., 1997).

It was thought that CCN proteins act in a similar fashion to classic growth factors, but its unique specific high-affinity signaling receptors are not found. The binding of some CCN members to integrin leads to a current view of action of CCN proteins, in which CCN proteins may act as matricellular proteins that bridge the functional and physical gap between ECM-associated proteins and cell surface molecules (Chen et al., 2004; Leu et al., 2003; Schober et al., 2002; Grzeszkiewicz et al., 2002; Jedsadayanmata et al., 1999; Kireeva et al., 1998). Their integrin binding with the assistance of heparin-sulfate proteoglycan activates downstream signaling molecules such as focal adhesion kinases, MAPK p42/44 and Rac. The downstream signal transduction pathways modulate cell motility, migration, proliferation and even extracellular matrix production. In addition, CCN proteins interact with and regulate other signaling molecules including TGF-β, vascular endothelial growth factor (VEGF), Notch and voltage independent calcium channels (Abeu et al., 2002; Inoki et al., 2002; (Li et al., 2002; Sakamoto et al., 2002). However, the modular architecture of CCN proteins remains to be fully and functionally characterized in future.

The CCN members modulate cell growth by either direct mitogenic action or potentiating the mitogenic activity of other growth factors. CTGF and CYR61 are products of immediate early genes in response to mitogenic stimuli (Kireeva et al., 1996; Bradham et al., 1991). They are transcriptionally activated by TGF-β, PDGF, EGF, FGF, TPA and cholera toxin and promote cell growth. Conversely, NOV, WISP-1 and WISP-2 are the negative regulators of cell growth (Manzow et al., 1996; Fleming et al., 1997).

Members of the CCN family also regulate cell adhesion and migration. Elm1 is expressed in low metastatic cell lines. It slows the rate of tumor growth and decreases the incidence of metastasis when transfected into high-metastatic cell lines (Hashimoto et al., 1998). CYR61 mediates adhesion and promotes angiogenesis and tumor growth (Kireeva et al., 1996; Babic et al., 1999). CTGF are also chemotactic and promote cell adhesion as reviewed in later section (Babic et al., 1998).

TGF−β inducibility of CTGF and cyr61 gene expression promotes ECM deposition by stimulating synthesis of ECM components and inhibiting their degradation. CTGF stimulates fibronectin, type IV collagen and integrin production and regulates the composition of the ECM, the net balance between its synthesis and degradation (Frazier et al., 1996). CYR61 enhances type II collagen production in mouse limb bud mesenchymal cells (Wong et al., 1997). Members of CCN family are involved in diverse physiology and pathological processes and exert their function through net induction of ECM protein deposition and content.

Abnormal expression of the CCN proteins is associated to tumourgenesis. Cyr61 overexpressing in gastric adenocarcinoma cells gave rise to larger and more vascularised tumours than parental cells when injected into nude mice (Babic et al., 1998). Elevated levels of Cyr61, CTGF, and WISP-1 but not NOV were associated with more advanced features in primary human breast carcinomas. CCN proteins play a positive role in tumourigenesis by providing the stimulatory effects on cell growth that are required for the increased lifespan of tumor cells. By decreasing the adhesives of the cells and by providing an increased ability to migrate and invade surrounding tissues, the CCN proteins might be key factors participating to the metastatic potential of tumor cells. The

identification of CCN protein partners should be very helpful in establishing whether abnormal interactions with physiological targets are involved in these processes.

Taken together, the adhesive matricellular proteins of the CCN family represent a new class of signaling molecules and play a critical role in the regulation of cell proliferation, migration, differentiation and apoptosis. The production of abnormal levels of normal or altered CCN proteins might be associated to or involved in the initiation and establishment of pathological processes.

CTGF Gene, Protein and Its Binding Proteins

Connective tissue growth factor (CTGF) gene is located on chromosome 1p12 in rat, 6q23.1 in human and D10Mit86 in mouse. CTGF gene in these species is organized into five exons and four introns. This arrangement is consistent with evolutionary shuffling of exons that encoded individual modular regions. CTGF amino acid sequence is predicted to contain 343-349 residues among species. The first approximate 30 residues are presumptive signal peptides and the most diverse region in all domains of CTGF. The other part of CTGF protein is highly conserved among these species.

CTGF protein is a secreted, cystine-rich peptide. The molecular weight of CTGF is predicted to be 36-38 kilo Daltons. The N-terminal 37 amino acid signal sequence directs newly synthesized CTGF to the Golgi apparatus and facilitates the secretion of CTGF to outside of cells (Chen et al., 2001b). The presence of four potentially functional domains in CTGF raises fundamental questions about their contribution to the biological properties of the protein. The current known binding proteins to domains of CTGF are listed in Figure 1-3. Domain I of CTGF is homologous to IGFPBs and has a low affinity to IGF (Kim et al., 1997). Whether this binding represents a physiological event is not clear. Domain II is homologous to those of other ECM associated protein such as von

Willebrand. The region in the amino terminal Von Willebrand factor domain of CTGF interacts with TGF-β and facilitates the TGF-β presentation to the high-affinity TGF-β type II receptor (Abreu et al., 2002). CTGF overexpression in Xenopus can antagonize BMP4 signaling through the same motif (Abreu et al., 2002). Using the yeast two-hybrid system, Inoki et al (2002) found that the TSP-1 domain of CTGF binds to the exon 7-coded region of VEGF. The interaction can block the angiogensis activity of VEGF by preventing VEGF and VEGF receptor binding. It is believed that CTGF binding sequensters these growth factors from their receptors.

The thrombospondin-1 of CTGF interacts with integrin on cell surface in a heparin sulfate proteoglycan dependent way. This binding contribute to cell adhesion ability of CTGF promote cell adhesion. The subtype of bound integrin varies on different types of cells. For instance, integrin-α6β1 on human foreskin fibroblasts, integrin-αII β3 on human platelets, integrin-αvβ3 on endothelial cells and stellate cells and integrin-αMβ2 on blood monocytes mediate cell adhesion by CTGF (Gao and Brigstock, 2004; Babic et al., 1999; Jedsadayanmata et al., 1999; Chen et al., 2001; Schober et al., 2002).

Several reports have documented the presence of CTGFs with lower molecular weight in different cell types, tissues, and body fluids (Riser et al., 2000; Brigstock et al., 1997; Ball et al., 1998). These proteins vary from 10 to 20 kDa and constitute principally domain IV alone or domain III and IV. At least some of these isoforms appear to be biologically active in that they bind to heparin and is sufficient for cell adhesion and capable of promoting fibroblast growth (Brigstock et al., 1997). Heparin is the earliest molecule identified to physically interact with 38-kDa human CTGF and 10- to 20-kDa pig CTGF and modulate the biological activity of CTGF (Brigstock et al. 1997; Frazier et

al. 1996). Residues 247-260, 274-286, and 305-328 of human CTGF are required for the binding to heparin (Brigstock et al. 1997).

In addition, exogenous addition of ^{125}I-labeled CTGF binds the multiligand low-density lipoprotein receptor (LRP) through its carboxyl-terminal domain (Segarini et al., 2001). CTGF is internalized and degraded in the endosome through LRP (Chen et al., 2001). The multiligand receptor, low density lipoprotein receptor-related protein/$_2$-macroglobulin receptor (LRP) binds to CTGF and forms cell surface complexes. This pathway represents a rapid internalization and degradation of CTGF (Segarini et al. 2001). So far, it is still unknown if this pathway represents a pathway for CTGF signaling.

Actin and perlecan is another CTGF binding protein using immunoprecipitation assay (Yosimichi et al., 2002; Nishida et al., 2003). Perlecan, a basement-membrane heparan sulfate proteoglycan is predominantly localized in the prehyphetrophic zone in muse growth plate. This binding between perlecan and CTGF is believed to regulate the proliferation and differentiation of chondrocyts. However, the specific binding region in CTGF is not determined (Nishida et al., 2003).

Taken together, an increasing body of evidence now suggests that CTGF exerts its biological properties through interact with partners on cell surface or in ECM. Although cognate signaling receptor(s) for CTGF is/are still unknown, the four modules may work dependently and independently to interact with partners. Identification of CTGF interactors and receptors as well as its signal components is the future direction to elucidate the molecular mechanism of CTGF action during physiological and pathological conditions.

The Biological Activities of CTGF

CTGF mRNA has been detected in multiple organs in physiological and pathological conditions. It has been implicated in several normal physiological processes, including those related to embryo development and differentiation, endochondral ossification, and female reproductive tract function in the uterus and ovary. Upregulation of CTGF has been linked to many pathogeneses including fibrosis tumor desmoplasia, wound healing and tissue regeneration (Moussad and Brigstock, 2000).

The role of CTGF in development is well-demonstrated by CTGF knockout mice (Ivkovic et al., 2003). The transgenic embryo died shortly after birth due to respiratory failure caused by skeletal defects. Mutant embryo displayed abnormal ossification and incapability of inducing the expression of bone-specific matrix, such as aggrecan, and an impairment of angiogenesis in growth plates. Conversely, transgenic mice overexpressing CTGF under the control of the type XI collagen promoter show decreased bone density (Nakanishi et al., 2001). These observations indicate a crucial role of CTGF in the regulation of angiogenesis, chondrogenesis and ECM remodeling during development.

CTGF was initially found to be mitogenic and chemotatic to cells of connective tissues such as fibroblasts (Bradham et al., 1991) in tissue culture condition. To date, CTGF has been found to be produced by and act on a much broader repertoire of cell and tissue types than its name would suggest. The biological function of CTGF has been found to be diverse, complex and cell type specific. In vitro condition, dependent on target cell types, it can stimulate cell proliferation, cell adhesion, cell migration, ECM production and angiogenesis. On the other hand, CTGF can act as cell growth inhibitor

and induce apoptosis. In some cases, it is intrinsically nonmitogenic but to augment the activity of other growth factors (Moussad and Brigstock, 2000).

Some signal pathways that are activated after CTGF stimulation have been reported. Chondrocyte differentiation induced by CTGF is believed through a p38 mitogen-activated protein kinase (p38MAPK) while chondrocyte proliferation is through a p44/42 MAPK/extracellular-signal regulated kinase (ERK) (Yosimichi et al., 2001). Exogenous CTGF induced fibronectin production, cell migration, and cytoskeletal rearrangement in primary mesangial cells. These functional responses were associated with recruitment of Src and phosphorylation of p42/44 MAPK and protein kinase B. Fibronectin induction required CTGF-induced p42/44 MAPK or phosphatidylinositol 3-kinase (PI3K)/protein kinase B pathway. Beta (3) integrin is involved in the regulation of fibronection induction and mesangial cell migration but not on transient actin cytoskeletal disassembly (Crean et al., 2002).

CTGF Mediates Downstream Fibrogenic Actions of TGF-β

There are several evidences to support the notion that CTGF is a downstream molecule mediating fibrotic action of TGF-β. At first, TGF-β is the most potent inducer of CTGF expression while other growth factors such as PDGF, EGF, and FGF only induce transient expression of CTGF (Igarashi et a., 1993). CTGF mRNA is specifically induced to significant levels by TGF-ß1 stimulation (Igarashi et al, 1993; Soma and Grotendorst, 1989). In activated scleroderma fibroblast, TGF-β initiated-CTGF upregulation persists even though the expression of TGF-β declines. This rapid and strong response to TGF-β stimulation is due to the existence of cis-elements in CTGF promoter. More detailed studies of TGF-β regulation of CTGF has been investigated

using fibroblast systems. TEF and Smad elements are essential for TGF-β induction of CTGF in normal fibroblasts (Holmes et al., 2001; Leask et al., 2001; Leask et al., 2002). The TGF β response element (TGFβRE, also called BCE-1, basal control element 1) in the CTGF promoter sequence controls the basal expression of fibroblast and increased constitutive CTGF expression in scleroderma fibroblasts (Grotendorst et al., 1996; Holmes et al., 2001). A functional Sp1 element also contributes to constitutive expression of CTGF in scleroderma fibroblasts in TGF-β independent manner (Holmes et al., 2003).

CTGF was noted to have mitogenic and chemotactic effects on fibroblasts (Braham et al., 1991). CTGF was also reported to enhance the mRNA expression of α1 (I) collagen, fibronectin, α5 integrin in fibroblasts (Frazier et al., 1996; Fan et al., 2000). These data suggest that CTGF may be a downstream mediator of TGF-ß1, specifically involved in the regulation of ECM proteins and promotion of fibroblast growth.

Given that CTGF signaling pathway remains unknown, there are two possible ways of CTGF functions as a downstream mediator of TGF-β. One is that CTGF itself may result in a prolonged induction of expression of ECM components. Alternately, CTGF may bind to TGF-β and potentiate TGF-β binding to the TGF-β type II receptors because it has been known that CTGF can bind to TGF-β in vitro. This binding contributes to the effects of TGF-β on cells by promoting the activation of Smads.

The Regulation of CTGF Gene Expression

CTGF was discovered in 1991 in the conditioned medium of human umbilical vein endothelial cells (HUVEC). Since then, CTGF expression has been found to be induced by many stimuli in cell type specific manner. The positive regulators of CTGF in endothelial cells and vascular smooth muscle cells include vascular endothelial growth

factor (Wunderlich et al., 2000; Suzuma et al., 2000), epidermal growth factor, fibroblast growth factor (Wunderlich et al., 2000), plasma clotting factor VIIa (Pendurthi et al., 2000; Camerer et al., 2000) and thrombin (Chambers et al., 2000). Bone morphologic protein 2 (BMP2) can induce CTGF expression in chondrocytes (Nakanishi et al., 1997). CTGF is also induced by lysophosphatidic acid and serotinin activation of heptahelical receptors in renal mesangial cells (Hahn et al., 2000). H_2O_2 stimulates CTGF transcription in retinal epithelial cells. Other positive regulators also include hypoxia for human breast cancer lines and vascular smooth muscle cells (Shimo et al., 2001; Paradis et al., 2001). glucose and insulin were found to upregulate CTGF expression in human Nonalcoholic steatohepatitis (Paradis et al., 2001). Among all positive regulators, TGF-β is the most potent regulator of CTGF to nearly all of cell type and will be discussed in detail in above section. In addition, physical effectors such as tension cyclic stretch, static pressure and shear forces induce transcription of CTGF (Schild and Trueb, 2002; Kessler et al., 2001; Hishikawa et al., 2001).

The negative regulators of CTGF include tumor necrosis factor-α and the Wilms tumor suppressor WT1 in scleroderma fibroblast, wilms tumor cell line, mesangial cells (Stanhope-Baker and Williams, 2000; Abraham et al., 2000; Hahn et al., 2000). IL-4 attenuated TGF-β induced CTGF expression in lung fibroblast (Rishikof et al., 2002). Prostaglandins and prostacyclins reduce steady-state CTGF mRNA levels through increasing adenylate cyclase activity and the high level of cAMP, which is known to inhibit CTGF expression in a protein kinase A dependent manner (Ricupero et al., 1999; Stratton et al., 2002; Stratton et al., 2001). The synthetic prostacyclin, Iloprost blocks CTGF expression in vivo and in vitro alleviates fibrosis in human and animal studies.

Besides cis-elements identified from fibroblast upon TGF-β stimulation, some other regulatory elements responsible for the differential expression of CTGF under a variety of biological conditions have been identified. Two cis acting regulatory elements in the CTGF gene appear to be important for expression in chondrocyte. One is the transcriptional enhancer dominant in chondrocyte (TRENDIC), which is located in the promoter region and appears to bind certain nuclear transcription factors in a chrondroctye specific manner (Eguchi et al., 2002). The other is a cis acting element for structure anchored repression (CAESAR) in the 3' untranslated region (Kubota et al., 2000). CAESAR appears to repress CTGF gene expression by affecting mRNA translation efficiency. In addition, a stretch-responsive element (GAGACC) in the promoter of CTGF may be involved in direct regulation of CTGF expression in mechanical stress.

The signaling molecules required for TGF-b-induced CTGF synthesis have been identified. Ras/MEK/ERK, c-jun NH2 terminal kinase (JNK), p38 MAP kinase and protein kinase C have been reported to be required for CTGF expression in fibroblasts (Stratton et al., 2002; Chowdhury and Chaqour, 2004; Chen et al., 2002; Utsugi et al., 2003). Activation of RhoA signaling is associated with CTGF gene expression triggered by either TGF-β or LPA. The microtubule disrupting agents, nocodazole and colchicine strongly up-regulate CTGF expression, but these activities are prevented upon stabilization of the microtubules by paclitaxel. Colchicine mediated disruption of the microtubular system was associated with the activation of RhoA, suggesting that RhoA is a molecular switch that translates changes in cell morphology into the expression of CTGF (Heusinger-Ribeiro et al., 2001).

CTGF and Liver Remodeling

In livers, CTGF is normally expressed in a very low level, except for a local upregulation in portal and central vein endothelia and in myocytes of portal arteries (Sedlaczek et al., 2001). However, a significant induction of CTGF transcripts has been found in liver injury and pathogenesis including liver fibrosis in animal models and in human chronic liver diseases (Ujike et al., 2000; Paradis et al., 1999). Activated stellate cells are found to be a major cellular source of CTGF in fibrotic and CCl_4-injuried rat livers. When added in primary stellate cell cultures, CTGF strongly promote stellate cell proliferation, migration and produce collagen type I (Paradis et al., 2002). CTGF stimulates c-fos gene activation and expression via phosphorylation of ERK1/2 in stellate cell (Gao et al., 2004).

Besides stellate cells, CTGF has been found to be expressed in other hepatic cells. Proliferating epithelial cells in bile duct are another source of CTGF mRNA by studying the temporal and spatial expression of CTGF in rats with acute and chronic hepatic fibrogenesis (Sedlaczek et al., 2001). In biliary atresia, CTGF is strongly expressed in stellate cells and hepatocytes and may play a major role in the pathogenesis of progressive fibrosis in this disease (Kobayashi et al., 2005). In hepatic fibrosis, CTGF is expressed in endothelial cells, epithelial cells, stellate cells and hepatocytes (Rachfal and Brigstock, 2003). However, the effect of CTGF in proliferating epithelial cells and other types of liver cells are still unknown. The role of upregulated CTGF in liver injury and fibrosis needs to be studied at a molecular level to ascertain its function.

Study Design and Rationale

Oval cell activation, as part of a process of the progenitor dependent liver regeneration must be an orchestrated response induced by specific external stimuli and

involves sequential changes in gene expression, growth factor production and morphological changes. However, little has been known about the molecular mechanism underlying oval cell activation. To elucidate the mechanism underlying oval cell activation, we first attempted to isolate genes differentially expressed in oval cells using suppression subtractive hybridization. It turned out that CTGF was identified as one of differentially expressed genes in Thy-1^+ oval cells. The overall hypothesis in this project was that CTGF plays an important role in oval cell-mediated liver regeneration. To test this hypothesis, CTGF mRNA and protein were first examined to verify the induction during the time course of oval cell mediated liver regeneration. The temporal patterns of TGF β, procollagen type I and fibronectin are investigated to compare that of CTGF. Cell types expressing CTGF were also studied to determine the source of CTGF. To determine the role of CTGF in vivo, Iloprost, an inhibitor of CTGF synthesis was adminstrated to animal undergone 2-AAF/PHx, and the effects of Iloprost on CTGF induction and on oval cell activation were examined. For more specific inhibition of CTGF, recombinant adenovirus was generated to express siRNA of two individual CTGF fragments. The efficiency of inhibition on CTGF synthesis was tested in tissue culture before the future experiment in animals.

The last aspect of the project is based on the fact that CTGF, the 38 kDalton secretory matricellular protein, must exert its biological actions through interacting with other molecules. To understand how CTGF is involved in oval cell mediated liver regeneration, a yeast two-hybrid cDNA library was constructed and screened using CTGF constaining different modules as a bait. This library, so far, to our knowledge, is the first yeast two hybrid cDNA library specific for oval cell mediated liver regeneration.

The identification of these interactors using the yeast two-hybrid approach would provide us insights on the molecular mechanism of CTGF in liver regeneration.

In summary, the general goal of this dissertation is to understand the molecular mechanism of oval cell mediated liver regeneration and the role of CTGF in regulating this process. These knowledge would broaden our understanding about the function of CTGF on tissue modeling, especially in oval cell mediated liver regeneration. Given that CTGF is a pathological factor during diverse tissue fibrosis, the better we understand the molecular mechanism of CTGF, the higher the chance will be for us to develop a therapeutic strategy for fibrotic disorders.

Table 1-1. Markers for several types of liver cells (Miyagawa et al. 2002; Buniatian et al. 1996; Thorgeirsson. 1996). + represents expression of the markers while – stands for no expression of markers in these liver cells.

Markers	oval cells	Hepatocytes	bile duct cells	Ito cells	endothelial cells
CK7	-	-	+	-	-
CK8	+	+	+	-	-
CK18	+	+	+	-	-
CK19	+	-	+	-	-
ALB	+/-	+	-	-	-
AFP	+	-	-	-	-
GGT	+	-	+	-	-
OV-6	+	-	+	-	-
OV-1	+	-	+	-	-
BDS7	+	-	+	-	-
BD1	-	-	+	-	-
HES6	-	+	-	-	-
OC.2	+	-	+	-	-
OC.3	+	-	+	-	-
H.1	-	+	-	-	-
HBD.1	-	+	+	-	-
A6	+	-	+	-	-
Desmin	-	-	-	+	-
GFAP	-	-	-	+	-
SE1	-	-	-	-	+

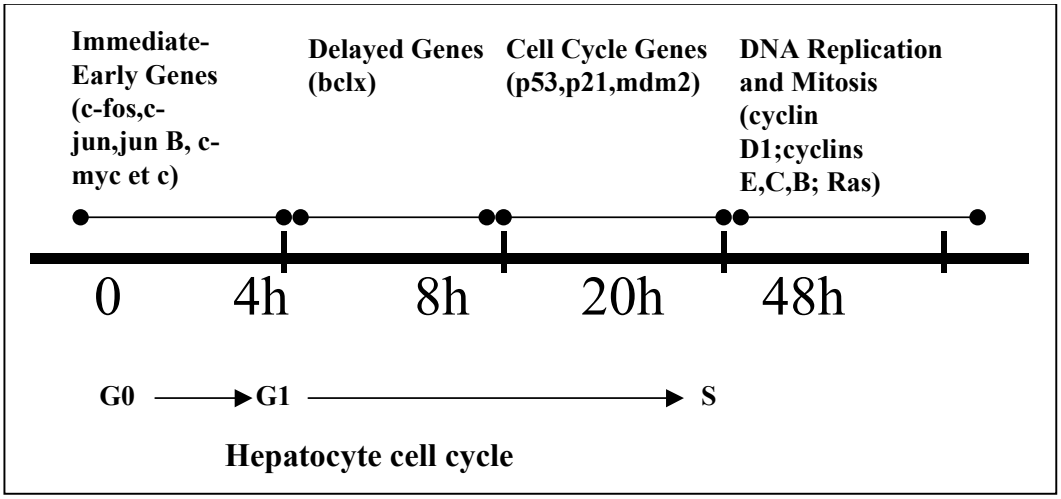

Figure 1-1. Sequence of gene activation in the regenerating liver after partial hepatectomy (Fausto, 2000).

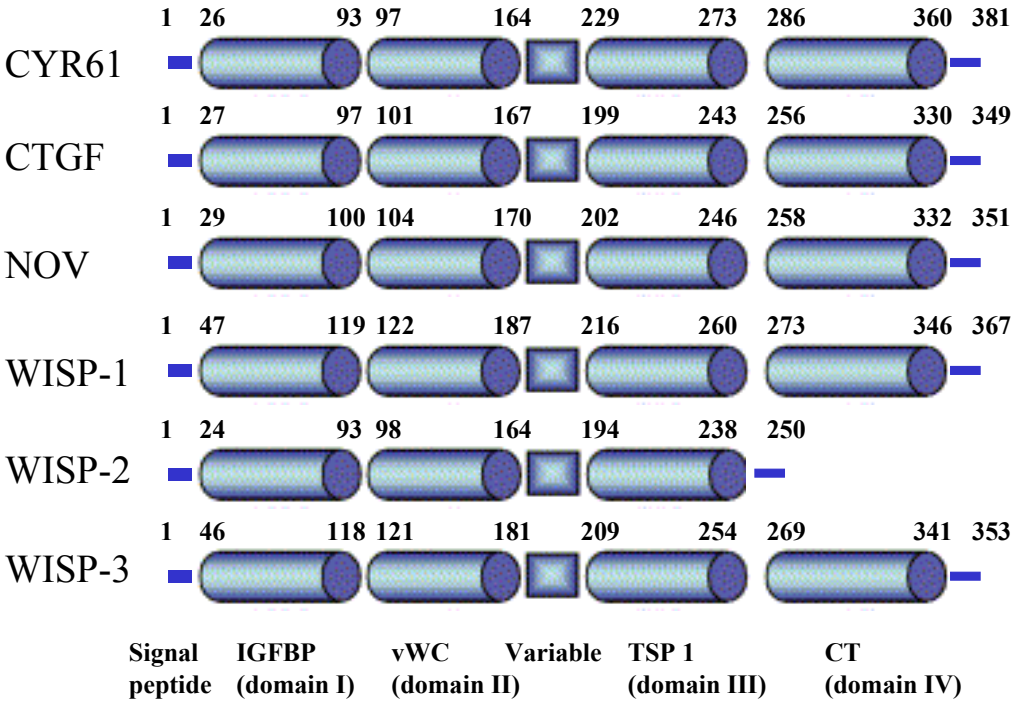

Figure 1-2. Structural organization of the CCN family. Residues are numbered according to the human orthologs of each protein. WISP-2 lacks domain IV. There are 25- to 30- residue signal peptide sequences preceding domain I in each protein.

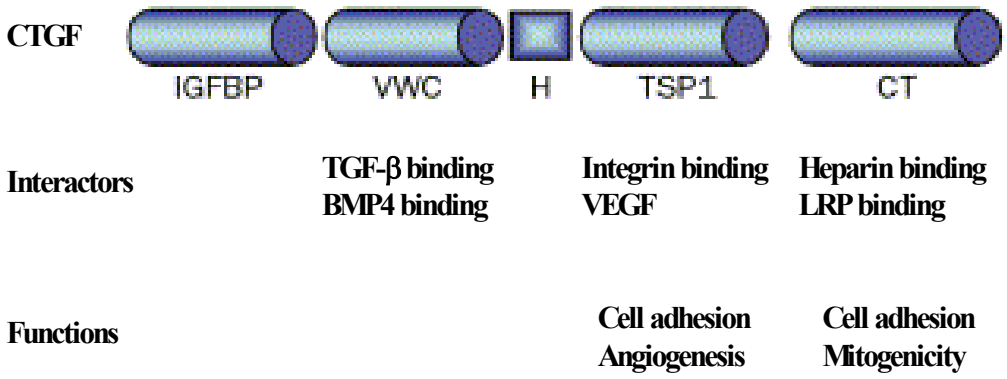

Figure 1-3. Known binding proteins of CTGF. Perlacan and actin were not in the diagram because CTGF binding regions arenot identified. VWC domain binds to both TGF-β and BMP4. TSP1 domain binds to integrin and VEGF. CT domain binds to heparin and LRP.

CHAPTER 2
GENERAL METHODS

Experimental Animals

Male Fischer 344 rats (120–150 g) were used for all experiments. All rats were housed in pairs in air-conditioned rooms with a temperature between 22-25° C. Animals were received constant food and water with 14 hours of lights per day. Before sacrifice, rats were euthanized with intraperitoneal injection of pentobarbital (Beuthanasia-D Special). All animal protocols were approved by the Institutional Animal Care and Use Committee (IACUC) at the University of Florida.

Oval Cell Induction by 2-AAF/PHx

2-Acetylaminofluorene (2-AAF) is metabolized through a cytochromP450 pathway in hepatocytes. Three main metabolites of 2-AAF in phase I include N-hydrooxy-AF, a sulfate esters and an O-glucuronide. All of them are mutagenic and carcinogenic compounds. 2-AAF in conjunction with hepatic injury can activate the hepatic oval cell compartment (Evarts et al., 1989). It is believed that inhibition of hepatocyte proliferation by 2-AAF is a necessary step for oval cell activation in the liver. Two third of partial hepatectomy is performed at day 5-7 after the implantation of 2-AAF to induce liver regeneration. The operation of PHx consist of the removal of the median and left lateral lobes, also referred to as anterior lobes, leaving intact the right lateral and caudate lobes (posterior lobes). All time points indicate days after PHx.

Sample Collection

Animals were sacrificed at appropriate time points and livers were cut into 1-2 cm slices. Some of them were snap frozen in liquid nitrogen and stored at -80° C for protein or RNA isolation. Some of them were buried into OCT and frozen. The rest of them were soaked in formalin and embedded later in paraffin blocks.

Tissue Sectioning and Processing

For in situ hybridization, livers were perfused with 4% paraformaldehyde and 0.05% glutaraldehyde according to a previously published method. Liver slice tissues were soaked in 30% sucrose before frozen in OCT and stored at -80^{o}C. Cryo-sections, 6 μm thick, were cut at –20^{o}C and dried overnight at 40^{o}C prior to analysis.

For paraffin blocks, 6um thick sections were cut with a microtome. Tissue sections were deparaffinized by two incubations in xylene for ten minutes, hydrated through absolute alcohol, 95% alcohol, 75% alcohol and 50% alcohol for 5 minutes at each step followed by a 1 minute wash in distilled water. Endogenous peroxidase activity was quenched by incubation with 0.3% H_2O_2 for 10 minutes at room temperature.

Immunohistochemical localization was then achieved through affinity-purified primary and secondary antibodies followed by the appropriate detection reagents.

Microscopy

Tissue sections mounted on glass slides were photographed using either bright field illumination or fluorescence microscopy with excitation/emission wavelengths for Texas Red and FITC staining. Photographs were taken at a constant exposure using a Peltier-cooled Olympus digital camera. Cell cultures fixed with paraformaldehyde or methanol on glass slides were photographed in a similar fashion, using an inverted-phase microscope using either bright field illumination or fluorescence microscopy with

excitation/emission wavelengths for Texas Red and FITC staining. Images were acquired using an Olym software.

CHAPTER 3
ISOLATION OF GENES DIFFERENTIALLY EXPRESSED IN HEPATIC OVAL CELLS BY SUPPRESSION SUBTRACTIVE HYBRIDIZATION

Introduction

Liver regeneration involves waves of liver cell proliferation, migration and differentiation mediated by a complex mixture of cytokines and chemokines to restore liver mass and function (Michalopoulos and DeFrances, 1997). When hepatocyte proliferation is suppressed by some hepatotoxin agents, a distinct progenitor cell, called the oval cell, is recruited to aid in liver regeneration (Evarts et al., 1989; Golding et al., 1995). This phenomenon is well demonstrated by the modified Solt-Farber liver injury model, in which, AAF administration combined with PHx triggers oval cell activation and proliferation in the periportal region of the liver lobule. AAF-induced oval cells originate from within the biliary ductular epithelia and are characterized by expression of phenotypic markers such as AFP, CK19 and Thy-1 surface antigen (Shiojiri et al., 1991; Petersen et al., 1998).

A number of cell types comprised of parenchymal hepatocytes as well as nonparachymal bile duct, stellate, endothelial, and Kupper cells may be involved in generating the oval cell response. We are interested in genes induced in oval cells by comparing to all of the NPC population from normal animals. The identification of these genes in oval cells could give a clue about the mechanism of oval cell activation.

Bisgaard (1999) used suppression subtractive hybridization to clone genes from NPC fraction of regenerating liver after a 70% PHx combined with the treatment of 2-

AAF. The NPC fraction containing oval cells were purified by centrifugation through a two-step Percoll gradient. This conventional isolation method enriches oval cells to as purity as high as around 80%. And the isolated cells are mixed populations of oval cells, stellate cells, endothelial cells and Kupffer cells. Basically, the authors attempt to identify genes differentially expressed in NPC fractions in regenerating livers in comparing to those of NPC fractions in normal livers. The identified genes are interferon-r receptor a subunit (IFN-γRα), gp91phox, interleukin-1β (IL-1β), lymphocyte function-associated molecule-1α (LFA-α), eukaryotic initiation factor-2-associated 67-kD protein (eIF-2-associated 67kD protein) and α-fetoprotein. Further characterizations indicate that the subunits of the IFN-γ receptor complex, IFN-γRα and IFN-γRβ, the secondary response genes uPAR and ICAM-1, the IFN-γ-inducing factor IL-18 and ICE are induced and expressed in ductular oval cells (Bisgaard et al., 1999). These results indicate that IFN-γ-mediated events are important in oval cell mediated liver regeneration triggered by 2-AAF/PHx. However, the tester population in these studies is mixed, heterogeneous nonparenchymal population in regenerating livers, rather a pure oval cell population.

We have developed a reliable method to enrich a relatively pure rat oval cell population (up to 93% purity) from the nonparenchymal cell fractions (NPC) by fluorescent activated cell sorting (FACS) based on the finding that oval cells express the cell surface marker Thy1 (Petersen et al. 1998). These $Thy1^+$ cells have been shown to express traditional oval cells markers such as α-fetal protein (AFP), cytokine 19 (CK-19), γ-glutamyltransferase (GGT) and OV6. Furthermore, these cells are not stellate cells as indicated by negatively desmin staining (Petersen et al. 1998). $Thy\text{-}1^+$ oval cells sorted by FACS represent a relatively pure population and provide a basis for us to identify genes

specifically expressed in them. In this chapter, suppression subtractive hybridization (SSH) was used to identify genes that are differentially expressed in the Thy1+ oval cells by comparing to NPC isolated from normal rat livers.

Materials and Methods

Thy-1$^+$ Oval Cell Isolation by FACS Analysis

Livers from AAF/PHx treated animals were perfused at day 7-11 post PHx by following a 2-step collagenase digestion. Hepatocytes were roughly removed by low centrifugation (50xg) and NPC populations containing oval cells were collected at higher speed (100xg). 80 millions of resuspended NPC cells were stained with fluorescein iosthiocyanate (FITC)-conjugated anti-rat Thy1 (1mg/1million cells). Thy1$^+$ and Thy1$^-$ populations were sorted using a Becton Dickinson FACStar flow cytometer.

RNA Isolation

The pools of sorted Thy-1$^+$ oval cells were isolated from 20 livers of 9-11 days post 2-AAF/PHx. NPCs were isolated from 3 normal rat livers. Total RNA and polyA RNA from both populations were isolated using RNEasy kit (QIAGEN, Chatsworth, CA, USA) and Poly(A)Purist™ mRNA Purification Kit (Ambion, Austin, TX, USA) according to the manufacturer's instructions.

Suppression Subtractive Hybridization (SSH)

A suppression subtractive hybridization (SSH) library was generated from Thy-1$^+$ oval cells and nonparenchymal cells (NPCs) as tester and driver population, respectively. The SSH was performed with the Clontech PCR-Select cDNA Subtraction Kit (Clontech Laboratories Inc., Palo Alto, CA) according to the manufacturer's instructions. Figure 3-1 shows sequences of the PCR-select cDNA synthesis primers, adaptors and PCR primers used in SSH. Briefly, samples of poly(A)$^+$ RNA were reverse-transcribed to cDNA. The

cDNA synthesized from oval cells was therefore used as tester cDNA and cDNA generated from control NPC mRNA as driver cDNA. The tester and driver cDNA were digested with RsaI and the tester cDNA ligated to the adapter DNA. After two repeated hybridizations of tester and driver cDNA, remaining unhybrideized sequences (representing cDNAs expressed highly in the tester sample) were amplified by polymerase chain reaction (PCR) using flanking and nested primers that anneal the adaptor cDNA. The subtracted PCR products ligated into pCR4 TOPO vector (TA Cloning kit, Invitrogen). The identity of the cDNA inserts was revealed by sequence analysis of purified plasmids and compared to known DNA sequences using the BLAST algorithm.

Northern Analysis

In Northern analysis, groups consisted of three animals each and were tested at time points 0, 3, 5, 7, 9, 11 and 13 day post PHx. Total RNA was prepared from snap-frozen liver tissues using RNAstat Reagent (Tel-Test Inc., Friendswood, TX). Total pooled RNA (approximately 20 μg) was used for Northern analysis. The clones of rat CTGF, fibronectin and proteoglycan peptide core protein gene obtained from cDNA library were used as a probe. Probes for TGF-β1 and pro-collagen type I were generated by PCR using published primers sequences (Chen et al., 2000). Hybridization was performed with [^{32}P]-dCTP labeled probes (Amersham Life Science; Piscataway, NJ) at 42^{o}C in 50% formamide, 5x SSPE, 5x Denhart, 2% SDS and 10% dextran sulfate.

Results

FACS Analysis Enriches a Relatively Pure Thy-1^{+} Oval Cell Population.

Thy-1 surface antigen has been found mainly in the hematopoietic system. Consistent with previous finding, very few Thy-1^{+} cells were observed in normal liver

(Figure 3-2A). At day 0 post PHx no increase in Thy-1$^+$ cells was seen (Data not shown), indicating that 2-AAF alone had no effect on Thy-1 antigen expression. By day 3 following PHx, an increase in Thy-1$^+$ cells was seen in the periportal region. By day 7-9 after PHx, a very robust Thy-1$^+$ cell response had developed (Figure 3-2B). Using FACS analysis, we were able to enrich the Thy-1$^+$ cell population to a purity of 95-97%. This enriched cell population was used in suppression subtractive hybridization studies to identify genes that are differentially expressed in Thy-1$^+$ oval cells as compared to normal nonparenchymal cells. Figure 3-3 shows FACS analysis of Thy1$^+$ cells before, during and after cell sorting. Green line represents unsorted NPC populations stained with Thy1$^+$. These populations comprise all of nonparenchymal cells including oval cells, bile duct, stellate, Kupffer and endothelial cells. Only a few percentages of cells are positive for Thy1 staining in the total NPC populations. Left side of purple line is the minimal gated fluorescent region chosen for sorting and blue line represents collected sorted cells. This distinct peak of blue line suggests a significant enrichment of Thy1$^+$ cells. The purity of Thy1$^+$ cells after sorting could reach to as high as 93%. 95% of these cells were viable based on trypan blue exclusion. These Thy1$^+$ cells have been shown to express traditional oval cells markers such as the traditional oval cell markers of α-fetal protein (AFP), cytokine 19 (CK-19), γ-glutamyltransferase (GGT) and OV6. Furthermore, these cells are not stellate cells indicated by negatively desmin staining (Petersen et al., 1998).

Identification of Genes Differentially Expressed in Thy-1$^+$ Oval Cells

We employed subtractive suppression hybridization (SSH) to identify the differentially expressed genes in Thy-1$^+$ oval cells. Poly +A RNA with the size of these

mRNA ranging from 4kb to 0.5kb was isolated from normal NPCs (called driver) and sorted Thy-1^+ oval cells (called tester). After double-stranded cDNA synthesis, the ds cDNAs were digested with RsaI restriction enzyme into small fragment (less than 300bp) and ligated with adaptor1 and adaptor2R. To monitor the ligation efficiency, a human skeletal muscle mRNA containing glyceraldehyde-3-phosphate dehydrogenase gene (GAPDH) was used as a control and the ligation efficiency of both adaptors was around 25%. Then the ligation products were subjected to the first and second hybridizations with excessive driver cDNA, which were not ligated with the adapters. The primary and secondary PCR were conducted and only cDNA with different adapters at their ends can be amplified exponentially. The products generated after secondary PCR reaction appeared to be a smear, typical products as the manual mentioned. These products were then cloned into the pCR4. TOPO vector and transformed into bacterial competent cells. SSH plasmids were digested with EcoR I restriction enzymes to check the presence and the size of cDNA inserts before sequencing analysis.

Table3-1 lists the top hit in Blast searches using the sequences of SSH clones as queries. Three of them, P31, P35 and P24, which encode CTGF, fibronectin and proteoglycan peptide respectively, were of our interest and were characterized further by Northern analysis.

The Induction Patterns of CTGF, Fibronectin and Proteoglycan Peptide Core Protein in Northern Analyses

To confirm if the genes cloned by SSH were modulated when oval cells were activated and recruited for liver regeneration, we performed a Northern blot analysis with whole liver total RNA extracts derived from a time course experiment with the AAF/PHx protocol using the isolated *CTGF* 3'UTR cDNA as probes. AAF/PHx treated animals

were sacrificed 1, 3, 5, 7, 9, 11, 13 and 15 days after PHx. Since the expansion and infiltration of the oval cell population into liver parenchyma start at day 3, reach to a maximum at day7-11 and the differentiation into basophilic hepatocyte occurs after 10-11 days post PHx, the selected time points should cover most of oval cell activation process and the early stage of oval cell differentiation in liver parenchyma region. In Figure 3-4, the Northern blot analysis shows that *CTGF* induction appears gradually from day 5 to day11 and reaches to the maximum at day 9. After that, the expression of this gene drop back to the normal level. The most steady-state levels of transcripts are detected at day 9 after partial hepatectomy, a time when the number of oval cells peaked. This result indicates that the steady-state RNA levels of CTGF increases in a manner consistent with activation of oval cells by AAF/PHx.

In Figure 3-5, we also examined fibronectin expression during the time course of oval cell activation. In normal liver, there was some endogenous level of expression while the expression was highly upregulated at the peak of oval cell proliferation at day 9. The total induction pattern of fibronectin was quite similar to that of CTGF, supporting that CTGF regulates and potentiates the expression of fibronectin.

Proteoglycan core peptide (*pgcp*) expression was not detectable in the total liver homogenates in normal liver and regenerating livers treated with 2-AAF/PHx (Figure 3-6). Interestingly, 1.5kb *pgp* was highly expressed in Thy-1^+ oval cells, indicating it is specifically present in oval cells.

Coordinated Expression of TGF-β1 and Pro-collagen Type I during Oval Cell Aided Liver Regeneration

It has been established that CTGF is a downstream mediator of the fibrogenic properties of TGF-β1, stimulating the expression of ECM genes in many biological

processes. Here, we performed a Northern blot analysis to compare the CTGF induction pattern with those of TGF-β1 and procollagen type I. TGF-β1 was induced at day 3 (Figure 3-7), just prior to CTGF induction. The level of TGF-β1 was maximal at day 9 and decreased there after. This pattern is consistent with the notion that TGF-β1 stimulates the transcription of CTGF following 2-AAF/PHx.

CTGF can induce extracellular matrix (ECM) genes. Pro-collagen type I and fibronectin were found to be upregulated following 2-AAF/PHx, reaching maximal expression at day 7 and 9 (Figure 3-5 and 3-7). This coincides with the induction of CTGF. These results support the hypothesis that CTGF is induced through the TGF-β1-mediated signaling pathway, which ultimately leads to the synthesis of ECM during liver regeneration.

Discussion

Oval cell mediated liver regeneration involves the secretion of a complex mixture of cytokines and growth factors to regulate the proliferation and expansion of oval cells. However, the molecular mechanism underlying this process is not fully understood. The present study utilized SSH technique to identify some candidate genes from a cDNA library enriched for genes expressed in Thy-1^+ oval cells (Table 3-1). Consistent with previous findings that CTGF is involved in tissue regeneration and remodeling, we detected a significant upregulation of CTGF mRNA during the regeneration process of rat liver following 2-AAF/PHx treatment (Figure 3-4B). The induction of CTGF occurs from day 5 to day 15 post PHx with a peak at day 9. Compared to CTGF expression during liver regeneration in rats following 70% PHx or D-galactosamine (GalN) exposure, the expression of CTGF in our liver injury model is prolonged (Ujike et al.,

2000). The sustained expression of CTGF may represent a critical component in the activation of oval cells, most likely through the TGF-β1 pathway.

Fibronectin is also a candidate gene identified in SSH. Northern analysis in Figure 3-5B verified its upregulation in the 2-AAF/PHx model. The pattern of induction of fibronectin is quite similar to that of CTGF except that it has a detectable basal level of expression. This result is consistent with the facts that fibronectin expression is induced by CTGF during oval cell mediated liver regeneration.

pgcp is another candidate identified from SSH. Interestingly, we barely detected *pgcp* expression in total liver homogenate but a strong expression of this gene was specifically present in Thy-1^+ oval cells. The biological relevance of *pgp* is unknown. If the other types of hepatic cells involved in oval cell mediated liver regeneration are not expressed it or express it in a low level, we may use it as a marker specific for oval cells.

It is known that TGF-β1 is one of the most potent inducers of CTGF, and promotes CTGF expression in fibroblasts through a complex network of transcriptional interactions requiring Smads, protein kinase C and Ras/MEK/ERK and a consensus transcriptional enhancer factor (TEF) binding element in the CTGF promoter (Leask A, 2003). Consistent with previous findings (Grisham J.W, Thorgeirsson S.S. 1997), the level of TGF-β1 mRNA is increased following 2-AAF/PHx (Figure 3-6). Both TGF-β1 and CTGF show a similar expression pattern with the exception of an earlier induction in TGF-β1 expression. The earlier induction of TGF-β1 supports the hypothesis that TGF-β1 stimulates CTGF following 2-AAF/PHx treatment. In contrast, the other ECM protein, procollagen type I is constitutively expressed during the course of oval cell aided

liver regeneration (Figure 3-7). This result is consistent with the notion that CTGF stimulates the expression of ECM proteins, at least in stellate cells.

In summary, we successfully identified several genes differentially expressed in sorted $Thy1^+$ oval cells. One of candidate gene, CTGF, is involved in tissue remodeling and regeneration process to regulate the production of ECM proteins but its role in oval cell mediated liver regeneration is not known. Therefore, the subsequent chapters in this dissertation focus on exploring the function of CTGF in the 2-AAF/PHx model.

cDNA synthesis primer

5’ –TTTTGTAC AAGCTT$_{30}$N$_{31}$N-3’
*Rsa*I *Hind*III

Adaptor1
*Not*I ***SrfI/SmaI*** *Rsa*I½-site
5’-CTAATACGACTCACTATAGGGCTCGAGCGGCCGCCCGGGCAGGT-3’
T7 Promoter 3’-GGCCCGTCCA-5’

Adaptor 2R
*Eag*I/*Eae*I *Rsa*I½-site
5’-CTAATACGACTCACTATAGGGCAGCGTGGTCGCGGCCGAGGT-3’
T7 Promoter 3’-GCCGGCTCCA-5’

PCR primer 1 5’-CTAATACGACTCACTATAGGGC-3’
T7 Promoter

Nested primer 1 5’-TCGAGCGGCCGCCCGGGCAGGT-3’
*Not*I ***SrfI/SmaI*** *Rsa*I½-site

Nested primer 2R 5-AGCGTGGTCGCGGCCGAGGT’-3’
*Eag*I/*Eae*I *Rsa*I½-site

Control Primers:

G3PDH 5’ primer 5’-ACCACAGTCCATGCCATCAC -3’
G3PDH 5’ primer 5’- TCCACCACCCTGTTGCTGTA-3’

Sequencing primers:
M13 reverse primer 5’-CAGGAAACAGCTATGAC-3’
M14 forward primer 5’- GTAAAACGACGGCCAG-3’

Figure 3-1. Sequences of the PCR-select cDNA synthesis primer, adaptors and PCR primers used in SSH. The ends of PCR-Select cDNA adaptors (1 and 2R) contain 20 nucleotides which are complementary. The formation of a pan-like secondary sequence suppresses undesirable amplification when an ss cDNA contains the same adaptors at its both ends during PCR with nested primer 1 and 2R. Only specific amplification of cDNA molecules with different adaptors at both ends can efficiently occur.

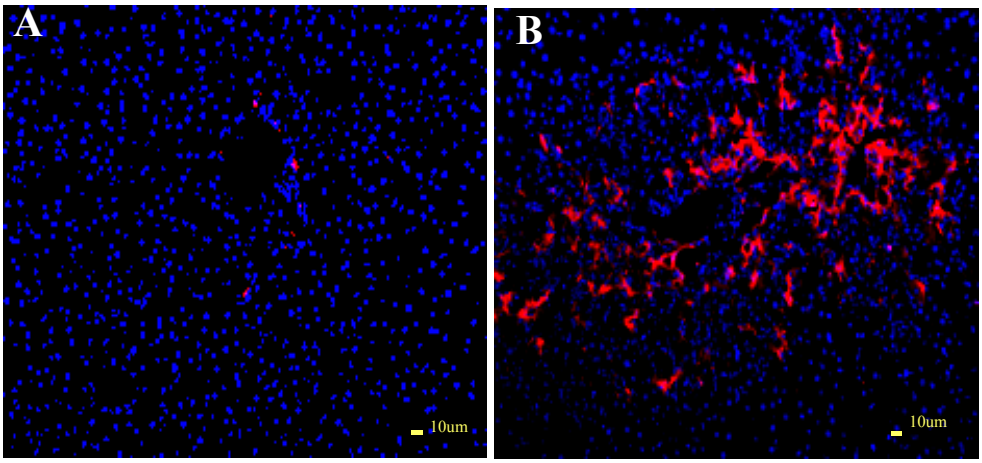

Figure 3-2. Massive proliferation of Thy-1^{+} oval cells in portal region during liver regeneration following 2-AAF/PHx. Frozen liver sections were examined by immunohistochemistry for Thy-1 antigen. Blue color indicates DAPI stained DNA while red indicates Texas red signal for Thy-1 antigen. (A) Normal. (B) 2-AAF/PHx treated liver (day 9). Both images were taken at 200X. Scale bar: 10um.

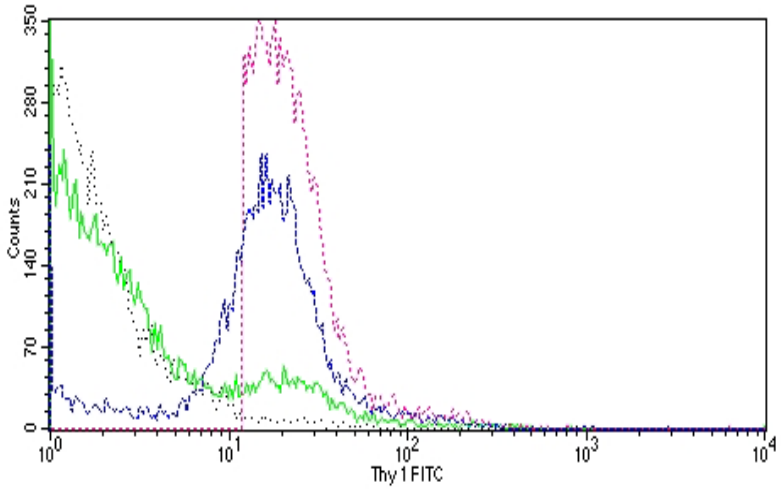

Figure 3-3. FACS analysis of Thy-1^+ and Thy-1^- sorted cells. Green line represents NPC population stained with FITC labeled Thy1 antibody before sorting. Grey dots represents NPC population stained with FITC labeled mouse IgG1 and serves as a control. Purple line represents gated $Thy1^+$ cells during sorting and left vertical line is the minimum of the gated regions. Blue line represents sorted $Thy1^+$ cells.

Table 3-1. Identities of SSH clones isolated from cDNA suppression subtractive library specific for oval cells after Blast search.

Sequencing#	The top hit after Blast search
P1	>gi|13124694|sp|P41233|ABC1_MOUSE ATP-binding cassette, sub-family A, member 1
P2	>gi|17486457|ref|XM_048404.2| Homo sapiens filamin A, alpha (actin binding protein 280) (FLNA),
P3	>gi|13278599|gb|BC004087.1|BC004087 Mus musculus, clone MGC:8296 IMAGE:3593425, mRNA
P4	>gi|12833999|dbj|AK003372.1|AK003372 homolog to translation initiation factor 3 subunit5
P5	Gi|18596934|ref|XM_050939.3| Homo sapiens KIAA0586 gene product (KIAA0586), mRNA
P7	gi|18606495|gb|BC023049.1| Mus musculus, proteasome (prosome, macropain) 26S subunit,
P8	gi|19909489|gb|AC098882.3| Mus musculus clone RP23-122D13, complete sequence
P11	>gi|12083658|ref|NM_022699.1| Rattus norvegicus ribosomal protein L30
P12	gi|19924078|ref|NM_138539.1| Rattus norvegicus deoxyribonuclease II
P13	gi|9910487|ref|NM_020074.1| Rattus norvegicus proteoglycan peptide
P15	>gi|2581790|gb|AAB82423.1| (U97674) cytochrome c oxidase chain I
P17	>gi|18257305|gb|BC021821.1|BC021821 Mus musculus, RIKEN cDNA 5033415K03
P31	Rattus norvegicus connective tissue growth factor (Ctgf), mRNA
P35	[NM_019143]Rattus norvegicus Fibronectin 1 (Fn1), mRNA
P36	Rattus norvegicus topoisomerase (DNA) II alpha (Top2a), mRNA
P37	Mus musculus B lymphocyte gene 1 (Bce1-pending), mRNA
P41	gi|19716095|dbj|AB072248.1| Rattus norvegicus cDNA, clone:a...
P43	Mus musculus, Similar to hypothetical protein FLJ20551, clone

A

ATTGTTCTTGTTTTAAGTGCTTTTGGAATTTTTAAACTGATAGCCTCAAACTCC
AAACACCATCGATAGGACATAAAGCTTGTCTGTGATTCAAAACAAAGGAGAT
ACTGCAGTGGAAACTGTAACCTGAGTGACTGTCTGTCAGAACATATGGTACCG
*Rsa*I
CCCGGGGCGGCCCGCTCGAAGGGCgaattcgtttaaacctgcagggactagtccctttagtgaggggtta
*EcoR*I
Attctgagcttggcgnaatcatggncatagctgtttcctgtgtgaaattgttatccgctcacaattccacacaacatacgagccgg
aagcataaagtgtaaagcctggggtgcctaatgagtgagctaactcacattaattgcgttgcgctcactggcccgctttccagtcg
ggaaacctgtcgtgncagctgcattaaatgaatcggcccaccgcgccggggaaaaggcggnttgcggtaattgggcgctcttt
ccgcttcctcgctcactgactcgctgcgctcggncgttcggctgcggcgagcgggaatcagctcactcaaaaggcgggnaata
acgggttatccccan

B

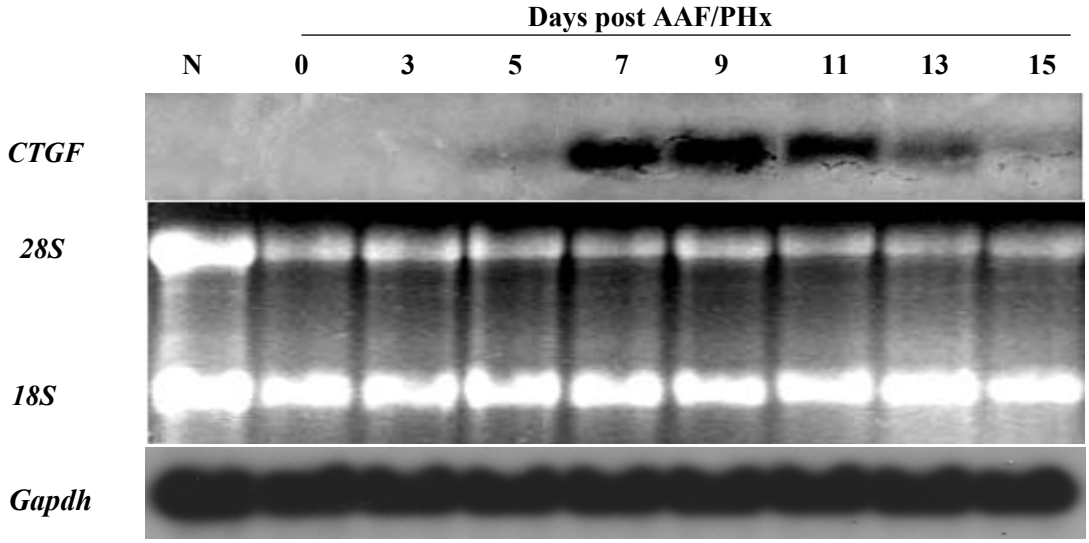

Figure 3-4. P31 represents CTGF gene, which is upregulated during oval cell activation in the 2-AAF/PHx model. A. shows that P31 contains sequences identical to 3' untranslated region of Rattus norvegicus CTGF gene (Genebank/EMBL accession number NM_022266). Rsa I is a site designed in primers of SSH and two EcoR I sites flank the pCR 4 vector during cloning. B. CTGF gene is induced in total liver homogenate in a Northern analysis using the cDNA insert of P31 as a probe.

A.

CGCGCGCGANGNGNCNCAAAAACGGGACCAAGNAAGNNAANCCAGNTTNTT
TTGCTTCTTTTGCCGNCTGACCTTGCAGCACTTGNCAGGGAGGCCTTGNCCNT
GGGGCTGTGNCCAAACACCCCACAGGGACTCACTTGTCCCAACAANCCTAAT
TGCCNANAAANANCTTNCTCTNACCNGTNATTNATCAATTTTCCCAGAATTTT
AATACGGAAAAAATTGNATTGAAGACACTTTGNATGCAGTTGATAAAAAG

*EcoR*I

Gaattcagnataattatggtnggggacnattttaatatggacccncgnccgcgaccaccgctaagggcgaattcgttaaacctg
caggactaagccccttaagngagggtaaatctgagcntggcggaaccatgggcataacnggttcctgggggaaattggtatcc
nctcnccaantcccancaacanaccaagccggaagcaaaaaagnggaaaggcctgggggngcccaaangagggggct
aaccncccattaaattgggggtggggctcnctggcccgctttttccaggccgggnaaaacctgnccggggncaagcctggaa
ttnaaaggaaaccgnnccaancncgccgggggaanaaaggggggntttgcngnaattggggccccccccttcccccctt

B.

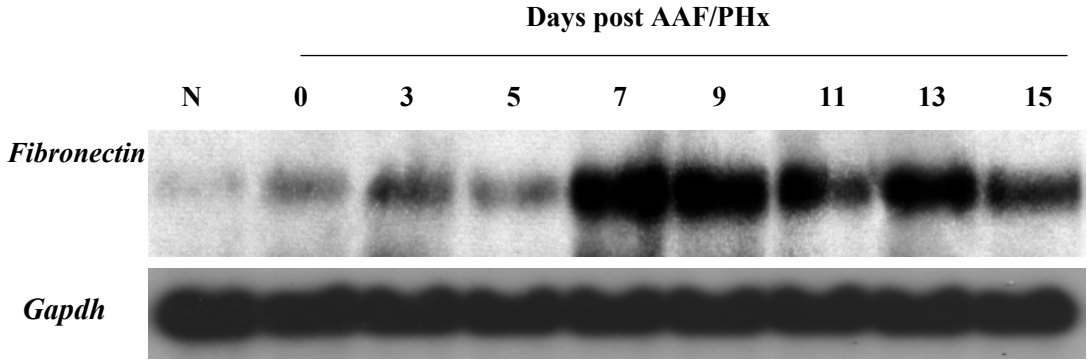

Figure 3-5. P35 represents fibronectin 1 gene, which is upregulated during oval cell activation in the 2-AAF/PHx model. A. P35 contains sequences identical to 3' region of Rattus norvegicus fibronectin 1 gene (Genebank/EMBL accession number NM_019143-1). EcoR I sites flank the pCR 4 vector during cloning. B. CTGF gene is induced in total liver homogenate in a Northern analysis using the cDNA insert of P35 as a probe.

A.

5’TTGCTAATCAAGAGGCTGCGAGGGGCTGAGCTGGTCAGGATGCGGCAGGTT
CCTGTGGGCACCAGGCTTGTCCTGGCTCTCGCCTTCGTCCTGGTTTGGGGATC
TTCAGTTCAAGGTTATCCTGCTCGGAGAGCCAGGTAC
*Rsa*I
CAATGGGTCCGCTGTAAACCAGATGGCATTTTTGCAAACTGCATTGAGGAGA
AAGGACCACGGTTCGACCTAATAGCAGAGGAATCCAACGTTGGCCCCCCGAT
GACCGATCCTGTTTTGATGAGAGGATTCCCGAATGATTTCTTCCCCATTTCTG
ATGACTATTCTGGCTCCGGCTCTGGCTCTGGCTCTGGCTCCGGCTCCGGCTCT
GGCTCTGGCTCTGGCTCTGGCTCAGGTTCCGGCTCCGGTTCCGGTTCTGGCTC
TGGCTCGGGTTCTGGCTCCGGCTCGGGCTCTGGCTCAGGAAGCGGCTCCCTA
GCTGACATGGAATGGGAATACCAGCCAACAGATGAAAACAATATTGTCTATT
TCAACTATGGGCCTTTTGATAGGATGCTCACCGAGCAAAACCAAGAACAACC
AGGAGATTTTATTATATGAAAGTAACCGTCTGTTTCCCCACCTCCACATGAAA
CAATGTGTTCAGTATACTTTGTGTACCACGTTTAAATGAGCAGTCTCAGGATA
AGTTTTACAGAAAATTTAAAATGCTTGGAAAAGACTCTTGAATCCTGTTACCC
CTTTCCTCATTAATTGATAAGGAATTATGCTTTAATGCTGTTATCTATCTTATT
GTTCTGGAAAATATCCGCAGCTATATGTGTATTGAATCATAACTTTAAAAGCC
ATACTGGTTTCGAAAACTTTATTTTGATAGCAAGTTGATGAACAATACTTCAT
ACCTAAACTGTTCCATTGTGAATTAAAGATATATTCCTATGTGATTAAAAAGA
AAATAAAATGAAACACAGTGGCCTCCTACCGTGGCTATGTGATGTGGTTT3’

B.

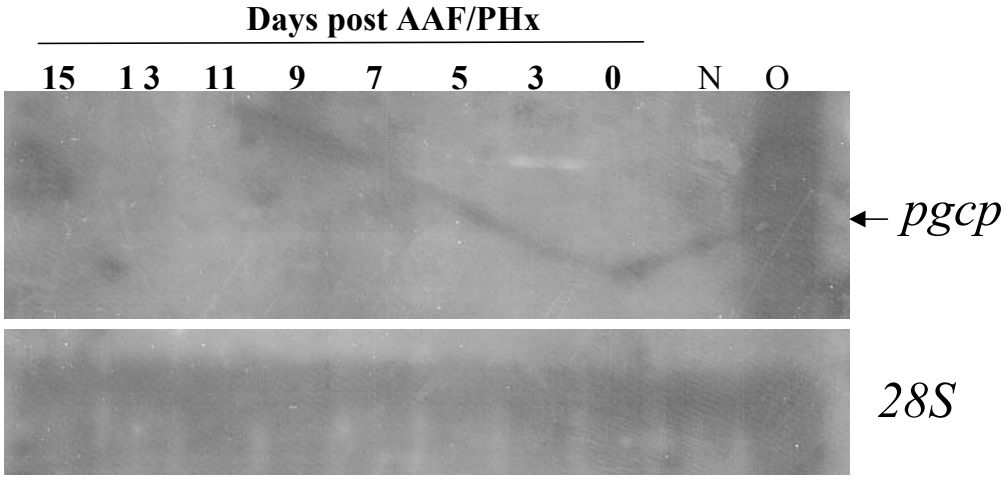

Figure 3-6. P24 represents a proteoglycan core peptide gene, which is expressed specifically in sorted Thy-1^+ oval cells. A. P24 contains sequences identical to part of a Rattus norvegicus chondroitin sulfate proteoglycan core protein (*pgcp*) (Genebank/EMBL accession number NM_020074). Rsa I is a site designed in primers of SSH. B. *pgcp* gene is not induced in total liver homogenate but specifically and highly unregulated in Thy-1^+ oval cells in a Northern analysis using the cDNA insert of P24 as a probe.

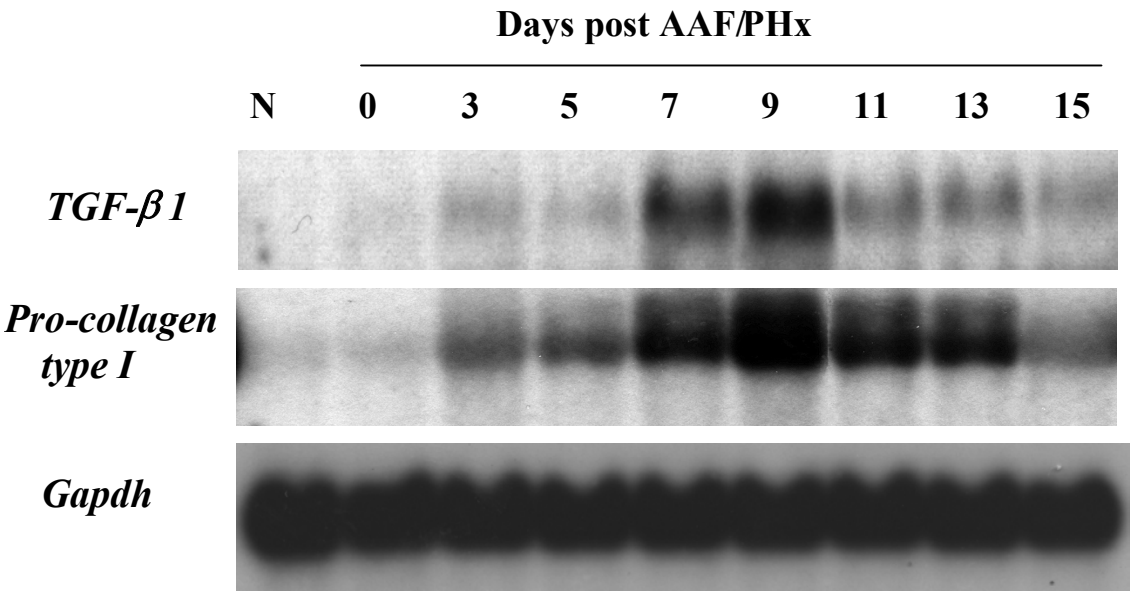

Figure 3-7. Inductions of TGF-β 1 and pro-collagen type I in oval cell aided liver regeneration in a Northern analysis. These induction patterns are concurrently associated with CTGF and fibronectin upregulations.

CHAPTER 4
CHARACTERIZATION OF CTGF GENE DURING OVAL CELL MEDIATED LIVER REGENERATION

Introduction

CTGF has been found to be produced by and act on a broad repertoire of cell and tissue types. Besides fibroblasts, it is expressed in and acts on endothelial cells, skeletal and smooth muscle cells, chondrocytes, epithelial cells and neural cells. It has also been implicated in several normal physiological processes including embryo development and differentiation, endochondral ossification and female reproductive tract function in the uterus and ovary. Upregulation of CTGF has been linked to many pathogeneses including fibrosis tumor desmoplasia, wound healing, and tissue regeneration (Moussad and Brigstock; 2000)

In normal livers, CTGF is expressed at a low level in venous endothelial cells and arterial myocytes. However, a significant induction of CTGF transcription has been noted in several human conditions including liver fibrosis, chronic liver diseases and non-alcoholic steatohepatitis. The upregulation of CTGF has also been reported in experimental liver injuries. Immunohistochemistry and *in situ* hybridization experiments in these models show the expression of CTGF in several types of hepatic cells including stellate cells and proliferating epithelial cells. Despite these studies, the cellular source of CTGF during oval cell mediated liver regeneration has not been characterized.

In addition, CTGF was discovered more than ten years again but progress on CTGF research has been limited by technical and biological peculiarities. There are no reliably

standardized reagents to purify active protein and no commercially available (recombinant) CTGF. Recombinant CTGF is currently being produced by several individual laboratories from different sources. The composite structure and the over 30 cystine residues in CTGF protein might complicate proper posttranslational processing in production of recombinant protein. To overcome this difficulties, we attempted to develop some tools including expressing flag-tagged CTGF in tissue culture and generating a stable WBF344 cell line overexrpessing flag-tagged CTGF. These tools were used to facilitate the biochemical characterization of CTGF protein in vitro and vivo. Finally, we combined in situ hybridization and immunofluorescent staining techniques to determine the cellular sources of CTGF in regenerating liver following 2-AAF/PHx.

Materials and Methods

Cloning of the Full-length CTGF cDNA

The full-length CTGF cDNA was amplified by RT-PCR with a primer set 5'GCTAGCCCTCCTGCCGCGCCCCGACCATGCTCGCC3'and 5'GGATCCCGCCATGTCTCCATACATCTTCCTGT3' and cloned into flag-pGEM-vector, which contained the flag epitope sequence (a generous gift from Dr W.Y. Song). The resulting clone was confirmed by sequencing. The CTGF cDNA and flag sequences were released by SpeI digestion and further cloned into pFastBac^{TM} vector (Invitrogen; Carlsbad, CA). CTGF-flag protein was expressed in Sf9 insect cells according to manufacture's instruction.

Expression of Flag CTGF in Baculovirus System

The full length CTGF cDNA with a flag epitope was cloned by RT-PCR into pcrII blunt vector based on published data (CTGF, GenBank accession number: NM_022266)

and verified by sequencing analysis. The flag tagged CTGF gene was further cloned into the 3' sequence of polyhedrin promoter in the baculouvirus expression vector pFASTBAC1 (Life technologies). The resulting construct was transfected into Sf9 cells and used for large-scale protein purification using M2 antibody conjugated affinity column.

Transfection of PIREs Flag CTGF into WBF-344 and NIH3T3 Cell Lines

The flag tagged CTGF gene was also cloned into mammalian expression vector pIRES2-EGFP vector under the control of CMV promoter and transfected in NIH3T3 and WBF344 cell lines by lipofectamin method. Single clone of GFP positive WBF344 cells was cloned and expanded to generate a stable CTGF expressing cell line. This cell line was used to evaluate the inhibitory efficiency of recombinant adenovirus carrying CTGF siRNA sequences in vitro in chapter 5.

Western Analysis of CTGF Protein

Total proteins were extracted from liver homogenates in RIPA buffer (50 mTris-HCl, pH 7.4, 1% NP-40, 0.25% Na-deoxycholate, 150 mM NaCl, 1 mM EDTA, 1 mM PMSF, 1 microgram/ml Aprotinin, leupeptin and pepstatin, 1 mM Na_3VO4, 1 mM NaF), separated in 10% SDS-PAGE gel and electro-transferred to PVDF membrane. Membrane was blocked in TBS containing 4% BSA and 0.1% Tween 20. A rabbit anti-mouse CTGF antibody (Abcam; Cambridge, MA) was used as a primary antibody at 1:2000 dilution in TBS containing 5% milk and 0.1% Tween 20. A calf anti-rabbit IgG (Santa Cruz biotechnologies; Santa Cruz, CA) was used as a secondary antibody at a 1: 5000 dilution. Detection was performed using the ECL plus kit (Amersham Life Science; Piscataway, NJ).

Tissue Staining and *In Situ* Hybridization

Immuno-fluorescent staining and *in situ* hybridization were performed on the same liver sections. Livers were perfused with 4% paraformaldehyde and 0.05% glutaraldehyde according to a previously published method (Fahimi, 1967). Cryo-sections, 6 μm thick, were cut at -20^0C and dried overnight at 40^0C prior to analysis.

Immunostaining was performed before *in situ* hybridization. Sections were washed in TBS containing 1 mM $CaCl_2$, permeablized in methanol at -20^0C and blocked with protein blocking agent (Thermo Shandon; Pittsburgh, PA). Slides were stained with mouse anti-rat Thy-1 antibody (PharMingen; San Diego, CA) at a dilution of 1:50. Alexa Fluor 594-labeled goat anti-mouse (Molecular Probes; Eugene, OR) was used as the secondary antibody at a dilution of 1:500.

In situ hybridization was performed immediately following immunostaining. The hybridization was performed according to published protocols in non-radioactive *In Situ* Hybridization Application Manual (Roche; Basel, Switzerland). A 430 bp region of rat CTGF cDNA (Genebank/EMBL accession number NM_022266) was amplified (Sedlaczek et al., 2001) and cloned into PCR4 TOPO vector. The linearized clones from both directions served as sense and antisense templates for digoxigenin (DIG)-riboprobe synthesis using T7 RNA polymerase. Sections were hybridized in buffer containing 40% deionized formamide, 10% dextran sulfate, 1x Denhardt's solution, 4x SSC, 10 mM DTT, 1 mg/ml denatured and sheared salmon sperm DNA with 5 ng/ul DIG- rRNA antisense or sense probes at 58^oC for 40 hours. After hybridization, slides were washed in 2x SSC followed by 1x SSC. Next, samples were digested in 10 μg/ml RNAase and washed in 0.1xSSC to remove non-hybridized RNA. The DIG signal was detected with

sheep, anti-DIG-alkaline phosphatase (Roche; Basel, Switzerland) and NBT/BCIP substrates were used for color detection.

Quantitative Real-time PCR

A two-step quantitative real time PCR reaction was carried out with the ABI PRISM 5700 Sequence Detection System (Perkin-Elmer Applied Biosystems, Foster City, CA). CTGF primers were based on published sequences[14] with the following modifications. Total RNA was extracted using the Qiagen RNA kit and any DNA contamination was removed by DNase I treatment (Ambion; Austin, TX). Total RNA was reverse transcribed with random hexamers using first strand cDNA synthesis kit (Invitrogen; Carlsbad, CA) following manufacture's instructions. Amplification reactions were performed using a SYBR Green PCR Core reagent kit (Applied Biosystems; Foster City, CA). Amplification conditions were as follows: 2 min at 50°C, 10 min at 95°C followed by 40 cycles of 15 sec at 95°C and 1 minute at 60°C in the presence of 500 nM forward and reverse primers, 5 mM $MgCl_2$, 50 mM KCl, 10 mM Tris buffer (pH 8.3), 200 mM dATP, dCTP, dGTP, 0.25 μl AMPUNG and 1 unit AmpliTaq. 0.5uM primers for 18s ribosome RNA and 2.0uM probe (Applied Biosystems; Foster City, CA) were used in the two-step real time PCR. The comparative-CT method against the expression level of 18s ribosomal RNA was used for quantitation.

Results

Cloning of the Full-length CTGF cDNA

To further characterize CTGF, we have designed reverse and forward primers 5'GCTAGCCCTCCTGCCGCGCCCCGACCATGCTCGCCT 3' and 5' GGATCCCGCCATGTCTCCATACATCTTCCTGT 3' to clone the whole coding region of rat *CTGF* cDNA according to published data (*CTGF*, GenBank accession number:

NM_022266). A NheI site was designed at the 5' region of reverse primer and a BamHI site was at the other end of forward primer. These two sites would be used for further cloning in expression vectors. As shown in Figure 4-1A, PCR products with the expected 1.1 kb size were amplified and cloned into pCR II blunt vector. The recombinants containing the 1.1kb insert were identified and the positive plasmids were further verified by restriction enzyme digestion with PstI, SmaI, EcoRI, NheI and BamHI. 1.1kb fragment was released by EcoRI enzyme, which recognizes two sites flanking the insert in vector. NheI and BamHI were engineered on reverse and forward primers and the digestions together with the two enzymes also produced a full-length insert (Figure 4-1B). There are two SmaI and two PstI recognition sites in the coding region of *CTGF* gene. The distance between two SmaI sites is about 300bp and the distance between two PstI is 597bp. The cloned cDNA has been sequenced and confirmed that there is no any mutation.

Expression of Flag-tagged CTGF in Culture

pIRES flag tagged CTGF-GFP was transfected into mammalian cell lines NIH3T3 and WBF344 cells. Flag tagged CTGF gene, which was linked to GFP with internal ribosomal entry site was coexpressed with GFP. We estimated the transfection efficiency by visualization of green fluorescence of GFP. 80% NIH3T3 cells and 45% WBF344 cells were GFP positive shown in Figure 4-2. CTGF expression in these transfected cells was detected by Western analysis as shown in Figure 4-3.

pFASTBAC1-flag CTGF was transfected and expressed in Sf9 insect cells. In Figure 4-3, untransfected cells didn't express any CTGF. In contrast, the 38 kD CTGF was detectable in transfected Sf9 cells and transfected mammalian cell lines WBF344 and NIH3T3. To generate a stable CTGF expressing cell line, we cloned GFP positive

WBF344 cells. After several passages, we successfully established a cell line with more than 95% cells expressing CTGF (Figure 4-4). This stable cell line was used to evaluate the inhibitory efficiency of recombinant adenovirus carrying CTGF siRNA sequences in vitro (chapter 5).

Western Analysis of CTGF Protein Level during Oval Cell Mediated Liver Regeneration

CTGF protein levels were measured during oval cell activation by Western blot analysis. Due to the multiple bands detected in total liver extracts, we engineered a construct containing a flag epitope sequence before the stop codon of the full length CTGF cDNA. The flag epitope consists of eight amino acids and adds 1.2 kDa to the molecular weight of the protein. Purified flag tagged CTGF protein was isolated from Sf9 insect cells and served as a positional marker for native CTGF from total liver protein extracts. A 38 kDa protein, consistent with the predicted size of CTGF, was observed in 2-AAF/PHx treated livers (Figure 4-5). A significant induction of CTGF protein was observed beginning at day 5 and peaking at days 7 and 9 following PHx. This pattern of CTGF protein expression is consistent with our observations regarding CTGF message expression during the oval cell response to 2-AAF/PHx.

CTGF is Expressed in Both Thy-1$^+$ Oval Cells and Stellate Cells

The possibility that oval cells are, themselves, a source of CTGF was investigated by two approaches. At first, CTGF gene expression in sorted Thy-1$^+$ oval cells was measured by quantitative real time PCR. In comparison to normal liver, a statistically significant 3.5-fold increase ($p<0.05$) in CTGF was detected in Thy-1$^+$ cells sorted from animals sacrificed at day 9 following 2-AAF/PHx. In contrast, the unsorted and total liver extract from animals sacrificed at the same time point showed only a 2.2-fold

increase in CTGF (Figure 4-6A). The higher expression of CTGF in the enriched Thy-1^+ oval cell population indicates that Thy-1+ oval cells are a source of CTGF.

Immunofluorescent staining for Thy-1 and *in situ* hybridization for CTGF message was used to localize CTGF message. The anti-Thy-1 antibody clearly labeled the periportal oval cell population (Figure 4-6C and 4-6E). The same Thy-1^+ cell population expressed CTGF transcripts (Figure 4-6D and 4-6F). As a control, sense CTGF riboprobe did not hybridize with any cells in the portal tract (Figure 4-6B). The co-labeling by immunostaining and *in situ* hybridization support the real time PCR results indicating Thy-1+ oval cells express CTGF.

To test if stellate cells express CTGF, we experienced difficulties in tissue section staining with CTGF antibody. As an alternative approach, we stained sorted cells prepared by cytospin to detect if CTGF is expressed in stellate cells. CTGF protein was detected with Texa red conjugated secondary antibody while desmin, the stellate cell marker, was detected with FITC conjugated secondary antibody. In Figure 4-7, some stellate cells were clearly positive for desmin and CTGF, indicating that stellate cells were a source of oval cells.

Discussion

We detected CTGF protein during the time course of oval cell-mediated liver regeneration. The Western result supports the previous finding by Northern analysis showing that CTGF was induced during oval cell activation process. The strong induction of CTGF occurred at day 5 at the protein level but only a slight RNA induction at that time. This may be due to the post translation modification of protein or a release of CTGF protein from ECM.

We detected that there are at least two sources of CTGF in oval cell aided regenerating livers. One is Thy^+ oval cells and the other is stellate cells. CTGF is expressed by Thy-1^+ oval cells. Thy-1^+ oval cells are scarce in normal liver, whereas a large population of Thy-1^+ immunoreactive cells has been observed in the 2-AAF/PHx model. By quantitative real time PCR, immunohistochemistry and *in situ* hybridization, we have demonstrated that Thy-1^+ oval cells express CTGF. Based on the fact that CTGF promotes the migration and proliferation of stellate cells in tissue culture condition, and that activated stellate cells are seen within the oval cell compartment, it is likely that the CTGF protein expressed by Thy-1^+ oval cells may be acting in a paracrine manner to promote the migration and proliferation of the stellate cells in the 2-AAF/PHx model. If so, CTGF may be assisting the oval cells indirectly by stimulating stellate cells to expand and remodel the extracellular matrix. Alternatively, CTGF may act on Thy-1^+ oval cells themselves. It is known that CTGF can stimulate cells via integrin and heparin-sulfate proteoglycan. One of the candidate genes differentially expressed in Thy-1^+ oval cells encodes proteoglycan peptide. Northern results show that the proteoglycan peptide gene is expressed specifically, and to a great extent, in the Thy-1^+ oval cell population (data not shown). It is likely that Thy-1^+ oval cells possess integrin and heparin-sulfate proteoglycan and are responsive to CTGF signaling. Future studies to test the biological activities of CTGF in Thy-1^+ oval cells *in vitro* would be needed to verify this possibility.

Taken together, using flag tagged CTGF generated in vitro as a marker, the expression of native CTGF protein during the course of regeneration following 2-AAF/PHx was determined. This expression kinetics at the protein level is roughly

consistent with that of mRNA level. Immunohistochemistry studies indicate that Thy-1+ oval cells and stellate cells are the source of CTGF.

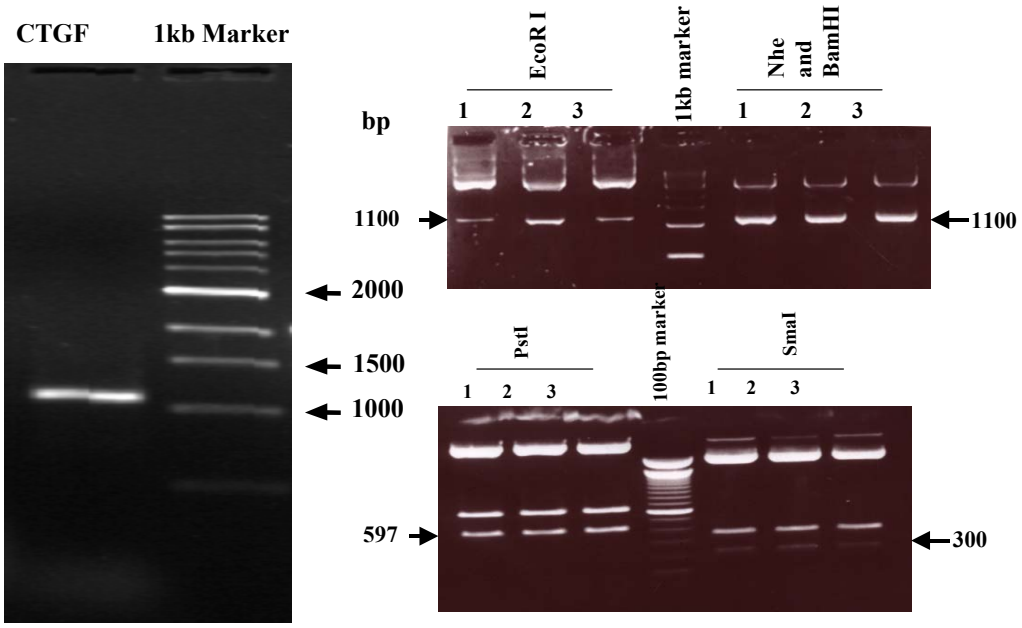

Figure 4-1. Cloning of Rat *CTGF* cDNA encoding the full length of CTGF protein by RT-PCR and verification of recombinants by restriction enzyme digestions. A shows PCR products with expected 1.1 kb size amplified by RT-PCR. The products were cloned into pCR II blunt vector (Invitrogen). B and C are results of restriction enzyme digestions of three individual candidate plasmids. In B,1.1kb fragment was released by EcoRI enzyme which recognizes two sites flanking the insert in vector and by the double digestion with NheI and BamHI which are engineered on reverse and forward primers. In C, *CTGF* specific fragments with the expected size of 395bp for SmaI and 380bp for PstI are released from all of three candidates.

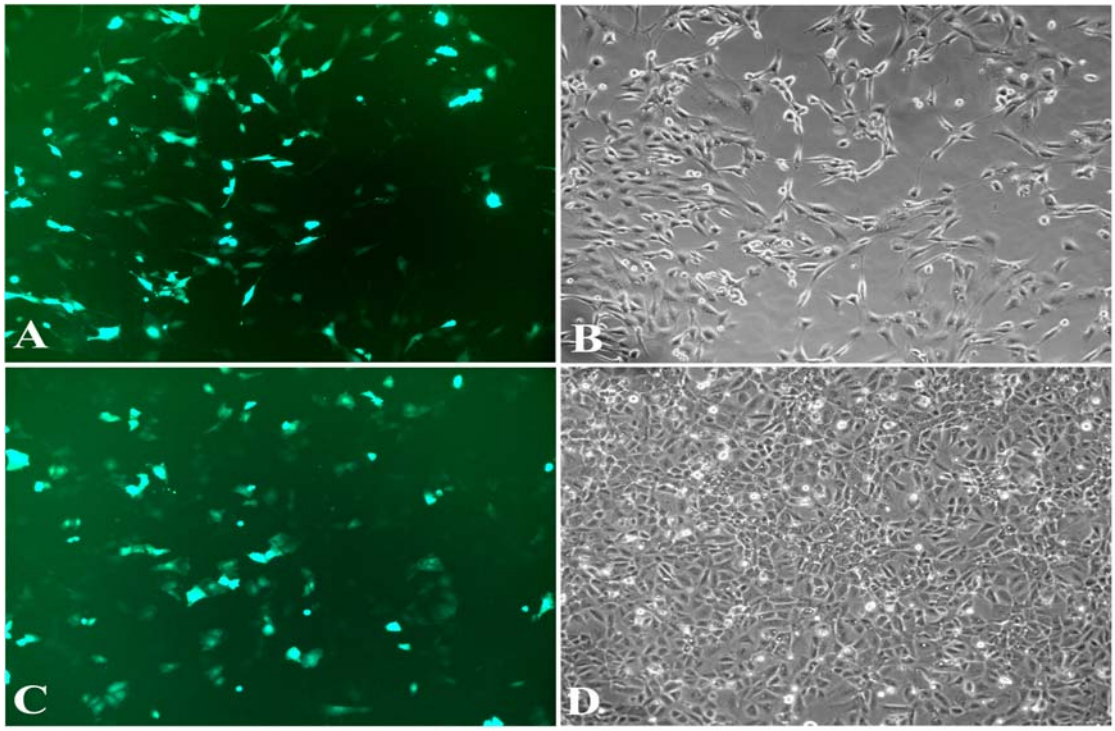

Figure 4-2. Transfection of pIRES-flag CTGF-eGFP construct in NIH3T3 cells (A and B) and WBF344 cells (C and D). (A) and (C) show GFP expression in transfected cells. (B) and (D) are phase contrast of total cells used for transfection. Magnification for A, B, C and D are 100x.

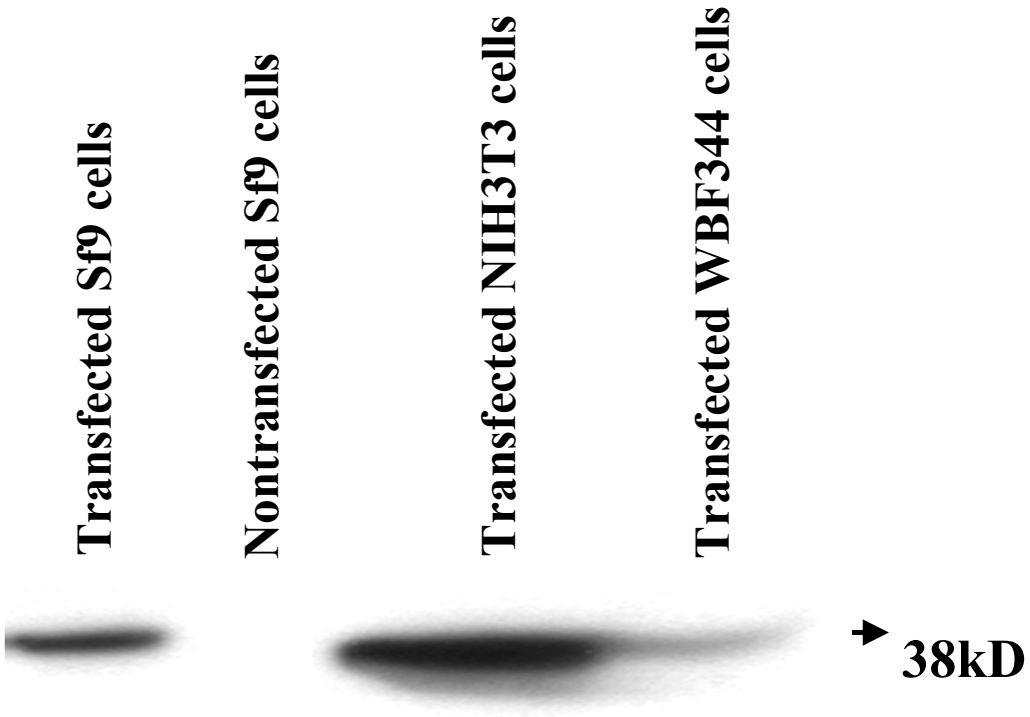

Figure 4-3. Detection of CTGF proteins in insect sf9 cells, NIH3T3 cell and WBF344 cells using anti-flag antibody.

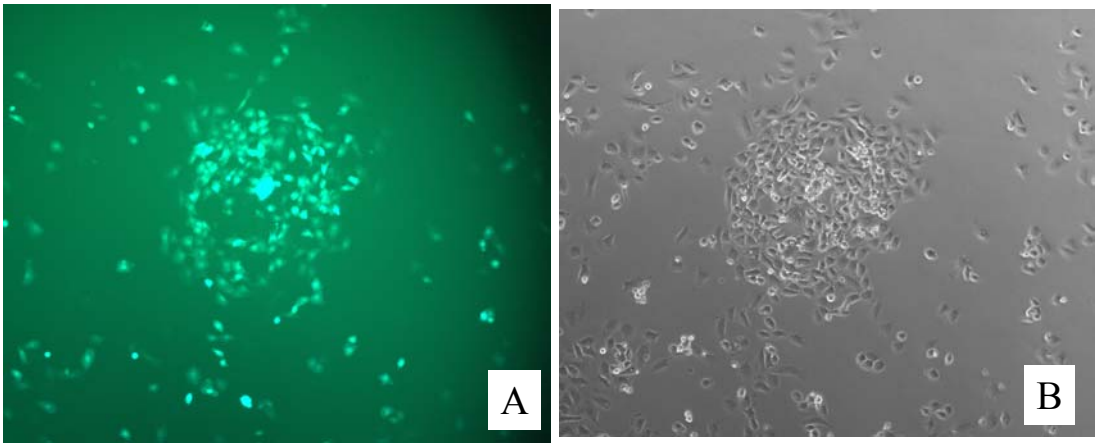

Figure 4-4. Establishment of a stable WBF344 cell line overexpressing flag-CTGF. A shows green fluorescent GFP positive cells while B is the phase-contrast picture of A. Magnification of A and B is 100x.

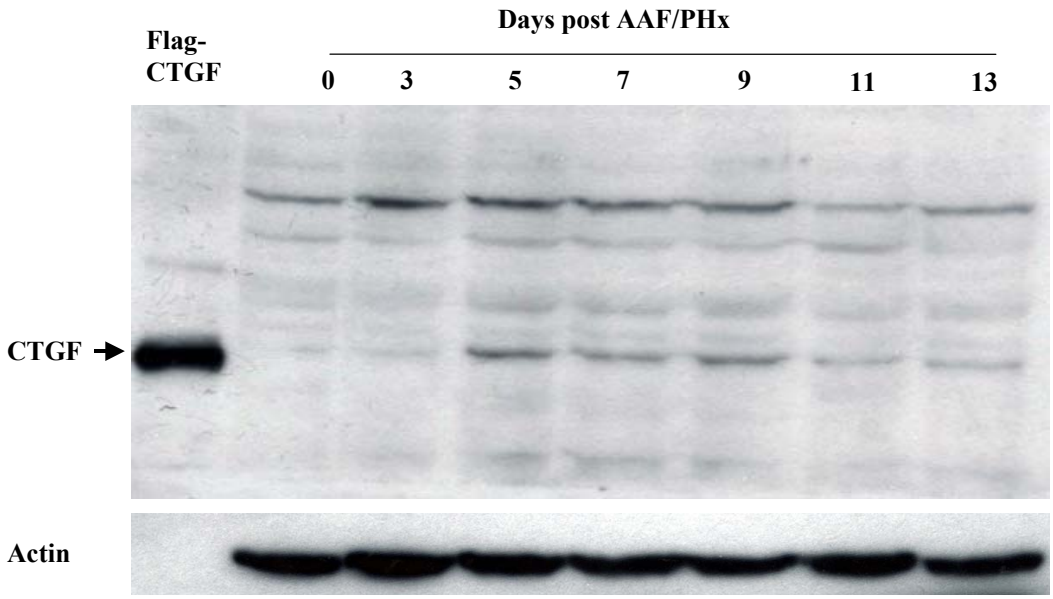

Figure 4-5. Induction of CTGF protein in the 2-AAF/PHx model. Western blot analysis of whole liver homogenate shows accumulation of CTGF protein. Actin was used as a loading control.

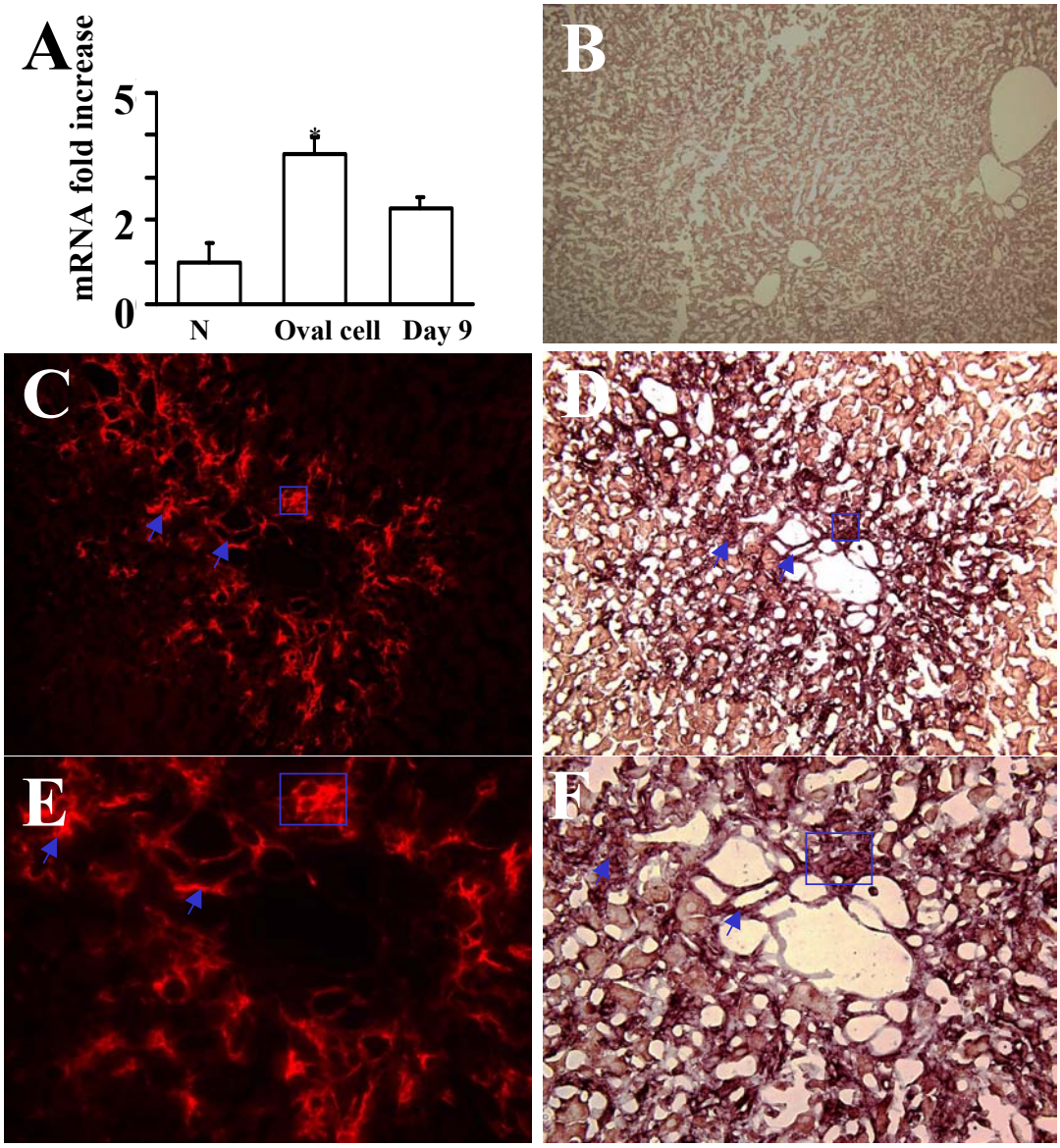

Figure 4-6. Thy-1^{+}oval cells express CTGF transcript. (A) Real Time PCR demonstrates induction of CTGF in both whole rat liver and Thy-1 sorted oval cells following 2-AAF/PHx comparing to those of normal livers. N indicates normal livers. Values in normal livers are arbitrarily assigned to 1 unit. Data represent the mean value $\pm$ SD ($n \geq 3$). *$P<0.05$. (B) *In situ* hybridization negative control, probed with sense *CTGF* (200X). Thy-1^{+} oval cells obtained at day 9 after 2-AAF/PHx treatment shown in (C) and (E) were stained in red. *In situ* hybridization of the same section with *CTGF* antisense probe in (D) and (F) show dark brown signals for CTGF transcripts. Blue arrows indicate the colocalization of CTGF transcripts in Thy-1^{+} oval cells. Images of (B), (C) and (D) were taken at 200X. (E) and (F) were taken at 400X. (E) and (F) were the large magnifications of (C) and (D) respectively.

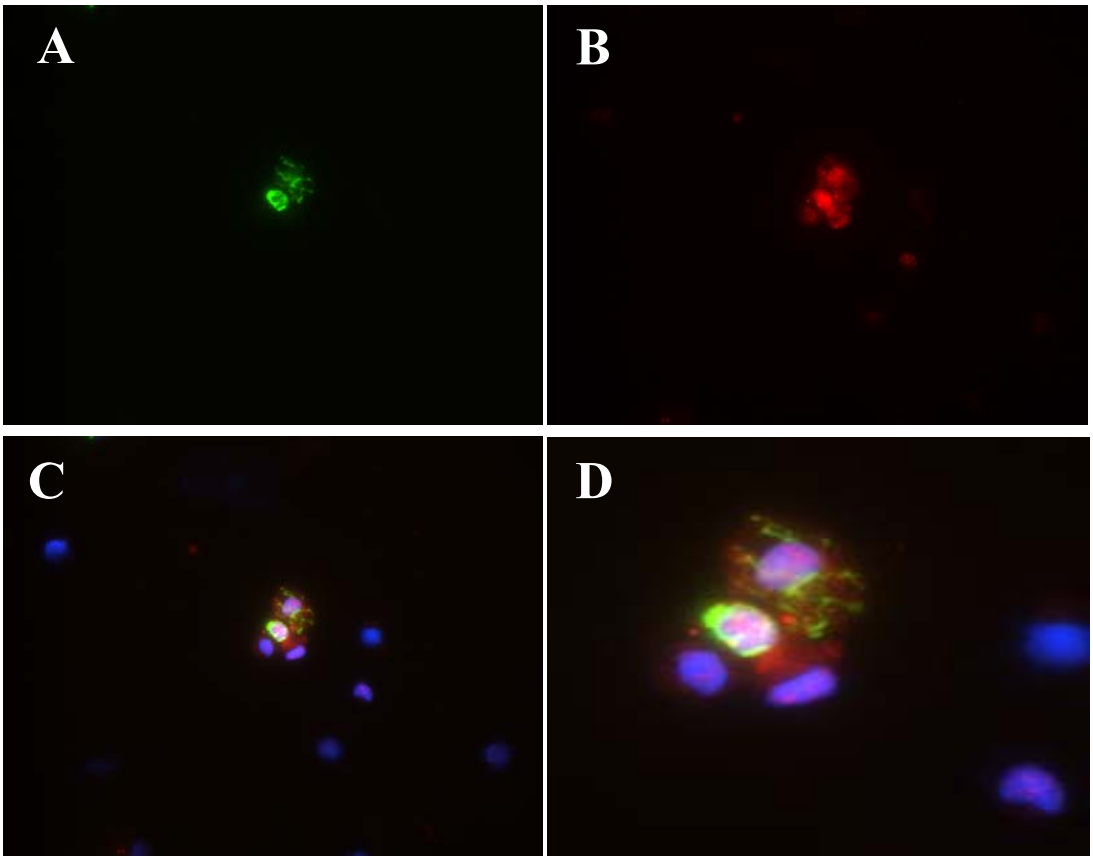

Figure 4-7. Colocalization of desmin and CTGF in sorted stellate cells. A (100x) was stained for desmin and B (100x) was for CTGF protein. C (100x) is the merge image of A and B. D (400x) is a large magnification of C. Blue is DAP-staining for nuclei.

CHAPTER 5
INHIBITION OF CTGF EXPRESSION DURING OVAL CELL MEDIATED LIVER REGENERATION

Introduction

CTGF gene expression is regulated transcriptionally by TGF-β signaling pathway. The CTGF promoter sequence contains a TGF-ß response element (Grotendorst et al, 1996), which is mainly important in regulation of basal expression of CTGF. A functional SMAD binding element is also located in the CTGF promoter region and is crucial in TGF-β induction of CTGF gene expression in fibroblasts and mesangial cells (Holmes et al., 2001 and 2003).

Recently, it has been found that the prostacyclin derivative, Iloprost, can effectively suppress TGF-β1 mediated induction of CTGF synthesis and decrease fibrosis in animal models and human studies (Stratton R et al, 2002 and 2001). Iloprost causes an elevation of cAMP, which, in turn, activates adenylate cyclase and protein kinase A. Inhibition of CTGF transcription is believed to involve activation of protein kinase A and subsequent inhibition of the Ras/MEK/ERK pathway (Stratton R et al, 2002) (Figure 5-1).

In chapter 2, we demonstrated that CTGF has a coordinate expression with TGF-β during oval cell activation in the 2-AAF/PHx model. This similar induction pattern suggests that CTGF upregulation is stimulated by TGF-β in regenerating livers following 2-AAF/PHx. Therefore, we tested the effect of Iloprost on CTGF induction during oval cell activation. We also investigated the oval cell response after Iloprost treatment in animal studies.

Other approaches to inhibit CTGF include antisense RNA or RNA interference and neutralizing antibody of CTGF. Neutralizing antibody of CTGF is impossible to use because of the expense and limited resources. Antisense or RNA interference approaches have been widely used in tissue culture condition. There are also some successful cases using these approaches in animal studies (Shimo et al., 1998; Uchio et al., 2004). In this chapter, we also attempted to generate CTGF siRNA using adenovirus system and assessed the efficiency of the CTGF siRNA adenovirus in vitro using a stable WBF344 cell line overexpressing flag-CTGF.

Materials and Methods

Iloprost Treatment and In Vivo BrdU Labeling

10 rats underwent 2-AAF/PHx as described in chapter 2. Half were injected with Iloprost through tail vein and the other half were injected with PBS solution as controls. For Iloprost treatment, Iloprost stock solutions in ethanol (Cayman Chemical; Ann Arbor, MA) were diluted to 5 μg/ml in PBS immediately before use. Approximately 33 μg/kg Iloprost was administered via the tail vein daily beginning at day 1 following PHx until the day before end points (day 5, 7 and 9 after PHx). 2 rats/ group were sacrificed at time point day 7 and day 9.

To perform *in vivo* BrdU labeling, 50mg/kg BrdU in 1xPBS was injected 2 hours before sacrifice. BrdU staining and H&E staining were preformed on liver sections with standard protocols.

Northern Analysis

Probes for CTGF and TGF-β 1 were the same ones used in chapter 3. AFP probes were generated using primers and cloned into pGEM-T vector based on Genebank

sequences (Genebank/EMBL accession number NM_012493.1). Hybridization was performed the same as described in chapter 3.

Quantitative Real Time PCR Analysis

The same two-step quantitative real time PCR reaction as described in chapter 4 was carried out to monitor CTGF expression with the ABI PRISM 5700 Sequence Detection System (Perkin-Elmer Applied Biosystems, Foster City, CA).

For AFP RNA quantification, AFP probe and primers were purchased (Applied Biosystems; Foster City, CA). One-step real time PCR was conducted on DNase I treated RNA samples using the following amplification conditions: 30 min at 48^{o}C and 10-minute step at 95° C, followed by 40 cycles of 15 sec at 95° C and 1 minute at 60° C. 0.5uM primers for 18s ribosome RNA and 2.0uM probe (Applied Biosystems; Foster City, CA) were used in both one-step and two-step real time PCR. The comparative-CT method against the expression level of 18s ribosomal RNA was used for quantitation.

Generation of Recombinant Adenovirus Carrying Sequences Specific for CTGF siRNA

The diagram in Figure 5-2 shows a schematic flow chart of how to generate recombinant adenovirus carrying sequences specific for CTGF siRNA. Briefly, siRNA CTGF1 sequences 5' AAGACCTGTGCCTGCCATTACAACTCTTGATTGTAATGGCAGGCACAGGTCG AGGT3' and siRNA CTGF2 5' AAAGAGTGGAGCGCCTGTTCTAACTCTTGATTAGAACAGGCGCTCCACTCTG AGGT3' were cloned into the 3 priming of H1 promoter at psiRNA-hH1GFPzeo vector (Invivogene) and transformed into GT116 bacterial strain. The recombinant clones can be identified based on the AseI restriction enzyme digestion because the positive clones only

contain one AseI site while the vector itself has two AseI sites. The sequences of positive clones were verified further by sequencing analysis. The sequences of H1 promoter and siRNA CTGF were released with SpeI and HindIII from psiRNA-hH1GFPzeo vector and further cloned into p-shuttle vector (Stratagene). The resulting clones were digested with XbaI and HindIII and cloned into 30 kb pADeasy adenovirus vector by homologous recombination in bacteria. PmeI restriction digestion can reveal the recombinant adenovirus which contains 3kb or 4.5 kb p-shuttle sequences. A recombinant virus carrying scramble siRNA sequence under the control of H1 promoter was generated using the control plasmid from psiRNA-hH1GFPzeo vector kit (Invivogen). Scramble siRNA sequence is

5'AAGCATATGTGCGTACCTAGCATCTCTTGAATGCTAGGTACGCACATA TGCGAGGT 3'.

The linearized and dephosphorylated recombinant adenovirus DNAs were used for transfection into AD293 cells to generate virus particles by lipofectamine reagent (invitrogen). The primary virus was amplified by infecting AD293 in tissue culture. AD293 was cultured in 10% FBS, DMEM media with 4.5g/L glucose. A virus titration kit (Invitrogen) was used to titer the activity of amplified recombinant CTGFsiRNA adenovirus.

Testing the Inhibition Efficiency of Recombinant CTGF siRNA Adenovirus in A CTGF Overexpressing WBF344 Cell Line

The stable WBF344 cell line overexpressing CTGF was grown on a 6-well plate in 10% FBS, DMEM/F12 media to 80% confluence. 1 MOI /each type of virus particles was used for transfection by incubating with 500 ul media in the 6-well plate for 4 hours.

Cells were lysated for protein analysis at 2 days after transfection. Western analysis was performed the same one as described in chapter 4.

Results

Iloprost Blocks Upregulation of CTGF But Does Not Affect TGF-β 1 Induction Following 2-AAF/PHx Treatment.

The synthetic prostacyclin derivative, Iloprost, has been shown to block TGF-β1 induced CTGF synthesis in both sclerotic diseases and in mouse wound healing models. 2-AAF/PHx treated rats were administered Iloprost (33 μg/kg/day i.p.) daily in an attempt to suppress CTGF induction. Three time points, day 5, 7, and 9 post PHx, representing the initial and peak points of CTGF expression in the 2-AAF/PHx model, were selected for Northern analysis. CTGF message levels were barely detectable at all three points in animals treated with Iloprost (Figure 5-3). As expected, strong CTGF induction was seen in control animals that received PBS alone in tail vein injection. Interestingly, TGF-β1 induction seemed not to be affected by Iloprost as evidenced by a similar elevation of TGF-β1 in both Iloprost treated and untreated animals at all three time points. These results indicate that Iloprost effectively blocks CTGF induction without affecting TGF-β1 upregulation in the 2-AAF/PHx model.

Decrease in the Number of Histologically Evident Oval Cells in Iloprost Treated Rat Liver Following 2-AAF/PHx.

H&E staining of paraffin sections was used to determine whether Iloprost causes any change of the oval cell response. Histological analysis showed a marked oval cell response in the periportal region of liver lobules at day 7 and 9 after following PHx (Figure 5-4A and 5-4C). In contrast, there was a minimal oval cell response in Iloprost treated animals (Figure 5-4B and 5-4D).

Decrease in the Number of Proliferating Cells in Iloprost Treated Rat Liver Following 2-AAF/PHx.

Next, oval cell proliferation was monitored by *in vivo* BrdU labeling. S-phase cells labeled by BrdU in Iloprost treated animals were compared to those of control animals. In control animals, more than 32.45±1.4 cells/periportal region were in S phase at day 7 post PHx. By day 9 post PHx, around 42.39±9.41 cells/periportal region were found to be in S phase (Figure 5-5A, 5-5C and 5-5E). In contrast, an approximate 3.26 fold decrease of S-phase cells at day 7 and a 2.42 fold decrease of S-phase cells at 9 post PHx in Iloprost treated animals were observed as compared to those of control animals (Figure 5-5B, 5-5D and 5-5E). Furthermore, the BrdU positive cells were more evenly distributed across the liver lobule in Iloprost treated animals. These observations indicate that Iloprost greatly diminishes proliferation of periportal oval cells in 2-AAF/PHx treated animals.

AFP Message Is Decreased in Iloprost Treated Rat Liver Following 2-AAF/PHx.

It is known that AFP is expressed by oval cells participating in oval cell aided liver regeneration. AFP expression decreases as oval cells begin to differentiate into hepatocytes, disappearing entirely upon completion of liver regeneration. AFP expression in Iloprost treated animals was determined by quantitative real time PCR. The AFP message level was decreased 3.4 fold at day 7 following PHx in Iloprost treated animals. By day 9, AFP message is decreased 4.76 fold as compared to the control group (Figure 5-6A). The decrease of AFP expression in Iloprost treated animals were further verified by Northern analysis shown in Figure 5-6B. These results suggest that Iloprost treatment can effectively suppress the oval cell response brought on by 2-AAF/PHx treatment.

Generation of Recombinant CTGFsiRNA Adenovirus

The two CTGF siRNA sequences and the scramble sequence (from scramble plasmid in psiRNA kit) under the control of H1 promoter were cloned into pADeasy adenovirus vector through an immediate p-shuttle vector. The best two recommended sequences for CTGF siRNA were selected using a program provided by Invivogen. The recombinant virus contained 3 kb p-shuttle H1-CTGF siRNA sequence. The linearized, dephosphorylated recombinant virus DNA was transfected into AD293 cells. The number of amplified virus particles was measured by staining Hexon, a structural protein of virus. The number of pADeasy-CTGF1 siRNA virus and CTGF2 siRNA virus were $1.146x10^{9}$ pfu/ml and the one of CTGF1 siRNA virus was $6.876x10^{10}$pfu/ml.

Recombinant CTGFsiRNA Adenovirus Inhibits CTGF Synthesis in the WBF344 Stable Cell Line Overexpressing CTGF.

We performed a Western analysis to examine the effect of recombinant CTGF siRNA adenovirus on CTGF synthesis. Compared to the cell lysate of pADeasy-scramble, CTGF protein was not decreased by CTGF2siRNA but decreased significantly by CTGF1siRNA adenovirus (Figure 5-7).

Discussion

It has been reported that Iloprost suppresses TGF-β1 induction of collagen and CTGF in fibroblasts in the skin of scleroderma patients. The inhibition of CTGF by Iloprost also reduces collagen levels during TGF- β1 induced fibrosis in the mouse wound chamber model (Stratton et al., 2002 and 2001). In this study we demonstrate that Iloprost effectively blocks CTGF induction during oval cell activation and proliferation in the 2-AAF/PHx model. CTGF expression was significantly decreased in Iloprost treated animals at all time points tested. Although treatment with Iloprost abolishes

CTGF expression, it has little effect on TGF-β1 induction. These results are in agreement with the proposed mechanism of Iloprost activity which blocks CTGF synthesis downstream of TGFβ1 induction. Iloprost treatment was found to be associated with a decreased number of histologically evident oval cells as well as a significantly decreased number of S-phase cells. Furthermore, we demonstrate that the oval cell compartment in Iloprost treated animals expresses lower levels of AFP, an oval cell marker. The concurrent decrease in AFP expression is clear evidence for impaired oval cell response. Of course, given that TGF-β regulates CTGF expression through a complex network of transcriptional interactions and the action of Iloprost on CTGF involves at least Ras/MEK/ERK signal pathway, it still remains to be determined if the impaired oval cell response truly results from the lack of CTGF induction rather than from silencing of another signaling pathway. However, Iloprost does not generally inhibit proliferation because hepatocytes divide normally in Iloprost treated animals that were given PHx alone.

In addition, CTGF siRNAs expressed in adenovirus system were generated in tissue culture system. In theory, compared to the activity of Iloprost, the action of CTGF siRNAs should be more specific to inhibit gene expression. One CTGF siRNA can decrease CTGF expression to 50% in tissue culture condition. This sequence can be delivered into regenerating liver with peak activation of oval cells using recombinant adenovirus in future studies. The inhibition activity can be tested based on determining the level of CTGF gene by Northern analysis. Of course, there is some limitation of this approach. One is that the efficiency by this sequence is not higher enough to see phenotypic change on liver regeneration. The other is due to the nature of adenovirus

system. Usually, the majority of adenovirus is uptaken, cleaned by kupffer cells rather than by stellate cells, oval cells and hepatocytes. If it is the case, siRNA will be able to target CTGF synthesis in those cells, which are one of the major cellular sources of CTGF.

In summary, Iloprost can inhibit CTGF upregulation during oval cell activation and proliferation in the 2-AAF/PHx model. Also, this inhibition was associated with a severely impaired oval cell response to 2-AAF/PHx. These data indicate that CTGF plays an important role in oval cell proliferation during liver regeneration in the 2-AAF/PHx model. In addition, RNA interference approach has been developed in vitro but future studies need to be done to test the efficiency of recombinant adenovirus CTGF siRNA #1 in vivo.

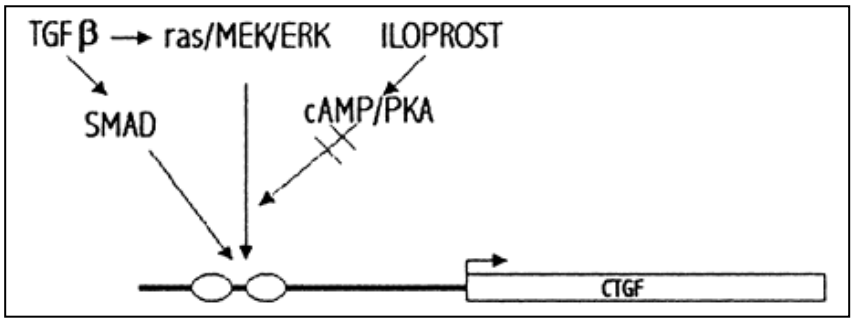

Figure 5-1. Inhibition of CTGF transcription is believed to involve activation of protein kinase A and subsequent inhibition of the Ras/MEK/ERK pathway (Stratton R et al., 2002).

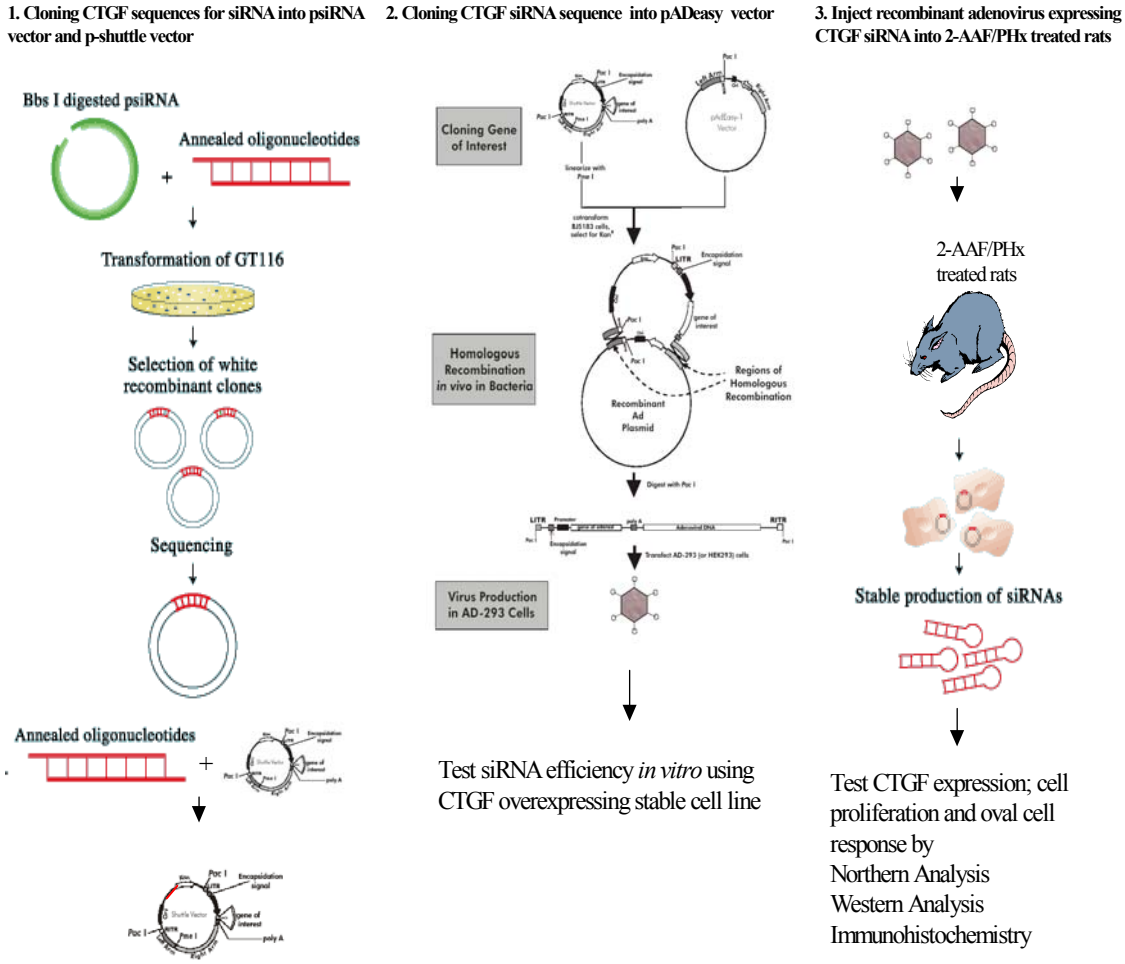

Figure 5-2. The flow chart of how to generate CTGF siRNA using adenovirus system.

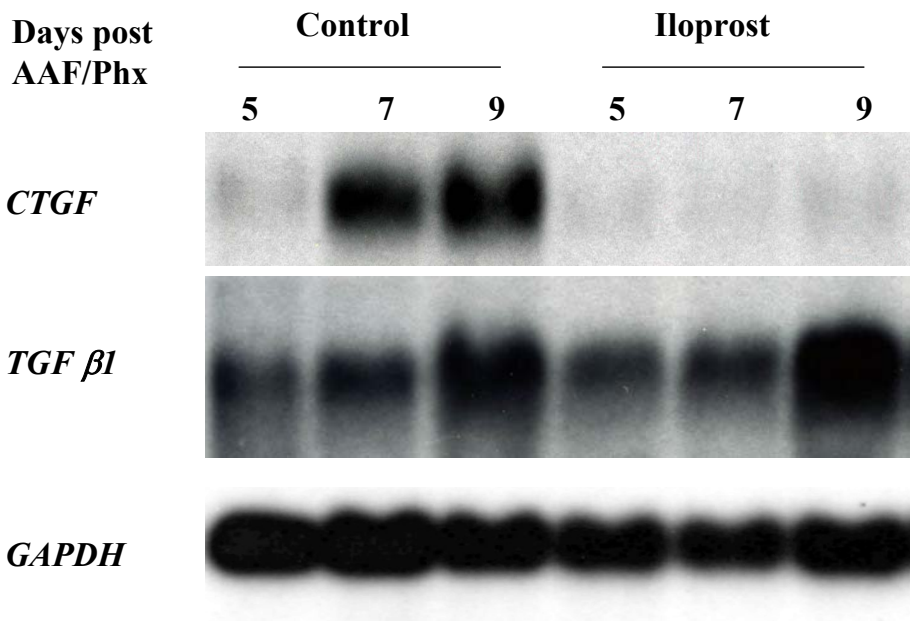

Figure 5-3. Iloprost blocks upregulation of CTGF but doesn't affect TGF-β 1 induction following 2-AAF/PHx treatment. Northern blot analysis showed that CTGF upregulation is block while TGF-β1 expression remains unaffected by Iloprost in 2-AAF/PHx treated rats. GADPH was used as a loading control.

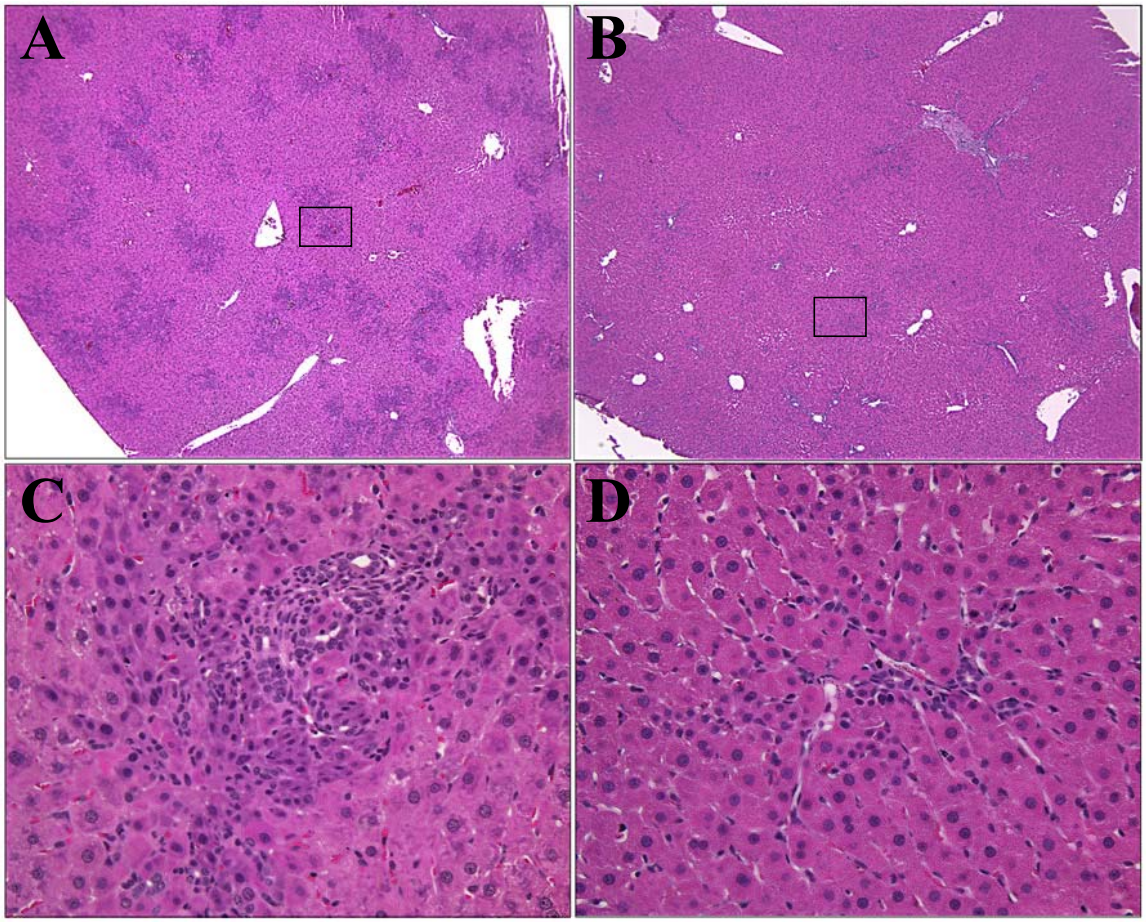

Figure 5-4. Decrease in the number of histologically evident oval cells in Iloprost treated rat liver following 2-AAF/PHx. (A) Portal regions of H&E stained liver sections from 2-AAF/PHx treated rats contain an abundance of cells with high nuclear to cytoplasm ratio (40X). (B) Far fewer of these cells are seen in sections from rats that received Iloprost (40x). (C) Magnification of the area outlined in A (400X). (D) Magnification of the area outlined in B (400X).

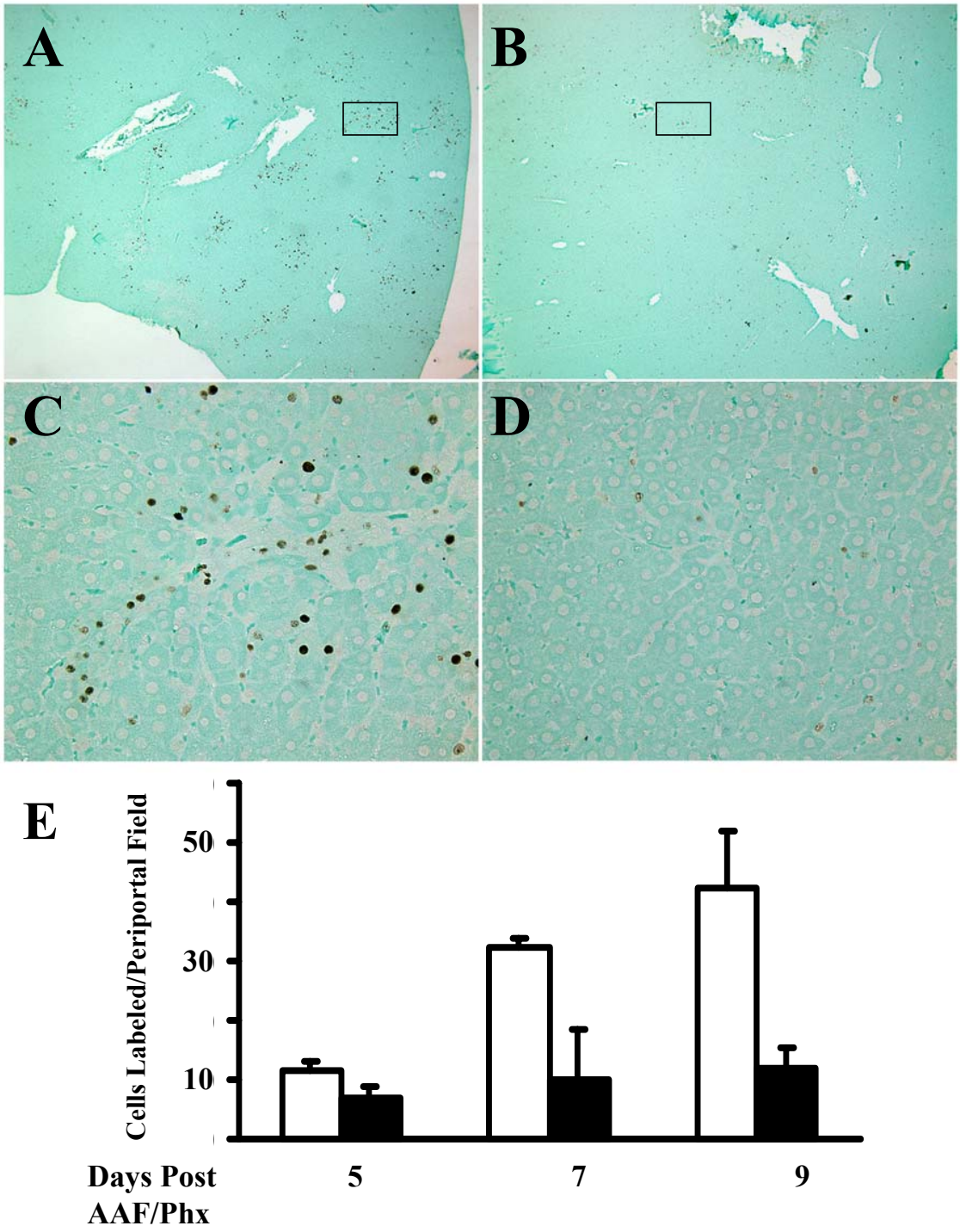

Figure 5-5. Decrease in the number of proliferating cells in Iloprost treated rat livers following 2-AAF/PHx. (A) Portal regions of BrdU stained liver sections from day 7, 2-AAF/PHx treated rats contain a high number of proliferating cells (40X). (B) A dramatic decrease in proliferation is seen in sections from rats that received Iloprost (40x). (C) and (E) Magnifications of the area outlined in A (100X and 400X respectively). (D) and (F) Magnifications of the area outlined in B (100X and 400X respectively).

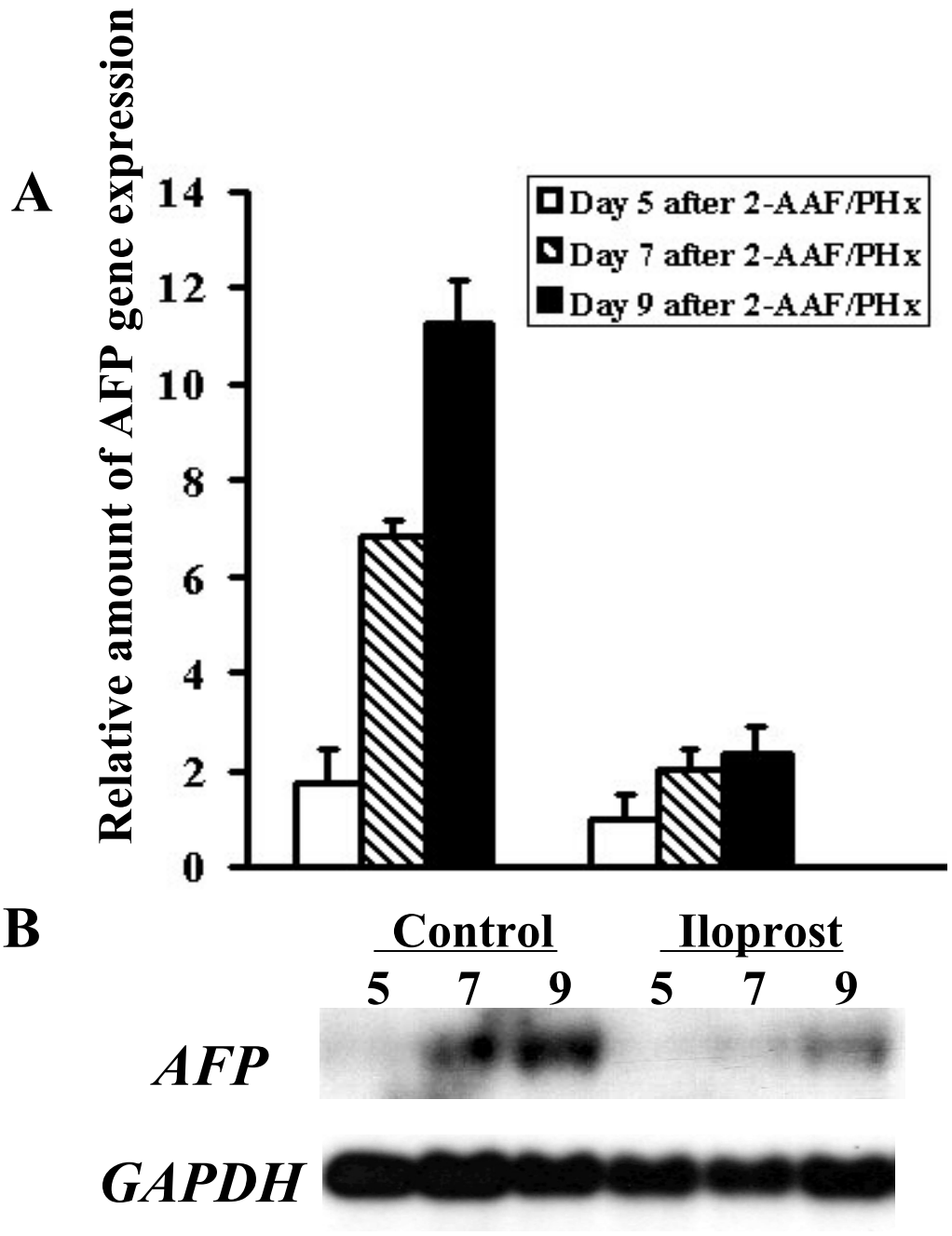

Figure 5-6. AFP message is decreased in Iloprost treated rat liver following 2-AAF/PHx. (A) Quantitative, real time PCR shows a substantial reduction in liver AFP message following 2-AAF/PHx treatment in rats that received Iloprost (second set of bars) as compared to control rats (first set of bars.) Data are normalized to the Iloprost treated sample at day 5 following 2-AAF/PHx. Data represent the mean value $\pm$ SD ($n \geq 3$). (B) AFP expressions at day 5, 7, and 9 in Iloprost treated animals were significantly reduced compared to those of control animals in a Northern analysis.

Figure 5-7. Recombinant CTGFsiRNA adenovirus #1 inhibits CTGF synthesis in the CTGF overexpressing WBF344 cell line in a Western analysis.

CHAPTER 6
IDENTIFICATION OF CTGF BINDING PROTEINS BY USING A YEAST TWO-HYBRID APPROACH

Introduction

Most of protein functions within complicated cellular pathways, interacting with other proteins either as pairs or as components of larger complexes. Such protein-protein interactions form the basis of regulation and coordination between different cellular activities. Direct interactions between proteins and ECM components modulate many biological processes such as cell adhesion, proliferation, migration and differentiation.

CTGF is an adhesive matricellular protein and belongs to the CCN family, which represents a new class of signaling molecule regulating cell proliferation, migration, differentiation and angiogenesis. CTGF contains an N-terminal signal peptide followed by the four structural domains that are largely conserved among the different members of the CCN family. Domain I immediately follows the signal peptide and resembles insulin-like growth factor binding proteins (IGFBPs). Domain II is a von Willebrand type C module and domain III is thrombospondin repeat 1 module. Domain IV is a putative cystine knot (Lau and Lam, 1999; Moussad and Brigstock, 2000; Perbal, 2001). Residues 247-260, 274-286, and 305-328 in module 3 of human CTGF bind strongly to heparin (Brigstock et al., 1997). The configuration of these domains may not only dictate direct actions of CTGF on target cells, but also its bioavailability, half-life, binding of other protein moieties and regulation in time and space. Using a yeast two-hybrid system, CTGF was found to bind to VEGF through specific interaction between the TSP-1

domain of CTGF and the exon 7-coded region of VEGF (Inoki et al., 2002). The interaction can block the angiogenesis activity of VEGF by preventing VEGF and VEGF receptor binding. The similar sequestration of CTGF was found to block BMP signaling by preventing BMP binding to its receptor in the early development of *Xenopus* (Abreu et al., 2002d). CTGF overexpression in *Xenopus* can antagonize BMP4 signaling through a binding site in the amino terminal Von Willebrand factor domain of CTGF. In addition, CTGF interacts with TGF-β through a similar binding site of CTGF and this binding is believed to facilitate the TGF-β presentation to the high-affinity TGF-β type II receptor (Abreu et al., 2002c). CTGF promotes cell adhesion through integrin and heparin sulfate proteoglycan on cell surface (Gao and Brigstock, 2004). The region of the CTGF protein that interacts with integrin $\alpha_v\beta_3$ is C terminus of CTGF. The multiligand receptor, low density lipoprotein receptor-related protein receptor (LRP) binds to CTGF in heparin dependent manner and forms cell surface complexes (Gao and Brigstock, 2003; Segarini et al., 2001). This pathway may represent a rapid internalization and degradation of CTGF while the function of this pathway in cell signaling is unknown (Chen et al., 2001).

Little has been known about the molecular mechanism of CTGF in matrix to regulate oval cell activation during liver regeneration. None of studies has been done on the role of CTGF during liver remodeling at the protein level. In this chapter, we used the HybriZAP-2.1 two-hybrid vector system and constructed a cDNA library to screen CTGF binding proteins. This system is designed to detect protein-protein interactions in vivo in the eukaryotic organism, yeast. It is based on the fact that transcription factor GAL4 contains two domains: the DNA binding domain (BD) capable of recognizing upstream activating sequences (UAS_{GAL1} or UAS_{GAL4}) of promoters of target genes, the

transcriptional activation domain (AD) capable of recruiting RNA transcriptional machinery. Separation of the two domains causes the loss of the activity of GAL4 to activate gene expression unless two fusion proteins bring the two domains together. In this system, two chimeric hybrid proteins are designed: baits are proteins of interest (X) fused with the carboxyl BD domain of GAL4; preys are a library of proteins (Y) fused with the carboxyl AD domain of GAL4. When expressed in yeast, X bait with BD domain can recognize UAS_{GAL1} or UAS_{GAL4} at the promoter region of reporter genes (*LacZ* encoding β-galactosidase and *His3* encoding Histidine) in the yeast chromosome. The expression of Y prey with AD domain can bind to the components of transcription machinery. Neither of the chimeric hybrids alone is capable of initiating specific transcription of reporter genes in yeast. However, specific transcription of reporter genes occurs when the interaction of X and Y brings AD and BD of GAL4 together.

Using this approach, several interesting interactors including fibronectin, extracellular matrix protein 1 and histidine rich glycoprotein were identified in this chapter. Further characterization of these candidates in future would help us to understand how CTGF regulates oval cell response during liver regeneration.

Materials and Methods

Media

LB Agar contains 10 g/liter of NaCl, 10 g/liter of tryptone, 5 g/liter of yeast extract, 20 g/liter of agar and PH 7.0. LB liquid is the same as LB Agar without agar. YPD-Agar media contain 20 g/liter of Difco peptone, 10 g/liter of yeast extract, 15–20 g/liter of agar, 2% glucose and PH5.8. YPD liquid is the same as YPD Agar without agar. SD agar contain 6.7g/LDifco yeast nitrogen base without amino acids; 20g/L agar; 2% glucose and PH5.8 and 1xdropout solution. SD liquid is the same as SD Agar without agar.

10Xdropout solution contains 300 mg/L L-Isoleucine; 1500 mg/L L-Valine; 200 mg/L L-Adenine hemisulfate salt; 200 mg/L L-Arginine HCl; 300 mg/L L-Lysine HCl; 200 mg/L L-Methionine; 500 mg/L L-Phenyalanine; 2000mg/L L-Threonine; 300 mg/L L-Tyrosine and 200 mg/L L-Uracil.

Yeast Transformation

Yeast transformation was carried out by PEG/ LiAc method. Y187 or HF7C strain was grown in YPD media before transformation. The transformants were grown in SD selection media. L-Leucine is a selection marker for preys of cDNA library. L-Tryptophan is a marker for baits. Histidine (*His3*gene) and β-galactidose (*LacZ* gene) are reporter genes for interaction.

Construction of a Yeast Two Hybrid cDNA Library

Livers with maximal oval cell activation (day 8 after 2-AAF/PHx) were used for RNA preparation. The HybriZAP-2.1 two-hybrid vector system (Stratagene) was used to identify genes encoding proteins that interact with CTGF baits. The library was constructed based on manual instruction. Briefly, total RNA of livers was reverse-transcripted into first- and second-strands of cDNAs. The cDNA termini were blunted and ligated to the EcoR I adaptors. The EcoR I ends were phosphorylated before cDNAs were digested with XhoI. The digested cDNAs were size fractionated to collect a population with a size larger than 400 bp. The fractioned cDNAs were ligated into the HybriZAP-2.1 vector and packaged using high-efficiency Gigapack III Gold packaging extract. XL1-Blue MRF^- cells were used to titer the package efficiency. The HybriZAP-2.1 library was amplified and the pAD-GAL4-2.1 phagemid vector was in vivo excised from the HybridZAP-2.1 vector in XLOLR strain with exAssist helper phage. The excised phagemid library was amplified in LB broth with 100ug/ml amplicillin. More

than 500 ug library cDNAs was isolated and transformed into Y187 strain. The pretransformed library was grown in SD agar lacking L-Leucine and yeast cells were collected in sorbital solution and stored in 25% glycerol at -80^{o}C before screening. The transformation efficiency was tested to see if it is high enough for library screening. The pretransformation efficiency is thawed and used before each screening.

Generation of Baits Carrying Different Domains of CTGF Protein and Auto-activation Testing

DNA fragments corresponding to different domains of CTGF were PCR amplified with primers shown in Figure 6-1. The Two hybrid Start primer has SalI restriction enzyme sites at 5' end. The other three primers contain NotI restriction enzyme sites at 3' end. PCR products were cloned into pGEM vector and verified by sequencing analysis. The CTGF domains were digested with SalI and NotI restriction and further cloned to the 3' of Gal 4 DNA binding domain DNA sequence of bait vector pXD86cycloheoxymide. The resulting plasmids contain a chimeric hybrid sequence encoding Gal 4 DNA binding domain and in-frame fused CTGF domains. All baits don't contain sequences encoding the signal peptide region of CTGF (1-20 amino acids).

To test if CTGF baits can self activate reporter genes in absence of preys, plasmids carrying CTGF baits were transformed into HF7C yeast strain and stored at -80^{o}C before use. The transformed yeast cells were plated on SD agar media lacking L-Tryptophan or lacking L-Tryptophan and L-Histidine. The growth was observed two or three days after plating.

Screening of the Yeast Two Hybrid cDNA Library

Single HF7C yeast colony carrying individual CTGF baits was cultured to OD_{600}=0.5 in SD liquid in presence of 20mg/liter of L-Tryptophan. The HF7C strain was

mated with Y187 strain of cDNA library. After mating, the yeast population was plated on SD agar media lacking L-Tryptophan, L-Leucine and L-Histidine and in presence of 5mM 3-AT. Candidates which were survived in the selection media after 10 days of growth were randomly picked up and grew on SD agar media lacking L-Tryptophan, L-Leucine and L-Histidine and in presence of 5mM 3-AT. Plasmid DNAs of 96 growing candidates were amplified by Rolling cycle amplification (RCA) using the TempliPhi 100 kit from Amersham followed by sequencing analysis using primer 5'-AGGGATGTTTAATACCACTAC-3' according to (Ding et al., 2004).

Results

CTGF Baits Are Not Self-activated in Yeast.

Four cDNA fragments encoding different domains of CTGF were fused in-frame to the C terminal end of DNA binding domain of GAL4 on the bait vector pXDcycloheximide86. The resulting plasmids were transformed into a type of yeast strain HF7C for mating and screening purpose. To rule out the possibility that these CTGF baits can activate reporter genes in absence of preys, we carried out self-activation test in media with or without selection markers Histidine and Tryptophan. Tryptophan is a marker for bait vector and histidine is a marker for activation of reporter gene. Bait empty vector is used as a negative control. As expected in Figure 6-2, all of individual yeast tranformed with four CTGF baits survived in media without Tryptophan but didn't grow in media without both Tryptophan and histidine, indicating that baits alone are incapable of initiating transcription of *His3*gene. Thus, all CTGF baits are feasible for screening.

Construction of a Yeast Two Hybrid cDNA Library Specific for Oval Cell Mediated Liver Regeneration

Because there is no available commercial yeast two-hybrid cDNA library specific for oval cell mediated liver regeneration, we have to construct a cDNA library for screening. We used the HybriZAP-2.1 two-hybrid vector system to construct the library. The size of cDNA was controlled by fractionation of pools of synthesized population. To monitor the range of cDNA size in this library, eighteen clones were randomly chosen after package, excision and amplification. Double digestion with NotI and SalI which are flanked the cDNA insertion sites on prey vector was performed to release inserts. Figure 6-3 shows that most of them carry inserts with the size ranging from 500 to 3 kb. The amplified cDNAs were transformed into α type of yeast strain Y187. The transformation efficiency of cDNA library was 9 million/ml after titration, which is sufficient for screening.

Candidates Binding to CTGF Baits

The screening was performed through mating HF7C strain carrying bait with Y187 strain carrying prey cDNA library. More than 25 million transformants were obtained in each screening. Ninety six clones which survived in SD agar media lacking L-Tryptophan, L-Leucine and L-Histidine and in presence of 5mM 3-AT were randomly picked up for sequencing analysis in screening for each bait. Table 6-1 lists all candidates identified.

Candidates Binding to Bait I

Using domain I (IGFBP domain) as a bait, we identified 5 different preys. One is fibronectin 1 (Genebank accession number NM_019143). The identified clone contains 6911-7251 bp of fibronectin 1 gene. This region encodes a sequence corresponding to

last two-fibronectin type 1 domains (FN1) and carboxyl terminus of fibronectin 1 (Figure 6-4). FN1 is one of three types of internal repeat within the plasma protein fibronectin. The similar domain is also located in coagulation factor XII, HGF activator and tissue-type plasminogen activator (t-PA). In t-PA and fibronectin, this domain type contributes to fibrin binding.

The second prey is Von Willebrand factor (vWF) (Genebank accession number XM_342759). vWF is associated with a 'pseudohemophilia' disease discovered in 1931 (Von Willebrand). This deficiency has a hemorrhagic syndrome with a prolonged bleeding time and is caused by a low level of antihemophilic globulin (AHG; factor III). A multimer circulates as a complex with factor VIII shielding factor VIII from degradation and localizing factor VIII at the site of vascular injury. Each mature vWF subunit (domains D', D3, A1, A2, A3, D4, B, C1, C2, CK) dimerizes through disulfide bonds near the carboxyl terminus. Each dimmer further multimerizes through disulfide bonds near the amino terminus (Figure 6-5A). In the damaged vessel wall, collagen and vWF of the subendothelial matrix become exposed to flowing blood and shear forces. Plasma vWF efficiently binds to exposed collagen and uncoils its structure, supporting the adhesion of circulating platelets in synergy with collagen. In our screening, the identified clone contains 7045-7718 bp of the vWF gene, which encodes a C terminal cystine knot-like domain (CTCK). This domain is also found in C terminus of CTGF, TGF-β, nerve growth factor (NGF), platelet-derived growth factor (PDGF) and gonadotropin. The predicted secondary structure of that region includes 2 highly twisted antiparallel pairs of beta-strands and three disulphide bonds. This domain is non-globular and little is conserved among these presumed homologues except for their cystine

residues. CT domains are predicted to form homodimers. Interestingly, C terminal region of CTGF is also a CT domain sharing some conserved amino acids (Figure 6-5B).

The third prey is Mus musculus ataxin 7-like 4 (Genebank accession number BC017546). Three clones were identified to carry the same cDNA of this gene with similar size. The longest clones contain 625-949bp of this gene. Strangely, the full-length gene is 1-1528 but the predicted coding region is very short, only 4-291 bp for 77 amino acids. Thus, the cDNA of the preys are not in the coding region. These clones may represent a false positive candidate.

The forth prey is an ATP-binding cassette, sub-family B (MDR/TAP), member 1A (Abcb1a) (Genebank accession number NM_133401). The identified clone contains 4735-4930bp of this gene, which is located at 3' untranslated region. Since this region doesn't encode any protein sequence, this clone may also represent a false positive candidate.

The fifth prey is histidine rich glycoprotein (HRG) (Genebank accession number NM_133428). HRG is a nonenzymatic protein present in plasma and platelets. The protein contains twelve tandem repetitions of Gly-His-His-Pro-His, which is referred to as a "histidine-rich region" (Koide et al., 1986). This region contains 53% histidine and showed a high degree of similarity to a histidine-rich region of high molecular weight kininogen. In our screening, more than fifty clones carry the sequences of this gene with varying lengths. The longest clone contains 583-1652 bp of this gene, which encodes the middle of and C terminal HRG. The shortest clone contains 1020-1652bp of this gene, which encodes a short region in the middle of HRG after the histidine-rich region. The short clones represent the minimal region for binding.

Candidates Binding to Bait II

The second bait for screening carries domain I and II of CTGF (IGFBP and VWC domains). Four types of preys were identified. Two of them, HRG and Mus musculus ataxin 7-like 4 are the same as the ones identified using bait I. These baits most likely bind to domain I region of bait II. Two other clones are unique to bind to domain II of CTGF. One is chordin (Genebank accession number XM_221307). The identified clone contains 1945-2526 bp of the gene, which encodes C terminal region of the protein (CR4 domain) (Figure 6-6A). Interestingly, VWC domain is also present in chordin and called as "CR" domain. Like Chordin CRs, the CTGF VWC is about 64 amino acids long and contains 10 conserved cystines. However, the conserved tryptophan residue is replaced by a phenylalanine and the motifs CXXCXC and CCXXC are replaced by CXXXCXC and CCXXXXC, respectively (Figure 6-6B). Chordin is a key developmental protein that dorsalizes early vertebrate embryonic tissues by binding to the ventralizing TGF-β-like bone morphogenetic proteins and sequestering them in latent complexes (Bachiller et al., 2000). No any data shows the involvement of chordin in oval cell mediated liver region. The binding of two VWC domains between CTGF and chordin indicates that CTGF regulates BMP signaling. Supporting evidence came from the observation that the injection of CTGF mRNA into Xenopus embryos induced anti-BMP phenotypes and CTGF physically bound to BMP and TGF-β1 through the VWC domain (Abreu et al., 2002b). How the BMP signaling is involved in oval cell mediated liver regeneration remains unknown.

The other unique prey for domain II binding is properdin (AA 5 - 441) (Genebank accession number XM_216784). Properdin is a plasma protein that regulates the

alternative complement pathway of the innate immune system. It binds and stabilizes the C3b.Bb complex (C3 convertase) that is formed from activated C3 (C3b) and one of the major cleavage products of Factor B (Bb). This interaction protects C3b in the complex from inactivation by Factor 1 with Factor H as co-factor that decreases the half-life of the C3b.Bb complex in plasma. Properdin contains six thrombospondin type 1 repeats (TSRs) as shown in Figure 6-7. TSRs have been reported to function as (a) attachment sites for many cell types, (b) inhibitors of angiogenesis, (c) protein binding sites, and (d) glycosaminoglycan (GAG) binding sites. Plasma properdin forms dimmer, trimer or tetramer in physiological condition (Sun et al., 2004). The molecular structures of dimeric and trimeric properdin were studied by X-ray scattering and analytical ultracentrifugation shown as Figure 6-7. The identified clones contain 600-1106bp of this gene. The encoded protein region is TSR3, TSR4, TSR5 and TSR6 of properdin as shown in Figure 6-7.

Candidates Binding to Bait III

The third type of baits for screening contains domain I (IGFBP domain), II (VWC domain), III (TSP-1 domain) and a hinge region between II and III domains of CTGF. Domain III is a thrombospondin type 1 (TSP1) with a cell-attachment motif WSXCSXXCG that binds sulfated glycoconjugates (Bork, 1993).

Using the third bait, we identified four types of preys. Two of them, HRG and Properdin are able to bind domain I and domain II respectively. The other two seem to be specific for binding to domain III. One prey is similar to a disintegrin and metalloprotease with thrombospondin motifs-7 (ADAMTS-7, Genebank accession number XM_236471). This protein belongs to a disintegrin-like and metalloprotease with thrombospondin type 1 motifs: the ADAMTS family which are complex secreted

enzymes containing a prometalloprotease domain and at least one thrombospondin type 1 repeat. The identified clone contains 2984-3436 bp of this gene, which encodes spacer region and last TSRs (Figure 6-7). Usually, the binding protein of ADAMTS is a substrate for the protease. Therefore, it is interesting to test if CTGF can be cleaved by ADAMTS-7 in future experiments.

The second prey is solute carrier family 13 (sodium/sulfate symporters, SLC13), member 4 (Slc13a4), (Genebank accession number NM_172892). The identified clone contains 2094-2792bp of this gene. This region encodes C terminal region of the protein, which includes part of permease SLC13 and the end of C terminus. Considering its function, CTGF binding to this protein may not represent significant biological activity during oval cell mediated liver regeneration.

Candidates Binding to the Full-length CTGF

Bait IV is the full-length CTGF lacking the first 20 amino acids of signal peptide region. Using bait IV, we identified 5 different preys. Two of them, HRG binding for domain I and Slc13a4 binding for domain III were also identified by screening using bait IV. Three other new preys seem be specific for domain IV. The first prey is extracellular matrix protein 1 (Genebank accession number NM_053882). The identified clone contains 288-965bp of this gene, which encodes almost a full-length protein. ECM 1 regulates endochondral bone formation by inhibiting alkaline phosphatase activity and bone mineralization (Deckers et al., 2001), stimulates proliferation of endothelial cells and induces angiogenesis in the chicken chorioallantoic membrane assay (Han et al., 2001).

The second prey encodes rat homologue of Drosophila slit protein (slit2). Slit family is composed of secreted guidance proteins, which regulate neuronal migration and

axon growth via interaction with their cellular roundabout receptor (Robo) in cell membrane (Wu et al., 1999; Li et al., 1999). Slits can also block leukocyte chemotaxis (Wu et al., 1999). The identified clone carries 4269-4859 bp region of the slit2. This region encodes the whole C terminus of the protein after 992 amino acids (Figure 6-10). Interestingly, there are two Calcium-binding EGF-like domain (EGF_CA) and cystine knot in that region. Calcium-binding EGF-like domain is usually present in a large number of membrane-bound and extracellular (mostly animal) proteins. Many of these proteins require calcium for their biological function. Calcium-binding sites have been found to be located at the N-terminus of particular EGF-like domains.

The third prey contains 4-483 bp of 40S ribosomal protein S20 gene, which encodes the full-length protein. 40S ribosomal protein S20 is a structure protein for ribosomal machinery. This binding between this protein and CTGF may not represent a biological process because of the location and function of 40S ribosomal protein S20.

Discussion

CTGF protein is composed of mosaic architecture with several modules, which can be found in other secreted and matricellular proteins. We designed four baits to cover different domains of CTGF and identified CTGF binding proteins. All four baits were designed not to contain the first 20 amino acids, a region of the signal peptide. Bait I contains 84 amino acids and covers the whole domain I. Comparing to bait I, bait II has addition 77 amino acids covering the whole domain II. Bait III is designed to cover domain I, II and III while Bait IV contains the full length of CTGF. Any repetitive prey identified by multiple baits should bind to the bait with minimal CTGF sequence. Using this strategy, we can identify interactors specific for each domain. Figure 6-4 summarizes predicted “true” binding proteins for each domain of CTGF.

It is known that domain I is homologous to the N-terminal cystine-rich regions of the six "classic" insulin like growth factor (IGF)-binding proteins, IGFBP-1 to -6 (Bork, 1993). It contains 10 of 12 conserved cystines in IGFBP family and a motif (GCGCCXXC) that is involved in binding IGF with low affinity (Kiefer et al. 1997). Excluding the false positive candidates, Domain I binding proteins include fibronectin 1, vWF and HRG, which are all plasma, extracellular protein. The location and function of them indicate that they are physiological partners of CTGF.

Fibronectin (FN) is a major adhesive, matricellular protein ubiquitously present in most tissues and in blood. As a large multidomain protein, fibronectin contains regions for binding to cells, to itself and to other ECM components such as fibrin, collagen and heparin (Figure 6.4). It is secreted as a disulfide bonded dimmer, which is then assembled by cells into a fibrillar matrix from which it functions (Baneyx et al., 2002). Fibronectin promotes cell adhesion through its interaction with different cell-surface receptors. The primary fibronectin receptors are members of the integrin superfamily of heterodimeric proteins (Tamkun et al., 1986). These receptors serve as a transmembrane link between fibronectin, the cytoskeleton, and cytoplasmic molecules that initiate intracellular signaling cascades that affect cell behavior (Clark and Brugge, 1995; Schwartz and Ingber, 1994). In chapter 3, fibronectin 1 was identified from the subtractive suppression cDNA library as one of genes differentially expressed in Thy-1^{+} oval cells. It was also induced in total liver homogenates and with a kinetic pattern similar to that of CTGF in livers following 2-AAF/PHx (Figure 3.5B). Using the IGFBP domain of CTGF as bait, we identified a clone containing sequences coding for the last two type-I repeats and C terminus of fibronectin 1. So far, no studies have been done to show the physical

interaction between fibronectin1 and CTGF. The binding between CTGF domain I to fibronectin1 displays a close relationship of CTGF and fibronectin in term of function and expression. This interaction may reflect a mechanism in that CTGF modulates cell adhesion and growth through the accessibility and availabilty to fibronectin in the ECM.

CTGF binds to the carboxyl-terminal CT domain of vWF. vWF is involved in platelet adhesiveness and contributes to vascular integrity. The biological relevance of the binding between CTGF and vWF is not clear, but it may indicate a role of CTGF in blood clotting. Interestingly, the IGFBP domain of CTGF can interact with the CT domain of vWF and CTGF is also composed a CT domain at its C terminal region. It will be interesting to test if C terminal CT domain of CTGF binds to its own N terminal IGFBP domain.

HRG represents 70-80% of clones identified using all four baits. The repetitive identification of the same prey with different cDNA size indicates a strong binding with CTGF domain I. It is known that HRG is an abundant plasma protein and binds to plasminogen and heparin. By binding to plasminogen, it reduces the amount of plasminogen in the circulating blood that is available for activation into plasmin and thus acts as an inhibitor of fibrinolysis. By binding to heparin, it reduces the amount of heparin and through this mechanism reduces the inhibition of coagulation by the heparin-antithrombin III complex. An excess of HRG is predicted to have a prothrombotic effect. HRG deficiency causes thrombophelia (Shigekiyo et al., 1998). HRG binding to IGFBP domain of CTGF may indicate a potential role of CTGF in blood coagulation. Perhaps, HRG is a carrier protein of CTGF and locates CTGF to the sites of tissue repairing.

Bait II contains an additional domain- a Von Willebrand type C domain (VWC) that occurs in Von Willebrand factor as well as various mucins, thrombospondins, and collagens (Bork, 1993). It is also present in chordin and called as "CR" domain. Like Chordin CRs, the CTGF CR is about 64 amino acids long and contains 10 cysteines. However, the conserved tryptophan residue is replaced by a phenylalanine and the motifs CXXCXC and CCXXC are replaced by CXXXCXC and CCXXXXC, respectively (Abreu et al., 2002a; Garcia et al., 2002). It will be interesting to see whether these particularities of the CTGF VWC alter its binding activities. Chordin dorsalizes early ventebrate early vertebrate embryonic tissues by binding to bone morphogenetic proteins (BMPs) and sequestering them in latent complexes. No any data shows the involvement of chordin in oval cell mediated liver region, but it may regulate this process by binding to CTGF and sequester BMPs.

Properdin is the other protein binding to domain II of CTGF. Properdin is a plasma protein that is active in the alternative complement pathway of the innate immune system. It is a positive regulatory factor that binds to many microbial surfaces. The identified clones contain 600-1106bp of this gene. The encoded protein region is TSR3, TSR4, TSR5 and TSR6 of properdin. Future study is needed to test which TSRs in properdin binds to VWC domain of CTGF. The biological significance between properdin and CTGF binding in oval cell mediated liver regeneration is not clear.

One interactor for domain III is similar to a disintegrin and metalloprotease with thrombospondin motifs-7, which belongs to a disintegrin-like and metalloprotease with thrombospondin type 1 motif: the ADAMTS family. Known functions of ADAMTS proteases include processing of procollagens and von Willebrand factor as well as

catabolism of aggrecan, versican and brevican. They have been demonstrated to have important roles in connective tissue organization, coagulation, inflammation, arthritis, angiogenesis and cell migration (Apte et al., 1995). ADAMTS-2 is procollagen N-proteinase (ADAMTS2) (Colige et al., 1997), ADAMTS4 is aggrecanase (Nagase and Kashiwagi, 2003) and ADAMTS13 is von Willebrand factor (vWF) protease (Zheng et al., 2003). A future experiment needs to test if CTGF is a substrate of ADAMTS-7. A supporting evidence for physiological cleavage of CTGF is the isolation of 10 kDa bioactive CTGF low molecules (Brigstock et al., 1997).

The other interactor for domain III is solute carrier family 13 (sodium/sulfate symporters). The biological relevance of the binding between CTGF and this protein is not clear considering its function.

Domain IV is a C-terminal (CT) module that also occurs in the C termini of a variety of unrelated extracellular mosaic proteins including TGF β and PDGF and is responsible for dimerization and receptor-binding (Bork, 1993). One of interactors for this domain is ECM 1. ECM1 binds to the major heparan sulphate proteoglycan, perlecan and plays an important role in the control of keratinocyte differentiation. Loss-of-function caused by mutations in the *ECM1* gene or by autoantibodies against ECM1 protein cause genodermatosis, lipoid proteinosis, which is characterized by thickening of the skin, mucosae, and certain viscera (Figure 6-9) (Hamada et al., 2002). It is believed that ECM1 may act as'biological glue' in the dermis, helping to regulate basement membrane and interstitial collagen fibril macro-assembly and growth factor binding. Therefore, CTGF binding to ECM1 may represent a mechanism to facilitate cell adhesion or migration.

The other interactor for CT domain is Slit2, which is similar to a family that plays a critical role in central nervous system midline formation. Slit family is composed of secreted guidance proteins, which regulate neuronal migration and axon growth via interaction with their cellular roundabout receptor (Robo) in cell membrane (Wu et al., 1999; Li et al., 1999). Slits can also block leukocyte chemotaxis (Wu et al., 2001). Recently, Slit 2 has been shown to physically bind to Drm/Gremlin and Dan, two homologous secreted antagonists of bone morphogenic proteins. Drm and Dan function as inhibitors for monocyte migration induced by stromal cell-derived factor 1 a (SDF-1a) or fMLP. SDF-1 appears to play an important role in oval cell migration into liver (Hatch et al., 2002). Therefore, Slit2 and CTGF binding may contribute to the migration of oval cell during liver regeneration in the 2-AAF/PHx model.

In summary, we identified some interesting candidate interactors for four domains of CTGF. After analysis, some more interesting ones were listed in Figure 6-11. These interactors link function of CTGF to cell adhesion (fibronectin1), migration/chemoattraction (Slit2), cell coagulation (properdin, vWF, HRG), modulator of BMP signaling (chordin) and cell proliferation and differentiaion (ECM 1). AMTMts7 may act as a protease to physically proteolysis of CTGF into smaller active molecules. Of course, more works need to be done to verify their binding to CTGF in vivo by methods such as immunoprecipitation. Characterization of these binding proteins would provide us an insight into how CTGF regulates oval cell mediated liver regeneration.

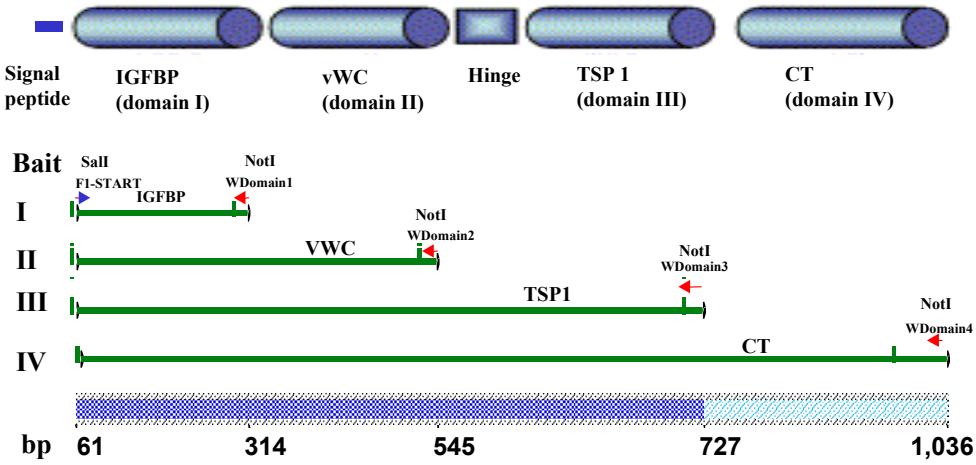

Sal site

CTGF 2HYB F1-START : 5'-GTCGACGCCTGCCACCGGCCAGGACT-3'

CTGF 2HYB F-WDomain1: 5'-GCGGCCGCTTAACACGGACCCACCGAAGACACA-3'

CTGF 2HYB F-WDomain2: 5'-GCGGCCGCTTAGTGTCTTCCAGTGGTAGGCAG-3'

CTGF 2HYB F-WDomain3: 5'-GCGGCCGCTTACCTCTAGGTCAGCTTCACAGGG-3'

CTGF 2HYB F-WDomain4: 5'-GCGGCCGCCTTACGCCATGTCTCCATACATCTTCCTGT-3'

NotI site

Figure 6-1. Baits containing domains of CTGF for Yeast two hybrid screening. All four baits were designed not to contain the first 60bp cDNA of the signal peptide. Bait I contains the 61-314 bp cDNA of IGFBP module. Bait II has additional 231bp cDNA covering vWC module. Bait III is designed to cover domain I, II and III while Bait IV contains the full length of CTGF. Primer pairs for amplification of each bait are shown: F1-START was used for all baits as the sense primer. Antisense primers were F-WDomain1 for bait I, F-WDomain2 for bait II, F-Wdomain3 for bait III and F-Wdomain4 for bait IV. Sal I and Not I were designed in primer pairs for the purpose of cloning into empty bait vector. Four cDNA fragments encoding different domains of CTGF were fused in-frame to the C terminal end of DNA binding domain of GAL4 on the bait vector pXDcycloheximide86.

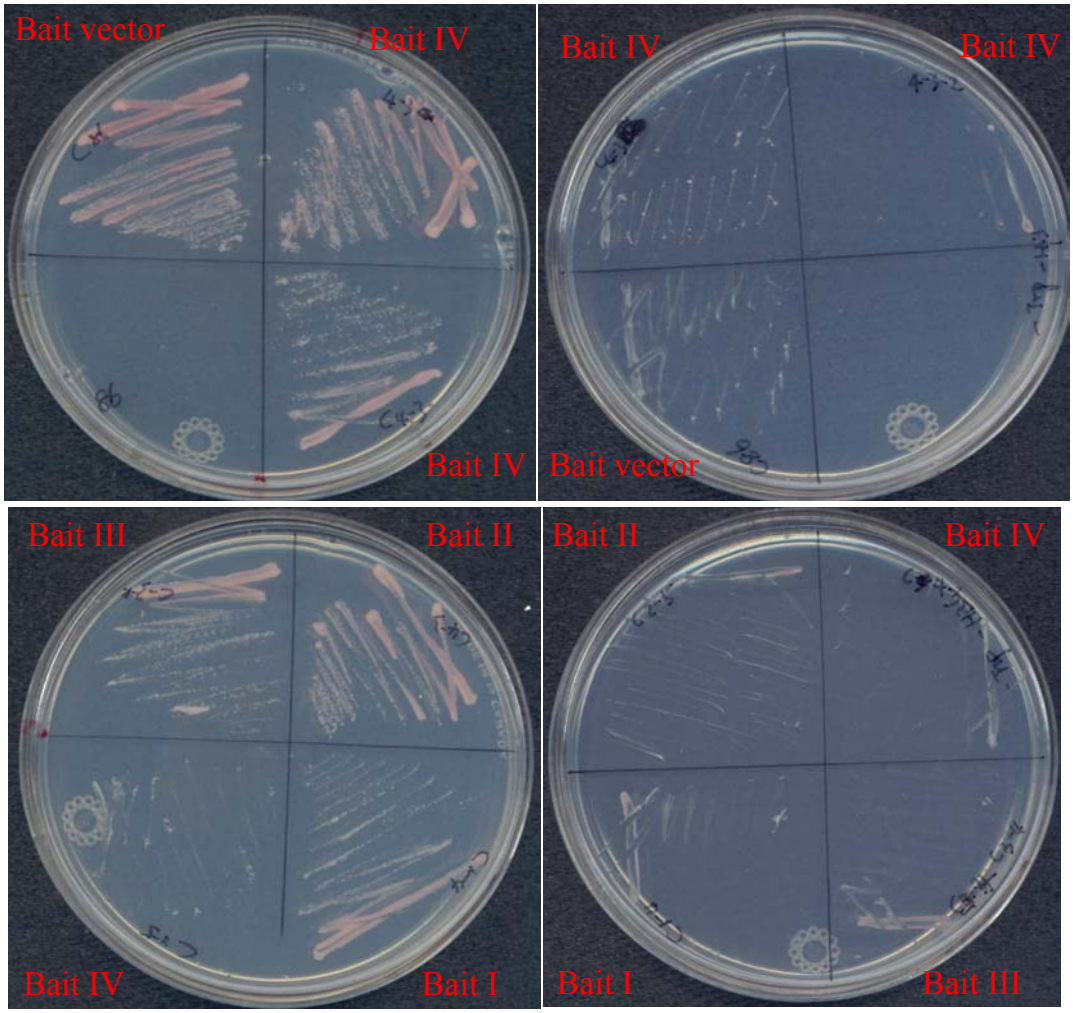

Figure 6-2. Autoactivation testing of pXDcycloheximide 86 baits. Two plates on the left panel were SD/-Trp media while the other two on the right panel were SD media lacking L-Tryptophan and L-Histidine. Tryptophan is a marker for bait vector and histidine is a marker for activation of reporter gene. Bait empty vector is a negative control. All of individual yeast transformed with four CTGF baits survived in media without L-Tryptophan but didn't grow in media without both L-Tryptophan and L-histidine.

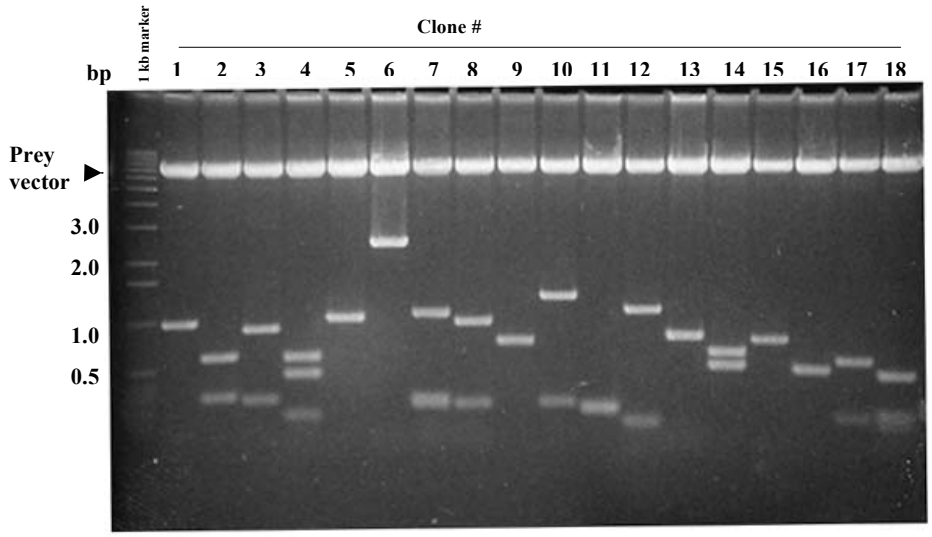

Figure 6-3. Representation of sizes of cDNA inserts in the cDNA library. Eighteen clones were randomly picked up and digested with SalI and NotI to release the insert of cDNA from prey vector. The digested products were separated on 0.7% agarose gel in TAE buffer.

Table 6-1. Summay of all preys identified from screening using CTGF baits containing different domains.

bait	Identities of interactors	Genebank accession #	cDNA of clones identical to sequences in Genebank	Identity
I	fibronectin 1	NM_019143	6911-7551bp	100%
I	Von Willebrand factor (Vwf)	XM_342759	7045-7718bp	97%
I	Mus musculus ataxin 7-like 4	BC017546	625-949bp	88%
I	ATP-binding cassette, sub-family B	NM_133401	4735-4930bp	100%
	member 1A (Abcb1a)			
I	Histidine rich glycoprotein	NM_133428	583-1652bp	100%
II	Histidine rich glycoprotein	NM_133428	583-1652bp	100%
II	properdin (AA 5 - 441)	XM_216784	600-1106bp	97%
II	chordin	XM_221307	1945-2526bp	98%
II	Mus musculus ataxin 7-like 4	BC017546	625-949bp	88%
III	Histidine rich glycoprotein	NM_133428	583-1652bp	100%
III	Properdin	XM_216784	600-1106bp	97%
III	a disintegrin and metalloprotease with	XM_236471	2984-3436bp	96%
	thrombospondin motifs-7 preproprotein			
III	solute carrier family 13	NM_172892	2094-2792bp	90%
	(sodium/sulfate symporters),			
	member 4 (Slc13a4)			
IV	Histidine rich glycoprotein	NM_133428	583-1652bp	100%
IV	extracellular matrix protein 1	NM_053882	288-965bp	99%
IV	rat homologue of Drosophila slit protein	AB011531	4269-4859bp	97%
IV	slit2/mRNA for MEGF5			
IV	Properdin	XM_216784	600-1106bp	97%
IV	40S ribosomal protein S20	XM_216327	4-483bp	99%

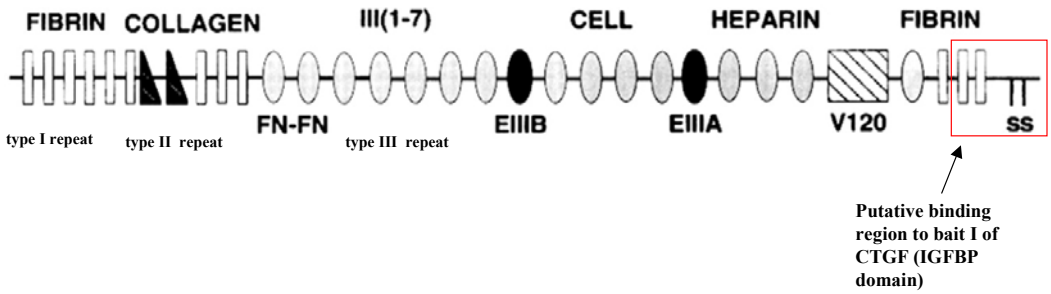

Figure 6-4. Structural organization of fibronectin and the putative binding region to bait I. FN is composed of three types of repeating modules, type I (*open rectangles*), type II (*triangles*), and type III (*ovals*). Domains for binding fibrin, collagen, cells, and heparin are indicated as is the location of an FN binding site in repeats $III_{1\text{-}2}$. Some domains are separated by alternatively spliced regions EIIIA and EIIIB (*dark ovals*) and the V region (*crosshatched box*). The pair of carboxyl terminal cystine required for dimmer formation are shown as SS (Sechler et al., 1998). Red box indicates the last two type I repeats and C terminus of fibronectin that are homology to the sequences on candidate interactors from screening.

A

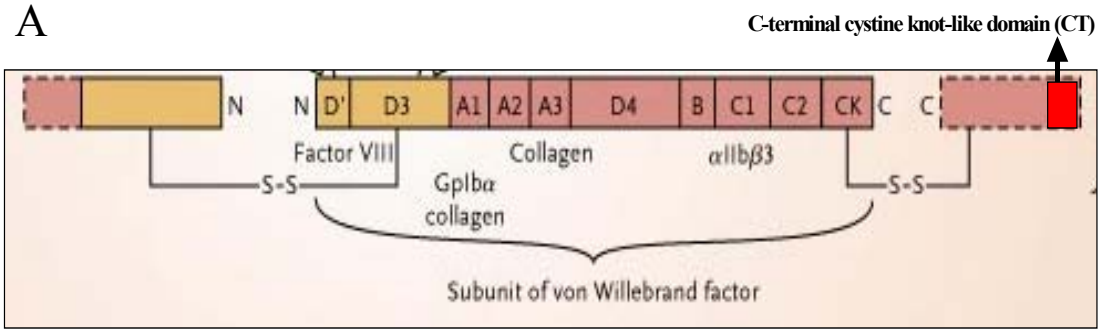

B

Figure 6-5. CT domain of vWF is a candidate binding site for IGFBP domain of CTGF. A is the diagram of von Willebrand factor structure. Each mature vWF subunit (domains D', D3, A1, A2, A3, D4, B, C1, C2, CK) dimerizes through disulfide bonds near the carboxyl terminus. Each dimmer further multimerizes through disulfide bonds near the amino terminus. IGFBP domain of CTGF binds to the carboxyl-terminal CT domain of vow as shown in a red box. B is the alignment of CT domain between vow and CTGF. Conserved amino acids are in red and similar amino acids are in blue.

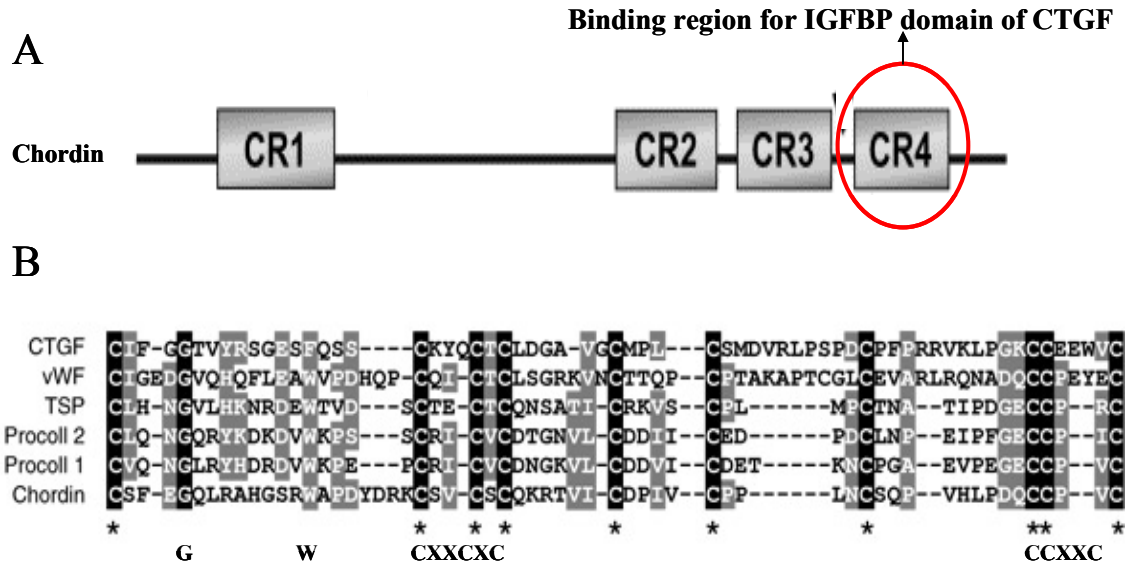

Figure 6-6. Chordin is a candidate interactor for VWC domain of CTGF. A is the schematic representation of chordin structure with four CR domain. CR4 is also called VWC domain. B is the alignment of VWC domains of xenopus CTGF, von Willebrand Factor, thrombospondin, procollagen 1 and 2 and Chordin. Black boxes represent identical amino acids and gray boxes similar amino acids; dashes indicate gaps introduced to optimize the alignment. Asterisks mark the ten identical cystine residues characteristic of CR domains. The conserved tryptophan residue in chordin is replaced by a phenylalanine and the motifs CXXCXC and CCXXC are replaced by CXXXCXC and CCXXXXC, respectively in CTGF (Abreu et al., 2002).

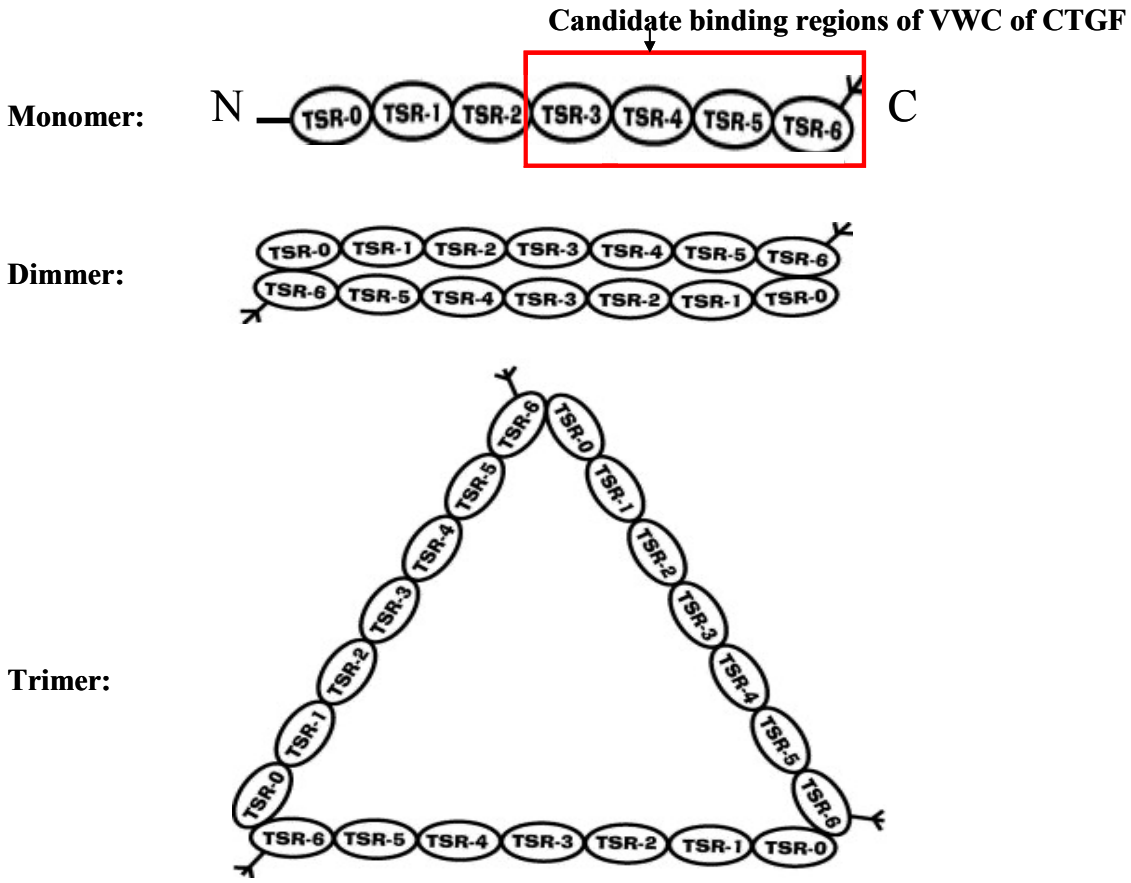

Figure 6-7. Structures of properdin monomer, dimmer and trimmer. N and C represent the N and C terminus of properdin monomer. Properdin monomer is composed of a series of TSRs and the dimmer and trimmer are formed as shown (Sun et al., 2004). The candidate binding region to VWC domain of CTGF is labeled in a red box.

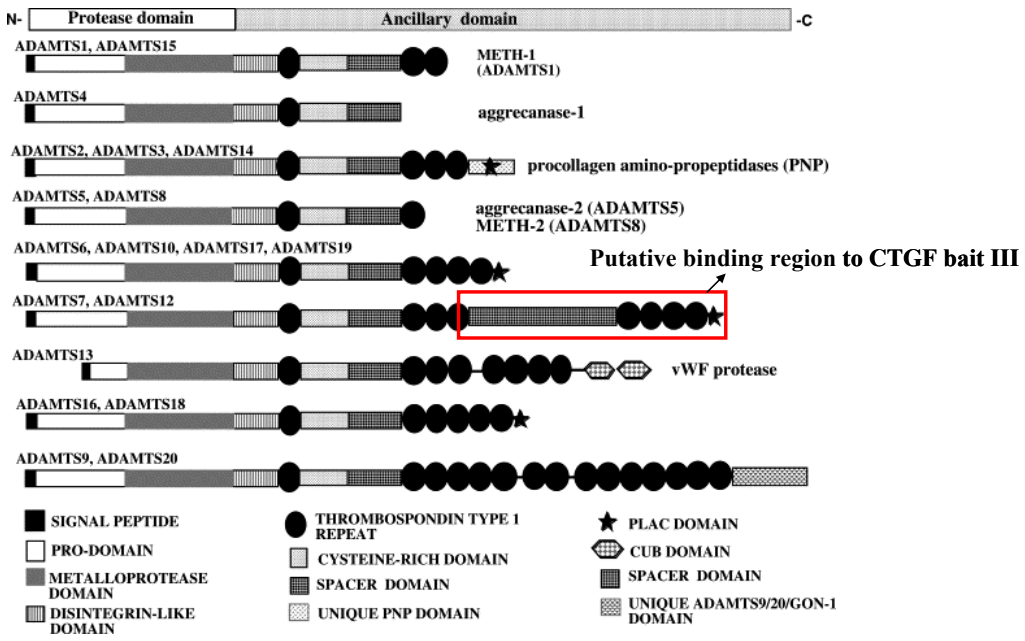

Figure 6-8. Domain organization in the ADAMTS family and ADAMTS7 is a candidate interactor of CTGF bait III. The putative binding region is labeled in a red box. ADAMTS7 contains a disintegrin-like domain and metalloprotease domain with eight TSRs (Ape, 2004).

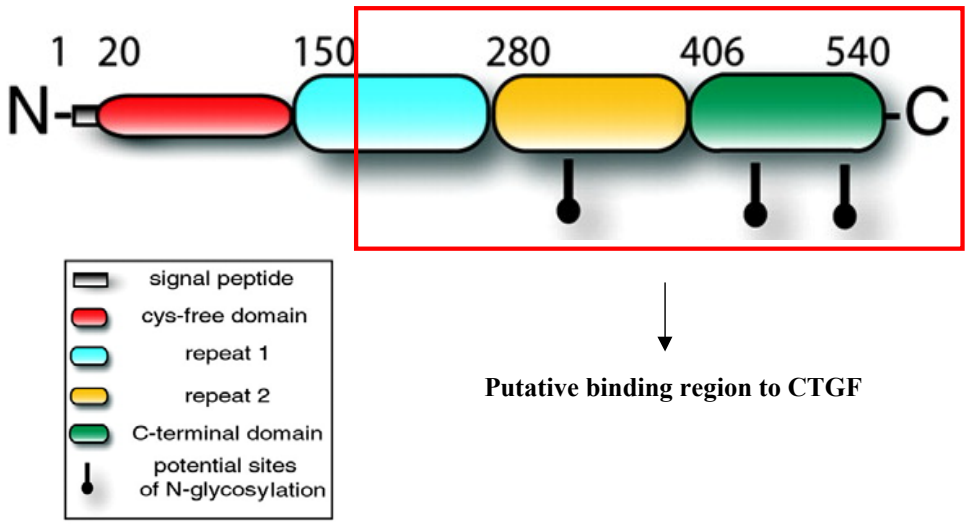

Figure 6-9. The structure of ECM 1 protein, a candidate to bind CTGF. The structure of ECM1 contains signal peptide, followed by cystine free domain, tandem repeat1, tandem repeat2 and C-terminal domain. Red box labels the putative binding region of ECM1 to CTGF.

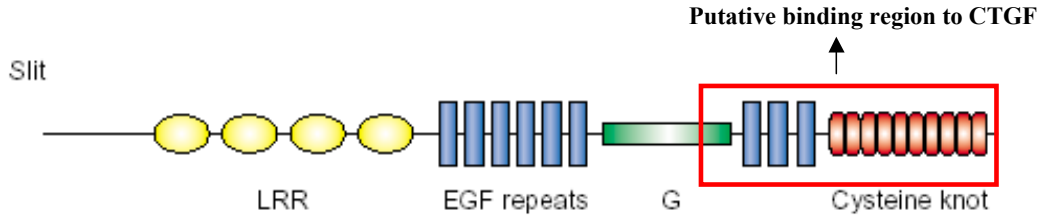

Figure 6-10. The general structure of Slit2 protein, a candidate binding to CTGF. The putative binding region in Slit2 to CTGF is labeled in a red box. The mammalian Slit protein contains four leucine rich repeats (LRRs), nine EGF repeats, a laminin G domain (G) and a cystine rich C terminus (cystine knot).

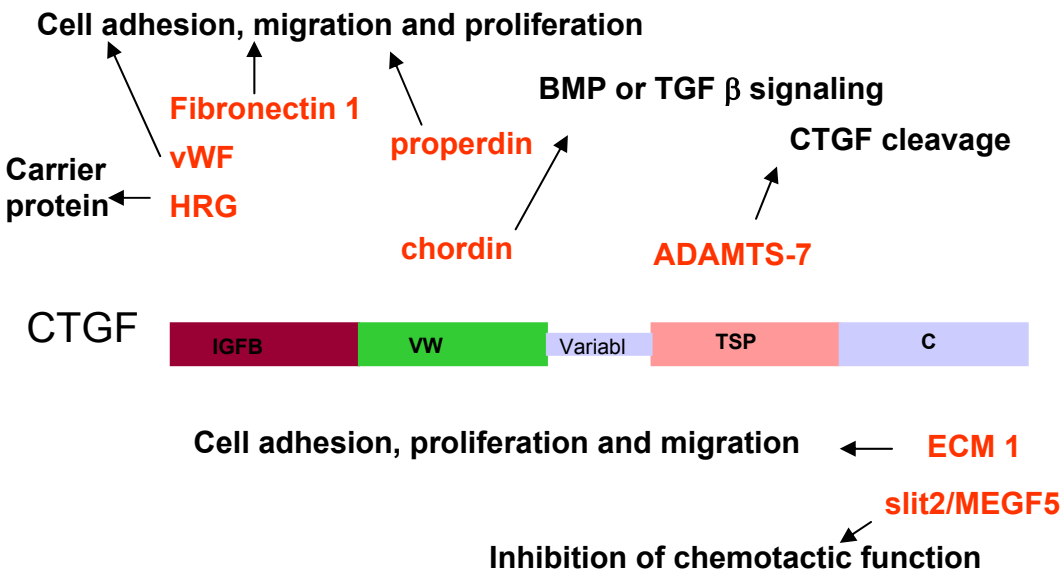

Figure 6-11. Summary of domains of CTGF binding to candidates and their potential functions. The CTGF interactors are in red and arrows point to the functions that they may mediate through binding to CTGF.

CHAPTER 7
SUMMARY AND CONCLUSIONS

The aim of this study was to gain a better insight into the molecular mechanisms of oval cell activation in the liver reparative process following 2-AAF/PHx. CTGF, the matricellular protein, came up to our scope as one of candidate genes differentially expressed in Thy-1$^+$oval cells. In this study, the important role of CTGF in oval cell activation was established through biochemical and genetic characterization of CTGF function in vivo and in vitro.

1. The Role of CTGF in Oval Cell Activation during Liver Regeneration in the 2-AAF/PHx Model.

The induction pattern of CTGF was examined at both the protein and RNA levels using the total liver homogenates. The kinetics of CTGF expression is correlated with that of TGF-β 1, pro-collagen type I and fibronectin 1, supporting the notion that TGF-β 1 upregulates CTGF expression and CTGF synergizes the induction of ECM proteins upon TGF-β 1 stimulation.

The cellular sources of CTGF were also investigated. Thy-1$^+$ oval cells and desmin$^+$ stellate cells are both the major sources of CTGF. Extensive proliferation of oval cells is a hallmark of reparative process in the 2-AAF/PHx model. Activation of stellate a cell, which have mesenchymal origin and are required during wound healing and other tissue remodeling processes, is closely associated with the activated oval cells (Puke et al., 2001). The intimate relationship between stellate cells and oval cells can be observed from ultrastructure of oval cell compartment. CTGF may promote cell migration and

proliferation of stellate cells and oval cells. Given that stellate cells are of mesenchymal origin and a major cell type to synthesize ECM proteins during tissue remodeling and normal wound healing, CTGF can stimulate stellate cells to produce ECM components in reparative livers following 2-AAF/PHx.

To establish the role of CTGF in oval cell-aided liver regeneration, we tested the effect of Iloprost, a known inhibitor for TGF-β induced CTGF synthesis. Iloprost administration effectively blocked CTGF induction during oval cell activation. Moreover, the inhibition of CTGF synthesis was associated with decreasing numbers of histologically evident oval cells and BrdU positive proliferating cells and a lower level of AFP expression. These results indicate that the inhibition of CTGF was associated with impaired oval cell response.

Considering that the inhibition of Iloprost on CTGF synthesis is through affecting protein kinase A and Ras/ MEK/ ERK pathways, RNA interference to target CTGF would be a more specific inhibition approach. In Chapter 5, we performed in vitro experiment and tested the efficiency of recombinant adenovirus specific for CTGF siRNA. The preliminary data indicate that one of the recombinant viruses is capable of inhibiting CTGF transcription in vitro. The effect of CTGF siRNA can be tested in regenerating livers following 2-AAF/PHx in future.

2. Identification of CTGF binding proteins

Another set of conclusions from this study relates to the molecular mechanism of CTGF signaling. CTGF is a matricellular protein with four conserved domains. It must exert its function through interaction with partners. The yeast two-hybrid approach was employed to identify these binding proteins. Since there is no commercially available

cDNA library specific for liver regeneration, we constructed the first yeast two-hybrid cDNA library for this purpose. We used four baits carrying different domains of CTGF to screen the library and identified several interesting candidates including fibronectin, von Willebrand factor, histidine rich glycoprotein, chordin, properdin, a disintegrin and metalloproteinase with thrombonspondin type I repeat 7, extracellular matrix protein 1 and slit2. Most of the candidates are ECM associated signal molecules. Their functions involve coagulation, cell adhesion, migration, chemoattraction and differentiation. The further characterization of molecules would provide us more insight into CTGF signaling pathway in ECM.

Despite the discovery of CTGF more than ten years ago, the knowledge of CTGF signaling remains elusive. A number of points such as how each domain contribute to the biological activities and function of CTGF need to be addressed. The work presented in this thesis answers some questions, and helps focus studies for future investigations.

LIST OF REFERENCES

Abraham,D.J., Shiwen,X., Black,C.M., Sa,S., Xu,Y., and Leask,A. (2000). Tumor necrosis factor alpha suppresses the induction of connective tissue growth factor by transforming growth factor-beta in normal and scleroderma fibroblasts. J. Biol. Chem. 19*;275*, 15220-15225.

Abreu,J.G., Ketpura,N.I., Reversade,B., and De Robertis,E.M. (2002d). Connective-tissue growth factor (CTGF) modulates cell signalling by BMP and TGF-beta 1. Nat. Cell Biol. *4*, 599-604.

Albrecht,J.H. and Hansen,L.K. (1999). Cyclin D1 promotes mitogen-independent cell cycle progression in hepatocytes. Cell Growth Differ. *10*, 397-404.

Albrecht,J.H., Hoffman,J.S., Kren,B.T., and Steer,C.J. (1993). Cyclin and cyclin-dependent kinase 1 mRNA expression in models of regenerating liver and human liver diseases. Am. J. Physiol. *265*, G857-G864.

Alison,M.R., Golding,M., Sarraf,C.E., Edwards,R.J., and Lalani,E.N. (1996a). Liver damage in the rat induces hepatocyte stem cells from biliary epithelial cells. Gastroenterology *110*, 1182-1190.

Alison,M.R., Golding,M.H., and Sarraf,C.E. (1996b). Pluripotential liver stem cells: facultative stem cells located in the biliary tree. Cell Prolif. *29*, 373-402.

Apte,S.S., Olsen,B.R., and Murphy,G. (1995). The gene structure of tissue inhibitor of metalloproteinases (TIMP)-3 and its inhibitory activities define the distinct TIMP gene family. J. Biol. Chem. *270*, 14313-14318.

Arii,S. and Imamura,M. (2000). Physiological role of sinusoidal endothelial cells and Kupffer cells and their implication in the pathogenesis of liver injury. J. Hepatobiliary. Pancreat. Surg. *7*, 40-48.

Babic,A.M., Chen,C.C., and Lau,L.F. (1999). Fisp12/mouse connective tissue growth factor mediates endothelial cell adhesion and migration through integrin alphavbeta3, promotes endothelial cell survival, and induces angiogenesis in vivo. Mol. Cell Biol. *19*, 2958-2966.

Babic,A.M., Kireeva,M.L., Kolesnikova,T.V., and Lau,L.F. (1998). CYR61, a product of a growth factor-inducible immediate early gene, promotes angiogenesis and tumor growth. Proc. Natl. Acad. Sci. U. S A. *95*, 6355-6360.

Bachiller,D., Klingensmith,J., Kemp,C., Belo,J.A., Anderson,R.M., May,S.R., McMahon,J.A., McMahon,A.P., Harland,R.M., Rossant,J., and De Robertis,E.M. (2000). The organizer factors Chordin and Noggin are required for mouse forebrain development. Nature *403*, 658-661.

Ball,D.K., Surveyor,G.A., Diehl,J.R., Steffen,C.L., Uzumcu,M., Mirando,M.A., and Brigstock,D.R. (1998). Characterization of 16- to 20-kilodalton (kDa) connective tissue growth factors (CTGFs) and demonstration of proteolytic activity for 38-kDa CTGF in pig uterine luminal flushings. Biol. Reprod. *59*, 828-835.

Baneyx,G., Baugh,L., and Vogel,V. (2002). Fibronectin extension and unfolding within cell matrix fibrils controlled by cytoskeletal tension. Proc. Natl. Acad. Sci. U. S A. *99*, 5139-5143.

Bisgaard,H.C., Muller,S., Nagy,P., Rasmussen,L.J., and Thorgeirsson,S.S. (1999). Modulation of the gene network connected to interferon-gamma in liver regeneration from oval cells. Am. J. Pathol. *155*, 1075-1085.

Bissell,D.M., Wang,S.S., Jarnagin,W.R., and Roll,F.J. (1995). Cell-specific expression of transforming growth factor-beta in rat liver. Evidence for autocrine regulation of hepatocyte proliferation. J. Clin. Invest. *96*, 447-455.

Bork,P. (1993). The modular architecture of a new family of growth regulators related to connective tissue growth factor. FEBS Lett. *327*, 125-130.

Bouwens,L., Baekeland,M., De Zanger,R., and Wisse,E. (1986). Quantitation, tissue distribution and proliferation kinetics of Kupffer cells in normal rat liver. Hepatology *6*, 718-722.

Bradham,D.M., Igarashi,A., Potter,R.L., and Grotendorst,G.R. (1991). Connective tissue growth factor: a cysteine-rich mitogen secreted by human vascular endothelial cells is related to the SRC-induced immediate early gene product CEF-10. J. Cell Biol. *114*, 1285-1294.

Brigstock,D.R., Steffen,C.L., Kim,G.Y., Vegunta,R.K., Diehl,J.R., and Harding,P.A. (1997). Purification and characterization of novel heparin-binding growth factors in uterine secretory fluids. Identification as heparin-regulated Mr 10,000 forms of connective tissue growth factor. J. Biol. Chem. *272*, 20275-20282.

Bucher,N.L. (1963). Regeneration of mammalian liver. Int. Rev. Cytol. *15:245-300.*, 245-300.

Camerer,E., Gjernes,E., Wiiger,M., Pringle,S., and Prydz,H. (2000). Binding of factor VIIa to tissue factor on keratinocytes induces gene expression. J. Biol. Chem. *275*, 6580-6585.

Carr,B.I., Hayashi,I., Branum,E.L., and Moses,H.L. (1986). Inhibition of DNA synthesis in rat hepatocytes by platelet-derived type beta transforming growth factor. Cancer Res. *46*, 2330-2334.

Chambers,R.C., Leoni,P., Blanc-Brude,O.P., Wembridge,D.E., and Laurent,G.J. (2000). Thrombin is a potent inducer of connective tissue growth factor production via proteolytic activation of protease-activated receptor-1. J. Biol. Chem. *275*, 35584-35591.

Chen,C., Michelini-Norris,B., Stevens,S., Rowsey,J., Ren,X., Goldstein,M., and Schultz,G. (2000). Measurement of mRNAs for TGFss and extracellular matrix proteins in corneas of rats after PRK. Invest Ophthalmol. Vis. Sci. *41*, 4108-4116.

Chen,C.C., Chen,N., and Lau,L.F. (2001). The angiogenic factors Cyr61 and connective tissue growth factor induce adhesive signaling in primary human skin fibroblasts. J. Biol. Chem. *276*, 10443-10452.

Chen,N., Leu,S.J., Todorovic,V., Lam,S.C., and Lau,L.F. (2004). Identification of a novel integrin alphavbeta3 binding site in CCN1 (CYR61) critical for pro-angiogenic activities in vascular endothelial cells. J. Biol. Chem. *279*, 44166-44176.

Chen,Y., Blom,I.E., Sa,S., Goldschmeding,R., Abraham,D.J., and Leask,A. (2002). CTGF expression in mesangial cells: involvement of SMADs, MAP kinase, and PKC. Kidney Int. *62*, 1149-1159.

Cheng,J. and Grande,J.P. (2002). Transforming growth factor-beta signal transduction and progressive renal disease. Exp. Biol. Med. (Maywood.) *227*, 943-956.

Chowdhury,I. and Chaqour,B. (2004). Regulation of connective tissue growth factor (CTGF/CCN2) gene transcription and mRNA stability in smooth muscle cells. Involvement of RhoA GTPase and p38 MAP kinase and sensitivity to actin dynamics. Eur. J. Biochem. *271*, 4436-4450.

Clark,E.A. and Brugge,J.S. (1995). Integrins and signal transduction pathways: the road taken. Science *268*, 233-239.

Colige,A., Li,S.W., Sieron,A.L., Nusgens,B.V., Prockop,D.J., and Lapiere,C.M. (1997). cDNA cloning and expression of bovine procollagen I N-proteinase: a new member of the superfamily of zinc-metalloproteinases with binding sites for cells and other matrix components. Proc. Natl. Acad. Sci. U. S A. *94*, 2374-2379.

Crawford,S.E., Stellmach,V., Murphy-Ullrich,J.E., Ribeiro,S.M., Lawler,J., Hynes,R.O., Boivin,G.P., and Bouck,N. (1998). Thrombospondin-1 is a major activator of TGF-beta1 in vivo. Cell *93*, 1159-1170.

Crean,J.K., Finlay,D., Murphy,M., Moss,C., Godson,C., Martin,F., and Brady,H.R. (2002). The role of p42/44 MAPK and protein kinase B in connective tissue growth factor induced extracellular matrix protein production, cell migration, and actin cytoskeletal rearrangement in human mesangial cells. J. Biol. Chem. *277*, 44187-44194.

Cressman,D.E., Greenbaum,L.E., DeAngelis,R.A., Ciliberto,G., Furth,E.E., Poli,V., and Taub,R. (1996). Liver failure and defective hepatocyte regeneration in interleukin-6-deficient mice. Science *274*, 1379-1383.

De Bleser,P.J., Niki,T., Rogiers,V., and Geerts,A. (1997). Transforming growth factor-beta gene expression in normal and fibrotic rat liver. J. Hepatol. *26*, 886-893.

De Bleser,P.J., Xu,G., Rombouts,K., Rogiers,V., and Geerts,A. (1999). Glutathione levels discriminate between oxidative stress and transforming growth factor-beta signaling in activated rat hepatic stellate cells. J. Biol. Chem. *274*, 33881-33887.

Deckers,M.M., Smits,P., Karperien,M., Ni,J., Tylzanowski,P., Feng,P., Parmelee,D., Zhang,J., Bouffard,E., Gentz,R., Lowik,C.W., and Merregaert,J. (2001). Recombinant human extracellular matrix protein 1 inhibits alkaline phosphatase activity and mineralization of mouse embryonic metatarsals in vitro. Bone *28*, 14-20.

Ding,X., Cory,G., and Song,W.Y. (2004). A high-throughput system to verify candidate interactors from yeast two-hybrid screening using rolling circle amplification. Anal. Biochem. *331*, 195-197.

DuBois, R.N., Hunter, E.B., and Russel, W. (1994) Molecular aspects of hepatic regeneration. In: Molecular basis of medicine. Dang CV and Feldman AM. Eds. New York, Marcel Decker. 234-256.

Eguchi,T., Kubota,S., Kondo,S., Kuboki,T., Yatani,H., and Takigawa,M. (2002). A novel cis-element that enhances connective tissue growth factor gene expression in chondrocytic cells. Biochem. Biophys. Res. Commun. *295*, 445-451.

Enenstein,J., Waleh,N.S., and Kramer,R.H. (1992). Basic FGF and TGF-beta differentially modulate integrin expression of human microvascular endothelial cells. Exp. Cell Res. *203*, 499-503.

Evarts,R.P., Hu,Z.Y., Omori,N., Omori,M., Marsden,E.R., and Thorgeirsson,S.S. (1996). Precursor-product relationship between oval cells and hepatocytes: Comparison between tritiated thymidine and bromodeoxyuridine as tracers. Carcinogenesis *17*, 2143-2151.

Evarts,R.P., Nagy,P., Nakatsukasa,H., Marsden,E., and Thorgeirsson,S.S. (1989). In vivo differentiation of rat liver oval cells into hepatocytes. Cancer Res. *49*, 1541-1547.

Fahimi,H.D. (1967). Perfusion and immersion fixation of rat liver with glutaraldehyde. Lab Invest *16*, 736-750.

Falcone,D.J., McCaffrey,T.A., Mathew,J., McAdam,K., and Borth,W. (1995). THP-1 macrophage membrane-bound plasmin activity is up-regulated by transforming growth factor-beta 1 via increased expression of urokinase and the urokinase receptor. J. Cell Physiol. *164*, 334-343.

Fan,W.H., Pech,M., and Karnovsky,M.J. (2000). Connective tissue growth factor (CTGF) stimulates vascular smooth muscle cell growth and migration in vitro. Eur. J. Cell Biol. *79*, 915-923.

Farber,E. (1956). Similarities in the sequence of early histological changes induced in the liver of the rat by ethionine, 2-acetylamino-fluorene, and 3'-methyl-4-dimethylaminoazobenzene. Cancer Res. *16*, 142-148.

Fausto,N. (2000). Liver regeneration. J. Hepatol. *32*, 19-31.

Fausto,N., Mead,J.E., Gruppuso,P.A., Castilla,A., and Jakowlew,S.B. (1991). Effects of TGF-beta s in the liver: cell proliferation and fibrogenesis. Ciba Found. Symp. *157:165-74; discussion 174-7.*, 165-174.

Fleming,J.V., Fontanier,N., Harries,D.N., and Rees,W.D. (1997). The growth arrest genes gas5, gas6, and CHOP-10 (gadd153) are expressed in the mouse preimplantation embryo. Mol. Reprod. Dev. *48*, 310-316.

Frazier,K., Williams,S., Kothapalli,D., Klapper,H., and Grotendorst,G.R. (1996). Stimulation of fibroblast cell growth, matrix production, and granulation tissue formation by connective tissue growth factor. J. Invest Dermatol. *107*, 404-411.

Friedman,S.L., Wei,S., and Blaner,W.S. (1993). Retinol release by activated rat hepatic lipocytes: regulation by Kupffer cell-conditioned medium and PDGF. Am. J. Physiol. *264*, G947-G952.

Fujio,K., Evarts,R.P., Hu,Z., Marsden,E.R., and Thorgeirsson,S.S. (1994). Expression of stem cell factor and its receptor, c-kit, during liver regeneration from putative stem cells in adult rat. Lab Invest. *70*, 511-516.

Gao,R., Ball,D.K., Perbal,B., and Brigstock,D.R. (2004). Connective tissue growth factor induces c-fos gene activation and cell proliferation through p44/42 MAP kinase in primary rat hepatic stellate cells. J. Hepatol. *40*, 431-438.

Gao,R. and Brigstock,D.R. (2003). Low density lipoprotein receptor-related protein (LRP) is a heparin-dependent adhesion receptor for connective tissue growth factor (CTGF) in rat activated hepatic stellate cells. Hepatol. Res. *27*, 214-220.

Garcia,A.J., Coffinier,C., Larrain,J., Oelgeschlager,M., and De Robertis,E.M. (2002). Chordin-like CR domains and the regulation of evolutionarily conserved extracellular signaling systems. Gene *287*, 39-47.

Garcia-Trevijano,E.R., Iraburu,M.J., Fontana,L., Dominguez-Rosales,J.A., Auster,A., Covarrubias-Pinedo,A., and Rojkind,M. (1999). Transforming growth factor beta1 induces the expression of alpha1(I) procollagen mRNA by a hydrogen peroxide-C/EBPbeta-dependent mechanism in rat hepatic stellate cells. Hepatology *29*, 960-970.

Georges-Labouesse,E.N., George,E.L., Rayburn,H., and Hynes,R.O. (1996). Mesodermal development in mouse embryos mutant for fibronectin. Dev. Dyn. *207*, 145-156.

Golding,M., Sarraf,C.E., Lalani,E.N., Anilkumar,T.V., Edwards,R.J., Nagy,P., Thorgeirsson,S.S., and Alison,M.R. (1995). Oval cell differentiation into hepatocytes in the acetylaminofluorene-treated regenerating rat liver. Hepatology *22*, 1243-1253.

Greenwel,P., Inagaki,Y., Hu,W., Walsh,M., and Ramirez,F. (1997). Sp1 is required for the early response of alpha2(I) collagen to transforming growth factor-beta1. J. Biol. Chem. *272*, 19738-19745.

Greenwel,P. and Rojkind,M. (1997). Accelerated development of liver fibrosis in CCl4-treated rats by the weekly induction of acute phase response episodes: upregulation of alpha1(I) procollagen and tissue inhibitor of metalloproteinase-1 mRNAs. Biochim. Biophys. Acta *1361*, 177-184.

Grotendorst,G.R., Okochi,H., and Hayashi,N. (1996). A novel transforming growth factor beta response element controls the expression of the connective tissue growth factor gene. Cell Growth Differ. *7*, 469-480.

Grzeszkiewicz,T.M., Lindner,V., Chen,N., Lam,S.C., and Lau,L.F. (2002). The angiogenic factor cysteine-rich 61 (CYR61, CCN1) supports vascular smooth muscle cell adhesion and stimulates chemotaxis through integrin alpha(6)beta(1) and cell surface heparan sulfate proteoglycans. Endocrinology *143*, 1441-1450.

Guo,N.H., Krutzsch,H.C., Negre,E., Vogel,T., Blake,D.A., and Roberts,D.D. (1992). Heparin- and sulfatide-binding peptides from the type I repeats of human thrombospondin promote melanoma cell adhesion. Proc. Natl. Acad. Sci. U. S A. *89*, 3040-3044.

Haber,B.A., Mohn,K.L., Diamond,R.H., and Taub,R. (1993). Induction patterns of 70 genes during nine days after hepatectomy define the temporal course of liver regeneration. J. Clin. Invest. *91*, 1319-1326.

Hahn,A., Heusinger-Ribeiro,J., Lanz,T., Zenkel,S., and Goppelt-Struebe,M. (2000). Induction of connective tissue growth factor by activation of heptahelical receptors. Modulation by Rho proteins and the actin cytoskeleton. J. Biol. Chem. *275*, 37429-37435.

Hall,M.C., Young,D.A., Waters,J.G., Rowan,A.D., Chantry,A., Edwards,D.R., and Clark,I.M. (2003). The comparative role of activator protein 1 and Smad factors in the regulation of Timp-1 and MMP-1 gene expression by transforming growth factor-beta 1. J. Biol. Chem. *278*, 10304-10313.

Hamada,T., McLean,W.H., Ramsay,M., Ashton,G.H., Nanda,A., Jenkins,T., Edelstein,I., South,A.P., Bleck,O., Wessagowit,V., Mallipeddi,R., Orchard,G.E., Wan,H., Dopping-Hepenstal,P.J., Mellerio,J.E., Whittock,N.V., Munro,C.S., van Steensel,M.A., Steijlen,P.M., Ni,J., Zhang,L., Hashimoto,T., Eady,R.A., and McGrath,J.A. (2002). Lipoid proteinosis maps to 1q21 and is caused by mutations in the extracellular matrix protein 1 gene (ECM1). Hum. Mol. Genet. *11*, 833-840.

Han,Z., Ni,J., Smits,P., Underhill,C.B., Xie,B., Chen,Y., Liu,N., Tylzanowski,P., Parmelee,D., Feng,P., Ding,I., Gao,F., Gentz,R., Huylebroeck,D., Merregaert,J., and Zhang,L. (2001). Extracellular matrix protein 1 (ECM1) has angiogenic properties and is expressed by breast tumor cells. FASEB J. *15*, 988-994.

Hartsough,M.T., Frey,R.S., Zipfel,P.A., Buard,A., Cook,S.J., McCormick,F., and Mulder,K.M. (1996). Altered transforming growth factor signaling in epithelial cells when ras activation is blocked. J. Biol. Chem. *271*, 22368-22375.

Hashimoto,Y., Shindo-Okada,N., Tani,M., Nagamachi,Y., Takeuchi,K., Shiroishi,T., Toma,H., and Yokota,J. (1998). Expression of the Elm1 gene, a novel gene of the CCN (connective tissue growth factor, Cyr61/Cef10, and neuroblastoma overexpressed gene) family, suppresses In vivo tumor growth and metastasis of K-1735 murine melanoma cells. J. Exp. Med. *187*, 289-296.

Hatch,H.M., Zheng,D., Jorgensen,M.L., and Petersen,B.E. (2002). SDF-1alpha/CXCR4: a mechanism for hepatic oval cell activation and bone marrow stem cell recruitment to the injured liver of rats. Cloning Stem Cells *4*, 339-351.

Heino,J. and Massague,J. (1989). Transforming growth factor-beta switches the pattern of integrins expressed in MG-63 human osteosarcoma cells and causes a selective loss of cell adhesion to laminin. J. Biol. Chem. *264*, 21806-21811.

Heusinger-Ribeiro,J., Eberlein,M., Wahab,N.A., and Goppelt-Struebe,M. (2001). Expression of connective tissue growth factor in human renal fibroblasts: regulatory roles of RhoA and cAMP. J. Am. Soc. Nephrol. *12*, 1853-1861.

Higgins,G.M., and Anderson,R.M. (1931). Experimental pathology of the liver: I. Restoration of the liver of the white rat following partial surgical removal. Arch Pathol. 12:186-202.

Hishikawa,K., Oemar,B.S., and Nakaki,T. (2001). Static pressure regulates connective tissue growth factor expression in human mesangial cells. J. Biol. Chem. *276*, 16797-16803.

Holmes,A., Abraham,D.J., Chen,Y., Denton,C., Shi-wen,X., Black,C.M., and Leask,A. (2003). Constitutive connective tissue growth factor expression in scleroderma fibroblasts is dependent on Sp1. J. Biol. Chem. *278*, 41728-41733.

Holmes,A., Abraham,D.J., Sa,S., Shiwen,X., Black,C.M., and Leask,A. (2001). CTGF and SMADs, maintenance of scleroderma phenotype is independent of SMAD signaling. J. Biol. Chem. *276*, 10594-10601.

Holt,G.D., Pangburn,M.K., and Ginsburg,V. (1990). Properdin binds to sulfatide [Gal(3-SO4)beta 1-1 Cer] and has a sequence homology with other proteins that bind sulfated glycoconjugates. J. Biol. Chem. *265*, 2852-2855.

Ichikawa,T., Zhang,Y.Q., Kogure,K., Hasegawa,Y., Takagi,H., Mori,M., and Kojima,I. (2001). Transforming growth factor beta and activin tonically inhibit DNA synthesis in the rat liver. Hepatology *34*, 918-925.

Inagaki,M., Wang,Z., and Carr,B.I. (1994). Transforming growth factor beta 1 selectively increases gene expression of the serine/threonine kinase receptor 1 (SKR1) in human hepatoma cell lines. Cell Struct. Funct. *19*, 305-313.

Inagaki,Y., Mamura,M., Kanamaru,Y., Greenwel,P., Nemoto,T., Takehara,K., Ten Dijke,P., and Nakao,A. (2001). Constitutive phosphorylation and nuclear localization of Smad3 are correlated with increased collagen gene transcription in activated hepatic stellate cells. J. Cell Physiol. *187*, 117-123.

Inoki,I., Shiomi,T., Hashimoto,G., Enomoto,H., Nakamura,H., Makino,K., Ikeda,E., Takata,S., Kobayashi,K., and Okada,Y. (2002). Connective tissue growth factor binds vascular endothelial growth factor (VEGF) and inhibits VEGF-induced angiogenesis. FASEB J. *16*, 219-221.

Ivkovic,S., Yoon,B.S., Popoff,S.N., Safadi,F.F., Libuda,D.E., Stephenson,R.C., Daluiski,A., and Lyons,K.M. (2003). Connective tissue growth factor coordinates chondrogenesis and angiogenesis during skeletal development. Development *130*, 2779-2791.

Jakowlew,S.B., Mead,J.E., Danielpour,D., Wu,J., Roberts,A.B., and Fausto,N. (1991). Transforming growth factor-beta (TGF-beta) isoforms in rat liver regeneration: messenger RNA expression and activation of latent TGF-beta. Cell Regul. *2*, 535-548.

Jedsadayanmata,A., Chen,C.C., Kireeva,M.L., Lau,L.F., and Lam,S.C. (1999). Activation-dependent adhesion of human platelets to Cyr61 and Fisp12/mouse connective tissue growth factor is mediated through integrin alpha(IIb)beta(3). J. Biol. Chem. 20*;274*, 24321-24327.

Jezequel,A.M., Novelli,G., Venturini C et al. Quantitative analysis of the perisinusoidal cells in human liver; the lipocytes. Front Gastrointest Res. 1984; 8:85-90.

Jones,A.L. and Schmucker,D.L. (1977). Current concepts of liver structure as related to function. Gastroenterology *73*, 833-851.

Kessler,D., Dethlefsen,S., Haase,I., Plomann,M., Hirche,F., Krieg,T., and Eckes,B. (2001). Fibroblasts in mechanically stressed collagen lattices assume a "synthetic" phenotype. J. Biol. Chem. *276*, 36575-36585.

Kim,H.S., Nagalla,S.R., Oh,Y., Wilson,E., Roberts,C.T., Jr., and Rosenfeld,R.G. (1997). Identification of a family of low-affinity insulin-like growth factor binding proteins (IGFBPs): characterization of connective tissue growth factor as a member of the IGFBP superfamily. Proc. Natl. Acad. Sci. U. S A. *94*, 12981-12986.

Kireeva,M.L., Lam,S.C., and Lau,L.F. (1998). Adhesion of human umbilical vein endothelial cells to the immediate-early gene product Cyr61 is mediated through integrin alphavbeta3. J. Biol. Chem. *273*, 3090-3096.

Kireeva,M.L., MO,F.E., Yang,G.P., and Lau,L.F. (1996). Cyr61, a product of a growth factor-inducible immediate-early gene, promotes cell proliferation, migration, and adhesion. Mol. Cell Biol. *16*, 1326-1334.

Kobayashi,H., Hayashi,N., Hayashi,K., Yamataka,A., Lane,G.J., and Miyano,T. (2005). Connective tissue growth factor and progressive fibrosis in biliary atresia. Pediatr. Surg. Int. *21*, 12-16.

Koide,T., Foster,D., Yoshitake,S., and Davie,E.W. (1986). Amino acid sequence of human histidine-rich glycoprotein derived from the nucleotide sequence of its cDNA. Biochemistry *25*, 2220-2225.

Kretzschmar,M., Doody,J., Timokhina,I., and Massague,J. (1999). A mechanism of repression of TGFbeta/ Smad signaling by oncogenic Ras. Genes Dev. *13*, 804-816.

Kubota,S., Kondo,S., Eguchi,T., Hattori,T., Nakanishi,T., Pomerantz,R.J., and Takigawa,M. (2000). Identification of an RNA element that confers post-transcriptional repression of connective tissue growth factor/hypertrophic chondrocyte specific 24 (ctgf/hcs24) gene: similarities to retroviral RNA-protein interactions. Oncogene *19*, 4773-4786.

Laiho,M., DeCaprio,J.A., Ludlow,J.W., Livingston,D.M., and Massague,J. (1990). Growth inhibition by TGF-beta linked to suppression of retinoblastoma protein phosphorylation. Cell *62*, 175-185.

Laiho,M., Saksela,O., and Keski-Oja,J. (1987). Transforming growth factor-beta induction of type-1 plasminogen activator inhibitor. Pericellular deposition and sensitivity to exogenous urokinase. J. Biol. Chem. *262*, 17467-17474.

Lau,L.F. and Lam,S.C. (1999). The CCN family of angiogenic regulators: the integrin connection. Exp. Cell Res. *248*, 44-57.

Leask,A., Holmes,A., and Abraham,D.J. (2002). Connective tissue growth factor: a new and important player in the pathogenesis of fibrosis. Curr. Rheumatol. Rep. *4*, 136-142.

Leask,A., Sa,S., Holmes,A., Shiwen,X., Black,C.M., and Abraham,D.J. (2001). The control of ccn2 (ctgf) gene expression in normal and scleroderma fibroblasts. Mol. Pathol. *54*, 180-183.

Lee,D.K., Park,S.H., Yi,Y., Choi,S.G., Lee,C., Parks,W.T., Cho,H., de Caestecker,M.P., Shaul,Y., Roberts,A.B., and Kim,S.J. (2001). The hepatitis B virus encoded oncoprotein pX amplifies TGF-beta family signaling through direct interaction with Smad4: potential mechanism of hepatitis B virus-induced liver fibrosis. Genes Dev. *15*, 455-466.

Leivonen,S.K., Chantry,A., Hakkinen,L., Han,J., and Kahari,V.M. (2002). Smad3 mediates transforming growth factor-beta-induced collagenase-3 (matrix metalloproteinase-13) expression in human gingival fibroblasts. Evidence for cross-talk between Smad3 and p38 signaling pathways. J. Biol. Chem. *277*, 46338-46346.

Leu,S.J., Liu,Y., Chen,N., Chen,C.C., Lam,S.C., and Lau,L.F. (2003). Identification of a novel integrin alpha 6 beta 1 binding site in the angiogenic inducer CCN1 (CYR61). J. Biol. Chem. *278*, 33801-33808.

Li,C.L., Martinez,V., He,B., Lombet,A., and Perbal,B. (2002). A role for CCN3 (NOV) in calcium signalling. Mol. Pathol. *55*, 250-261.

Li,H.S., Chen,J.H., Wu,W., Fagaly,T., Zhou,L., Yuan,W., Dupuis,S., Jiang,Z.H., Nash,W., Gick,C., Ornitz,D.M., Wu,J.Y., and Rao,Y. (1999). Vertebrate slit, a secreted ligand for the transmembrane protein roundabout, is a repellent for olfactory bulb axons. Cell *96*, 807-818.

Lindroos,P.M., Zarnegar,R., and Michalopoulos,G.K. (1991). Hepatocyte growth factor (hepatopoietin A) rapidly increases in plasma before DNA synthesis and liver regeneration stimulated by partial hepatectomy and carbon tetrachloride administration. Hepatology *13*, 743-750.

Loyer,P., Glaise,D., Cariou,S., Baffet,G., Meijer,L., and Guguen-Guillouzo,C. (1994). Expression and activation of cdks (1 and 2) and cyclins in the cell cycle progression during liver regeneration. J. Biol. Chem. *269*, 2491-2500.

Lund,L.R., Riccio,A., Andreasen,P.A., Nielsen,L.S., Kristensen,P., Laiho,M., Saksela,O., Blasi,F., and Dano,K. (1987). Transforming growth factor-beta is a strong and fast acting positive regulator of the level of type-1 plasminogen activator inhibitor mRNA in WI-38 human lung fibroblasts. EMBO J. *6*, 1281-1286.

Manzow,S., Brancolini,C., Marks,F., and Richter,K.H. (1996). Expression of growth arrest-specific (Gas) genes in murine keratinocytes: Gas2 is specifically regulated. Exp. Cell Res. *224*, 200-203.

Mars,W.M., Liu,M.L., Kitson,R.P., Goldfarb,R.H., Gabauer,M.K., and Michalopoulos,G.K. (1995). Immediate early detection of urokinase receptor after partial hepatectomy and its implications for initiation of liver regeneration. Hepatology *21*, 1695-1701.

Mars,W.M., Zarnegar,R., and Michalopoulos,G.K. (1993). Activation of hepatocyte growth factor by the plasminogen activators uPA and tPA. Am. J. Pathol. *143*, 949-958.

Martinez-Hernandez,A. and Amenta,P.S. (1993). The hepatic extracellular matrix. II. Ontogenesis, regeneration and cirrhosis. Virchows Arch. A Pathol. Anat. Histopathol. *423*, 77-84.

Martinez-Hernandez,A. and Amenta,P.S. (1995). The extracellular matrix in hepatic regeneration. FASEB J. *9*, 1401-1410.

Massague,J. (1990). The transforming growth factor-beta family. Annu. Rev. Cell Biol. *6:597-641.*, 597-641.

McCuskey,R.S. and Reilly,F.D. (1993). Hepatic microvasculature: dynamic structure and its regulation. Semin. Liver Dis. *13*, 1-12.

Mead,J.E. and Fausto,N. (1989). Transforming growth factor alpha may be a physiological regulator of liver regeneration by means of an autocrine mechanism. Proc. Natl. Acad. Sci. U. S A. *86*, 1558-1562.

Michalopoulos,G.K. (1990). Liver regeneration: molecular mechanisms of growth control. FASEB J. *4*, 176-187.

Michalopoulos,G.K. and DeFrances,M.C. (1997). Liver regeneration. Science *276*, 60-66.

Moussad,E.E. and Brigstock,D.R. (2000). Connective tissue growth factor: what's in a name? Mol. Genet. Metab *71*, 276-292.

Mulder,K.M. (2000). Role of Ras and Mapks in TGFbeta signaling. Cytokine Growth Factor Rev. *11*, 23-35.

Mulder,K.M. and Morris,S.L. (1992). Activation of p21ras by transforming growth factor beta in epithelial cells. J. Biol. Chem. *267*, 5029-5031.

Munger,J.S., Huang,X., Kawakatsu,H., Griffiths,M.J., Dalton,S.L., Wu,J., Pittet,J.F., Kaminski,N., Garat,C., Matthay,M.A., Rifkin,D.B., and Sheppard,D. (1999). The integrin alpha v beta 6 binds and activates latent TGF beta 1: a mechanism for regulating pulmonary inflammation and fibrosis. Cell *96*, 319-328.

Nagase,H. and Kashiwagi,M. (2003). Aggrecanases and cartilage matrix degradation. Arthritis Res. Ther. *5*, 94-103.

Nakamura,T., Tomita,Y., Hirai,R., Yamaoka,K., Kaji,K., and Ichihara,A. (1985). Inhibitory effect of transforming growth factor-beta on DNA synthesis of adult rat hepatocytes in primary culture. Biochem. Biophys. Res. Commun. *133*, 1042-1050.

Nakanishi,T., Kimura,Y., Tamura,T., Ichikawa,H., Yamaai,Y., Sugimoto,T., and Takigawa,M. (1997). Cloning of a mRNA preferentially expressed in chondrocytes by differential display-PCR from a human chondrocytic cell line that is identical with connective tissue growth factor (CTGF) mRNA. Biochem. Biophys. Res. Commun. *234*, 206-210.

Nakanishi,T., Yamaai,T., Asano,M., Nawachi,K., Suzuki,M., Sugimoto,T., and Takigawa,M. (2001). Overexpression of connective tissue growth factor/hypertrophic chondrocyte-specific gene product 24 decreases bone density in adult mice and induces dwarfism. Biochem. Biophys. Res. Commun. *281*, 678-681.

Niki,T., De Bleser,P.J., Xu,G., Van den,B.K., Wisse,E., and Geerts,A. (1996). Comparison of glial fibrillary acidic protein and desmin staining in normal and CCl4-induced fibrotic rat livers. Hepatology *23*, 1538-1545.

Niki,T., Pekny,M., Hellemans,K., Bleser,P.D., Berg,K.V., Vaeyens,F., Quartier,E., Schuit,F., and Geerts,A. (1999). Class VI intermediate filament protein nestin is induced during activation of rat hepatic stellate cells. Hepatology *29*, 520-527.

Nishida,T., Kubota,S., Fukunaga,T., Kondo,S., Yosimichi,G., Nakanishi,T., Takano-Yamamoto,T., and Takigawa,M. (2003). CTGF/Hcs24, hypertrophic chondrocyte-specific gene product, interacts with perlecan in regulating the proliferation and differentiation of chondrocytes. J. Cell Physiol. *196*, 265-275.

Oberhammer,F., Bursch,W., Parzefall,W., Breit,P., Erber,E., Stadler,M., and Schulte-Hermann,R. (1991). Effect of transforming growth factor beta on cell death of cultured rat hepatocytes. Cancer Res. *51*, 2478-2485.

Oe,S., Lemmer,E.R., Conner,E.A., Factor,V.M., Leveen,P., Larsson,J., Karlsson,S., and Thorgeirsson,S.S. (2004). Intact signaling by transforming growth factor beta is not required for termination of liver regeneration in mice. Hepatology *40*, 1098-1105.

Omori,M., Evarts,R.P., Omori,N., Hu,Z., Marsden,E.R., and Thorgeirsson,S.S. (1997). Expression of alpha-fetoprotein and stem cell factor/c-kit system in bile duct ligated young rats. Hepatology *25*, 1115-1122.

Paku,S., Schnur,J., Nagy,P., and Thorgeirsson,S.S. (2001). Origin and structural evolution of the early proliferating oval cells in rat liver. Am. J. Pathol. *158*, 1313-1323.

Paradis,V., Dargere,D., Bonvoust,F., Vidaud,M., Segarini,P., and Bedossa,P. (2002). Effects and regulation of connective tissue growth factor on hepatic stellate cells. Lab Invest. *82*, 767-774.

Paradis,V., Dargere,D., Vidaud,M., De Gouville,A.C., Huet,S., Martinez,V., Gauthier,J.M., Ba,N., Sobesky,R., Ratziu,V., and Bedossa,P. (1999). Expression of connective tissue growth factor in experimental rat and human liver fibrosis. Hepatology *30*, 968-976.

Paradis,V., Perlemuter,G., Bonvoust,F., Dargere,D., Parfait,B., Vidaud,M., Conti,M., Huet,S., Ba,N., Buffet,C., and Bedossa,P. (2001). High glucose and hyperinsulinemia stimulate connective tissue growth factor expression: a potential mechanism involved in progression to fibrosis in nonalcoholic steatohepatitis. Hepatology *34*, 738-744.

Pendurthi,U.R., Allen,K.E., Ezban,M., and Rao,L.V. (2000). Factor VIIa and thrombin induce the expression of Cyr61 and connective tissue growth factor, extracellular matrix signaling proteins that could act as possible downstream mediators in factor VIIa x tissue factor-induced signal transduction. J. Biol. Chem. *275*, 14632-14641.

Perbal,B. (2001). NOV (nephroblastoma overexpressed) and the CCN family of genes: structural and functional issues. Mol. Pathol. *54*, 57-79.

Petersen,B.E., Goff,J.P., Greenberger,J.S., and Michalopoulos,G.K. (1998). Hepatic oval cells express the hematopoietic stem cell marker Thy-1 in the rat. Hepatology *27*, 433-445.

Petersen,B.E., Zajac,V.F., and Michalopoulos,G.K. (1997). Bile ductular damage induced by methylene dianiline inhibits oval cell activation. Am. J. Pathol. *151*, 905-909.

Qi,Z., Atsuchi,N., Ooshima,A., Takeshita,A., and Ueno,H. (1999). Blockade of type beta transforming growth factor signaling prevents liver fibrosis and dysfunction in the rat. Proc. Natl. Acad. Sci. U. S A. *96*, 2345-2349.

Rachfal,A.W. and Brigstock,D.R. (2003). Connective tissue growth factor (CTGF/CCN2) in hepatic fibrosis. Hepatology Research *26*, 1-9.

Rappaport, A.M. (1963) Acinas units and the pathophysiology of the liver. In: *The liver. Morphology. Biochemistry. Physiology*. Vol I. Rouiller CH. Ed. New York, Academic Press. 265-328.

Rich,K.A., George,F.W., Law,J.L., and Martin,W.J. (1990). Cell-adhesive motif in region II of malarial circumsporozoite protein. Science *249*, 1574-1577.

Ricupero,D.A., Rishikof,D.C., Kuang,P.P., Poliks,C.F., and Goldstein,R.H. (1999). Regulation of connective tissue growth factor expression by prostaglandin E(2). Am. J. Physiol. *277*, L1165-L1171.

Riser,B.L., Denichilo,M., Cortes,P., Baker,C., Grondin,J.M., Yee,J., and Narins,R.G. (2000). Regulation of connective tissue growth factor activity in cultured rat mesangial cells and its expression in experimental diabetic glomerulosclerosis. J. Am. Soc. Nephrol. *11*, 25-38.

Rishikof,D.C., Ricupero,D.A., Kuang,P.P., Liu,H., and Goldstein,R.H. (2002). Interleukin-4 regulates connective tissue growth factor expression in human lung fibroblasts. J. Cell Biochem. *85*, 496-504.

Roberts,A.B., Sporn,M.B., Assoian,R.K., Smith,J.M., Roche,N.S., Wakefield,L.M., Heine,U.I., Liotta,L.A., Falanga,V., Kehrl,J.H., and . (1986). Transforming growth factor type beta: rapid induction of fibrosis and angiogenesis in vivo and stimulation of collagen formation in vitro. Proc. Natl. Acad. Sci. U. S A. *83*, 4167-4171.

Roulot,D., Sevcsik,A.M., Coste,T., Strosberg,A.D., and Marullo,S. (1999). Role of transforming growth factor beta type II receptor in hepatic fibrosis: studies of human chronic hepatitis C and experimental fibrosis in rats. Hepatology *29*, 1730-1738.

Ruoslahti,E. and Engvall,E. (1997). Integrins and vascular extracellular matrix assembly. J. Clin. Invest. *99*, 1149-1152.

Russell,W.E., Coffey,R.J., Jr., Ouellette,A.J., and Moses,H.L. (1988). Type beta transforming growth factor reversibly inhibits the early proliferative response to partial hepatectomy in the rat. Proc. Natl. Acad. Sci. U. S A. *85*, 5126-5130.

Sakamoto,K., Yamaguchi,S., Ando,R., Miyawaki,A., Kabasawa,Y., Takagi,M., Li,C.L., Perbal,B., and Katsube,K. (2002). The nephroblastoma overexpressed gene (NOV/ccn3) protein associates with Notch1 extracellular domain and inhibits myoblast differentiation via Notch signaling pathway. J. Biol. Chem. *277*, 29399-29405.

Schild,C. and Trueb,B. (2002). Mechanical stress is required for high-level expression of connective tissue growth factor. Exp. Cell Res. *274*, 83-91.

Schnabl,B., Kweon,Y.O., Frederick,J.P., Wang,X.F., Rippe,R.A., and Brenner,D.A. (2001). The role of Smad3 in mediating mouse hepatic stellate cell activation. Hepatology *34*, 89-100.

Schober,J.M., Chen,N., Grzeszkiewicz,T.M., Jovanovic,I., Emeson,E.E., Ugarova,T.P., Ye,R.D., Lau,L.F., and Lam,S.C. (2002). Identification of integrin alpha(M)beta(2) as an adhesion receptor on peripheral blood monocytes for Cyr61 (CCN1) and connective tissue growth factor (CCN2): immediate-early gene products expressed in atherosclerotic lesions. Blood *99*, 4457-4465.

Schultz-Cherry,S. and Murphy-Ullrich,J.E. (1993). Thrombospondin causes activation of latent transforming growth factor-beta secreted by endothelial cells by a novel mechanism. J. Cell Biol. *122*, 923-932.

Schuppan,D., Schmid,M., Somasundaram,R., Ackermann,R., Ruehl,M., Nakamura,T., and Riecken,E.O. (1998). Collagens in the liver extracellular matrix bind hepatocyte growth factor. Gastroenterology *114*, 139-152.

Schwartz,M.A. and Ingber,D.E. (1994). Integrating with integrins. Mol. Biol. Cell. *5*, 389-393.

Sedlaczek,N., Jia,J.D., Bauer,M., Herbst,H., Ruehl,M., Hahn,E.G., and Schuppan,D. (2001). Proliferating bile duct epithelial cells are a major source of connective tissue growth factor in rat biliary fibrosis. American Journal of Pathology *158*, 1239-1244.

Segarini,P.R., Nesbitt,J.E., Li,D., Hays,L.G., Yates,J.R., III, and Carmichael,D.F. (2001). The low density lipoprotein receptor-related protein/alpha2-macroglobulin receptor is a receptor for connective tissue growth factor. J. Biol. Chem. *276*, 40659-40667.

Serini,G., Bochaton-Piallat,M.L., Ropraz,P., Geinoz,A., Borsi,L., Zardi,L., and Gabbiani,G. (1998). The fibronectin domain ED-A is crucial for myofibroblastic phenotype induction by transforming growth factor-beta1. J. Cell Biol. *142*, 873-881.

Shek,F.W. and Benyon,R.C. (2004). How can transforming growth factor beta be targeted usefully to combat liver fibrosis? Eur. J. Gastroenterol. Hepatol. *16*, 123-126.

Shigekiyo,T., Yoshida,H., Matsumoto,K., Azuma,H., Wakabayashi,S., Saito,S., Fujikawa,K., and Koide,T. (1998). HRG Tokushima: molecular and cellular characterization of histidine-rich glycoprotein (HRG) deficiency. Blood *91*, 128-133.

Shimo,T., Kubota,S., Kondo,S., Nakanishi,T., Sasaki,A., Mese,H., Matsumura,T., and Takigawa,M. (2001). Connective tissue growth factor as a major angiogenic agent that is induced by hypoxia in a human breast cancer cell line. Cancer Lett. *174*, 57-64.

Shimo,T., Nakanishi,T., Kimura,Y., Nishida,T., Ishizeki,K., Matsumura,T., and Takigawa,M. (1998). Inhibition of endogenous expression of connective tissue growth factor by its antisense oligonucleotide and antisense RNA suppresses proliferation and migration of vascular endothelial cells. J. Biochem. (Tokyo) *124*, 130-140.

Shinozuka,H., Lombardi,B., Sell,S., and Iammarino,R.M. (1978). Early histological and functional alterations of ethionine liver carcinogenesis in rats fed a choline-deficient diet. Cancer Res. *38*, 1092-1098.

Shiojiri,N., Lemire,J.M., and Fausto,N. (1991). Cell lineages and oval cell progenitors in rat liver development. Cancer Res. *51*, 2611-2620.

Stanhope-Baker,P. and Williams,B.R. (2000). Identification of connective tissue growth factor as a target of WT1 transcriptional regulation. J. Biol. Chem. *275*, 38139-38150.

Stratton,R., Rajkumar,V., Ponticos,M., Nichols,B., Shiwen,X., Black,C.M., Abraham,D.J., and Leask,A. (2002). Prostacyclin derivatives prevent the fibrotic response to TGF-beta by inhibiting the Ras/MEK/ERK pathway. FASEB J. *16*, 1949-1951.

Stratton,R., Shiwen,X., Martini,G., Holmes,A., Leask,A., Haberberger,T., Martin,G.R., Black,C.M., and Abraham,D. (2001). Iloprost suppresses connective tissue growth factor production in fibroblasts and in the skin of scleroderma patients. J. Clin. Invest. *108*, 241-250.

Sun,Z., Reid,K.B., and Perkins,S.J. (2004). The dimeric and trimeric solution structures of the multidomain complement protein properdin by X-ray scattering, analytical ultracentrifugation and constrained modelling J. Mol. Biol. *343*, 1327-1343.

Suzuma,K., Naruse,K., Suzuma,I., Takahara,N., Ueki,K., Aiello,L.P., and King,G.L. (2000). Vascular endothelial growth factor induces expression of connective tissue growth factor via KDR, Flt1, and phosphatidylinositol 3-kinase-akt-dependent pathways in retinal vascular cells. J. Biol. Chem. *275*, 40725-40731.

Tahashi,Y., Matsuzaki,K., Date,M., Yoshida,K., Furukawa,F., Sugano,Y., Matsushita,M., Himeno,Y., Inagaki,Y., and Inoue,K. (2002). Differential regulation of TGF-beta signal in hepatic stellate cells between acute and chronic rat liver injury. Hepatology *35*, 49-61.

Tamkun,J.W., DeSimone,D.W., Fonda,D., Patel,R.S., Buck,C., Horwitz,A.F., and Hynes,R.O. (1986). Structure of integrin, a glycoprotein involved in the transmembrane linkage between fibronectin and actin. Cell. *46*, 271-282.

Taub,R. (1996). Liver regeneration 4: transcriptional control of liver regeneration. FASEB J. *10*, 413-427.

Uchio,K., Graham,M., Dean,N.M., Rosenbaum,J., and Desmouliere,A. (2004). Down-regulation of connective tissue growth factor and type I collagen mRNA expression by connective tissue growth factor antisense oligonucleotide during experimental liver fibrosis. Wound Repair Regen. *12*, 60-66.

Ueda,S., Yamanoi,A., Hishikawa,Y., Dhar,D.K., Tachibana,M., and Nagasue,N. (2003). Transforming growth factor-beta1 released from the spleen exerts a growth inhibitory effect on liver regeneration in rats. Lab Invest. *83*, 1595-1603.

Ujike,K., Shinji,T., Hirasaki,S., Shiraha,H., Nakamura,M., Tsuji,T., and Koide,N. (2000). Kinetics of expression of connective tissue growth factor gene during liver regeneration after partial hepatectomy and D-galactosamine-induced liver injury in rats. Biochem. Biophys. Res. Commun. *277*, 448-454.

Utsugi,M., Dobashi,K., Ishizuka,T., Masubuchi,K., Shimizu,Y., Nakazawa,T., and Mori,M. (2003). C-Jun-NH2-terminal kinase mediates expression of connective tissue growth factor induced by transforming growth factor-beta1 in human lung fibroblasts. Am. J. Respir. Cell Mol. Biol. *28*, 754-761.

Vanderkerken,K., Bouwens,L., De Neve,W., Van den,B.K., Baekeland,M., Delens,N., and Wisse,E. (1993). Origin and differentiation of hepatic natural killer cells (pit cells). Hepatology *18*, 919-925.

Varela-Rey,M., Montiel-Duarte,C., Oses-Prieto,J.A., Lopez-Zabalza,M.J., Jaffrezou,J.P., Rojkind,M., and Iraburu,M.J. (2002). p38 MAPK mediates the regulation of alpha1(I) procollagen mRNA levels by TNF-alpha and TGF-beta in a cell line of rat hepatic stellate cells(1). FEBS Lett. *528*, 133-138.

Wenner,C.E. and Yan,S. (2003). Biphasic role of TGF-beta1 in signal transduction and crosstalk. J. Cell Physiol. *196*, 42-50.

Wong,M., Kireeva,M.L., Kolesnikova,T.V., and Lau,L.F. (1997). Cyr61, product of a growth factor-inducible immediate-early gene, regulates chondrogenesis in mouse limb bud mesenchymal cells. Dev. Biol. *192*, 492-508.

Wu,J.Y., Feng,L., Park,H.T., Havlioglu,N., Wen,L., Tang,H., Bacon,K.B., Jiang,Z., Zhang,X., and Rao,Y. (2001). The neuronal repellent Slit inhibits leukocyte chemotaxis induced by chemotactic factors. Nature *410*, 948-952.

Wu,W., Wong,K., Chen,J., Jiang,Z., Dupuis,S., Wu,J.Y., and Rao,Y. (1999). Directional guidance of neuronal migration in the olfactory system by the protein Slit. Nature *400*, 331-336.

Wunderlich,K., Senn,B.C., Todesco,L., Flammer,J., and Meyer,P. (2000). Regulation of connective tissue growth factor gene expression in retinal vascular endothelial cells by angiogenic growth factors. Graefes Arch. Clin. Exp. Ophthalmol. *238*, 910-915.

Yamada,Y. and Fausto,N. (1998). Deficient liver regeneration after carbon tetrachloride injury in mice lacking type 1 but not type 2 tumor necrosis factor receptor. Am. J. Pathol. *152*, 1577-1589.

Yamada,Y., Kirillova,I., Peschon,J.J., and Fausto,N. (1997). Initiation of liver growth by tumor necrosis factor: deficient liver regeneration in mice lacking type I tumor necrosis factor receptor. Proc. Natl. Acad. Sci. U. S A. *94*, 1441-1446.

Yang,L., Li,S., Hatch,H., Ahrens,K., Cornelius,J.G., Petersen,B.E., and Peck,A.B. (2002). In vitro trans-differentiation of adult hepatic stem cells into pancreatic endocrine hormone-producing cells. Proc. Natl. Acad. Sci. U. S A. *99*, 8078-8083.

Yin,L., Ghebranious,N., Chakraborty,S., Sheehan,C.E., Ilic,Z., and Sell,S. (1998). Control of mouse hepatocyte proliferation and ploidy by p53 and p53ser246 mutation in vivo. Hepatology *27*, 73-80.

Yin,L., Lynch,D., and Sell,S. (1999). Participation of different cell types in the restitutive response of the rat liver to periportal injury induced by allyl alcohol. J. Hepatol. *31*, 497-507.

Yosimichi,G., Kubota,S., Hattori,T., Nishida,T., Nawachi,K., Nakanishi,T., Kamada,M., Takano-Yamamoto,T., and Takigawa,M. (2002). CTGF/Hcs24 interacts with the cytoskeletal protein actin in chondrocytes. Biochem. Biophys. Res. Commun. *20;299*, 755-761.

Yosimichi,G., Nakanishi,T., Nishida,T., Hattori,T., Takano-Yamamoto,T., and Takigawa,M. (2001). CTGF/Hcs24 induces chondrocyte differentiation through a p38 mitogen-activated protein kinase (p38MAPK), and proliferation through a p44/42 MAPK/extracellular-signal regulated kinase (ERK). Eur. J. Biochem. *268*, 6058-6065.

Yu,Q. and Stamenkovic,I. (2000). Cell surface-localized matrix metalloproteinase-9 proteolytically activates TGF-beta and promotes tumor invasion and angiogenesis. Genes Dev. *14*, 163-176.

Yue,J. and Mulder,K.M. (2000). Requirement of Ras/MAPK pathway activation by transforming growth factor beta for transforming growth factor beta 1 production in a smad-dependent pathway. J. Biol. Chem. *275*, 35656.

Yue,J., Sun,B., Liu,G., and Mulder,K.M. (2004). Requirement of TGF-beta receptor-dependent activation of c-Jun N-terminal kinases (JNKs)/stress-activated protein kinases (Sapks) for TGF-beta up-regulation of the urokinase-type plasminogen activator receptor. J. Cell Physiol. *199*, 284-292.

Zheng,X., Nishio,K., Majerus,E.M., and Sadler,J.E. (2003). Cleavage of von Willebrand factor requires the spacer domain of the metalloprotease ADAMTS13. J. Biol. Chem. *278*, 30136-301.

BIOGRAPHICAL SKETCH

Liya Pi was born in P.R. China, November 10, 1970. She graduated from Lanzhou University and entered the Institute of Genetics, Academia Sinica, for an M.S degree in 1992. However, she did not complete her M.S degree and accompanied her husband, Wen-Yuan Song, to the United States in 1995. One year later, she resumed her graduate study under the guidance of Dr. Pamela Ronald in the Biochemistry and Molecular Biology Program at the University of California, Davis. In 1999, Wen-Yuan's movement from California to Florida interrupted her Ph.D. study and she had to write a M.S thesis based on the works done in Dr. Ronald's laboratory. To test her ability and seek a dream for her research career, she restarted her Ph.D. study in the Interdisciplinary Program in Biomedical Sciences at the University of Florida, College of Medicine, in 2000. After five years' hard work, she will receive her doctorate in Molecular Cell biology in May 2005.

Her scholastic accomplishments include being an Alumni fellow at the University of Florida during her Ph.D. study. She also won “Excellent international student” award twice from the International Office at the University of Florida.